TECHNISCHE UNIVERSITÄT MÜNCHEN

Lehrstuhl für Analytische Chemie und Wasserchemie

Institut für Klinische Chemie und Pathobiochemie

Incorporation of platelet glycoprotein receptors into lipid bilayer nanodiscs for the detection of autoantibodies in autoimmune thrombocytopenia

Stefanie Alexandra Mak

Vollständiger Abdruck der von der Fakultät für Chemie der Technischen Universität München zur Erlangung des akademischen Grads eines

Doktors der Naturwissenschaften (Dr. rer. nat.)

genehmigten Dissertation.

Vorsitzender:	Prof. Dr. Lukas Hintermann
Prüfer der Dissertation:	1. Prof. Dr. Reinhard Nießner
	2. apl. Prof. Dr. Peter B. Luppa

Die Dissertation wurde am 23.10.2019 bei der Technischen Universität München eingereicht und durch die Fakultät für Chemie am 25.11.2019 angenommen.

Teile der vorliegenden Arbeit wurden bereits veröffentlicht unter:

S. Mak, R. Sun, M. Schmalenberg, C. Peters, and P. B. Luppa. Express incorporation of membrane proteins from various human cell types into phospholipid bilayer nanodiscs. Biochemical Journal, 474(8):1361–1371, Apr. 2017.

R. Sun, S. Mak, J. Haschemi, P. Horn, F. Boege, and P. B. Luppa. Nanodiscs Incorporating Native β1 Adrenergic Receptor as a Novel Approach for the Detection of Pathological Autoantibodies in Patients with Dilated Cardiomyopathy. The Journal of Applied Laboratory Medicine, jalm.2018.028225, May 2019.

What if I fall?
Oh, but my darling, what if you fly?

Erin Hanson

Danksagung

Diese Doktorarbeit entstand in der Zeit von Oktober 2015 bis Juni 2019 am Institut für Klinische Chemie und Pathobiochemie am Klinikum rechts der Isar der Technischen Universität München.

Vor allem danke ich Herrn Prof. Luppa von ganzem Herzen für die Möglichkeit, meine Doktorarbeit in seiner Arbeitsgruppe zu schreiben. Durch sein entgegengebrachtes Vertrauen gab er mir den Freiraum, selbstständig und eigenverantwortlich zu arbeiten, wobei seine Tür jederzeit für Fragen offen stand. Ich hätte mir keinen besseren Betreuer für diese Arbeit wünschen können.

Herrn Prof. Nießner möchte ich für die offizielle Betreuung der Arbeit danken, sowie dafür, in Diskussionen immer die richtigen Fragen zu stellen und direkt zum Kern des Problems vorzudringen.

Herrn Prof. Bakchoul vom Blutspendezentrum Tübingen danke ich für die Bereitstellung von Probenmaterial, sowie für die Möglichkeit, in seinem Labor zu arbeiten.

Ohne die stets tatkräftige Hilfe aller meiner Kollegen wäre diese Arbeit nicht zustande gekommen. Vor allem Dr. Michael Schmalenberg und Dr. Ruoyu Sun sind mir immer zur Seite gestanden, und waren eine große Hilfe bei allen Schritten von der Themenfindung bis zum Korrekturlesen der Arbeit. Ich danke ihnen für ihre Hilfe bei der Lösung von Problemen aller Art und die vielen unterhaltsamen Momente in Arbeit und Freizeit. Auch ihr Beitrag zum Arbeitsklima, zum Erhalt der guten Laune und zur Versorgung mit Süßigkeiten aus aller Welt war maßgeblich für diese Arbeit.

Allen Laborleitern, die meine Arbeit begleitet und betreut haben, danke ich sehr. Dr. Alexander Le Blanc, Dr. Andreas Poschenrieder und Dr. Susanne Weber haben ihre Geduld und ihr beträchtliches Fachwissen immer wieder unter Beweis gestellt durch anregende Diskussionen, frühzeitiges Finden von Fehlern und ihre Unterstützung bei allen kleinen und großen Problemen.

Unsere technischen Assistenten Anita Schreiegg und Christine Grubmüller haben mir sehr viel über die praktische Arbeit im Labor beigebracht und mich immer in allen Aspekten der Arbeit unterstützt. Ohne ihren unermüdlichen Kampf gegen die Entropie wäre dieses Labor nicht so ein angenehmer Ort zum Arbeiten.

Meine Kollegen Dr. Andreas Bietenbeck, Melina Grasmeier, Andreas Kratzert, Janine Potreck, Dr. Markus Thaler, Christine Schönmann und Martina Simon haben die Arbeit immer zu einem Vergnügen gemacht. Neben ihrer fachlichen Unterstützung war vor allem

der geistige Beistand entscheidend, die spannenden Diskussionen, Film-, Spiel-, Koch- und sonstigen Abende sowie die schönen Reisen zu verschiedenen Konferenzen. Dank ihnen hat mir die Arbeit auch in schwierigen Zeiten immer Spaß gemacht.

Auch bei allen anderen Kollegen des Instituts, vom Sekretariat über die Routine bis hin zu den anderen Forschungsgruppen, möchte ich mich bedanken für eine immer hervorragende Arbeitsatmosphäre, tatkräftige Hilfe bei ausgefallenen Experimenten und Ermunterungen zur richtigen Zeit.

Peer hat mich vor allem in der letzten und anstrengendsten Phase der Arbeit bei der Stange gehalten, bekocht, motiviert, mein Gejammer geduldig angehört und mich nicht zu ernst genommen. Ihm danke ich auch für andere Blickwinkel auf mein Thema und Ablenkung in den richtigen Momenten.

Ich danke meinen Eltern und meinem Bruder für Ihre Unterstützung nicht nur während der Doktorarbeit, sondern auch in allen anderen Bereichen meines Lebens. Ohne ihre Hilfe und Ermutigung wäre ich nicht so weit gekommen. Das Wissen, dass ich immer einen Platz habe, zu dem ich zurückkommen kann, hat das verrückte Experiment Doktorarbeit erst möglich gemacht.

Zusammenfassung

Autoimmunthrombozytopenie (AITP) ist eine erworbene Autoimmunkrankheit, bei der reife Thrombozyten sowie ihre Vorläuferzellen durch immunologische Prozesse zerstört werden. Dies beschleunigt den Abbau von Thrombozyten und hemmt deren Neubildung, was zu einer verringerten Thrombozytenzahl führt. Symptome sind Petechien, verlängerte Blutungszeiten, Hämatomneigung schon bei geringen Traumen und in seltenen Fällen sogar lebensbedrohliche intrazerebrale Blutungen. Die meisten Therapieansätze unterdrücken entweder die Immunreaktion gegenüber Thrombozyten oder fördern deren Neubildung. Allerdings wird eine angemessene Behandlung von AITP häufig durch eine anfängliche Fehldiagnose der Patienten behindert.

Der Hauptgrund dafür ist, dass AITP in erster Linie als Ausschlussdiagnose festgestellt wird und daher von der klinischen Erfahrung des behandelnden Arztes abhängt. Obwohl verschiedene Versuche unternommen wurden, thrombozytenspezifische Autoantikörper als Biomarker für AITP zu etablieren und Testmethoden für deren Nachweis im Blutserum zu entwickeln, wird derzeit keiner dieser Assays in der Routinediagnostik verwendet. Dies ist teilweise auf die komplizierte Natur dieser Assays zurückzuführen, die zumeist von frischen Spender- oder Patiententhrombozyten als Antigenquelle abhängen. Das schwerwiegendere Hindernis ist allerdings ihre schlechte Leistung. Letzteres zeigt sich durch eine im Allgemeinen akzeptable Spezifität, jedoch geringen Sensitivität der Tests. Dies liegt vor allem an der schwierigen Immobilisierung von Thrombozytenrezeptoren mit intakter Struktur auf Assayoberflächen, da diese bei der Isolierung aus der Thrombozytenmembran zur Denaturierung neigen.

Ziel dieser Doktorarbeit war es, ein neues Assay-Format zum Nachweis von Autoantikörpern gegen Thrombozytenrezeptoren bei AITP zu entwickeln. Dieses neuartige Testsystem sollte die Nachteile früherer Assays umgehen, insbesondere die Notwendigkeit von intakten menschlichen Thrombozyten und die komplizierte und zeitintensive Handhabung. Zu diesem Zweck wurden die Glykoprotein (GP) -Rezeptoren GPIIb/IIIa und GPIb/IX in HEK-293-Zellen rekombinant exprimiert, wodurch die begrenzte Verfügbarkeit menschlicher Spenderthrombozyten überwunden wurde und die Rezeptoren für eine einfachere Assayentwicklung modifiziert werden konnten. Die korrekte Expression, Assemblierung und Struktur dieser GP-Rezeptoren in HEK-293-Zellen wurde durch Western Blot, Durchflusszytometrie und Adhäsionsassays verifiziert.

Um ihre Anwendung in den meisten für lösliche Proteine entwickelten Standardtechnologien zu ermöglichen, wurden die Thrombozyten-GP-Rezeptoren in Nanodiscs eingebaut. Nanodiscs sind runde Scheiben einer Phospholipiddoppelschicht mit einem Durchmesser von 7 bis 17 nm, die durch einen Gürtel aus sogenannten Membrane Scaffold Proteinen stabilisiert werden. Die native Struktur und Funktionalität der GPIIb/IIIa- und GPIb/IX-Rezeptoren blieb auch nach ihrem Einbau in Nanodiscs erhalten, wie durch immunologische Assays mit komplexspezifischen Antikörpern sowie durch Oberflächenplasmonenresonanz(SPR)-Spektroskopie mit ihren jeweiligen Liganden, Fibrinogen und von Wille-

brand-Faktor, gezeigt wurde.

Die Nanodiscs mit eingebauten GP-Rezeptoren wurden als Liganden in einem ELISA-basierten Verfahren zum Nachweis von Autoantikörpern in humanen Serumproben verwendet. Der Aufbau dieses Testformats ermöglicht eine einfache Bedienung und einen hohen Durchsatz von Proben. Der Assay wurde für die Differenzierung von Serumproben mit und ohne spezifischen Antikörpern gegen die GP-Rezeptoren optimiert. Schließlich wurde der auf GPIIb/IIIa-Nanodiscs basierende Test mit humanen Serumproben validiert. Insgesamt wurden 150 Proben gemessen, davon 69 von AITP-Patienten und 81 von gesunden Kontrollpersonen. Die ermittelten Inter-Assay- und Intra-Assay-Variationskoeffizienten lagen weit unter den akzeptablen Grenzen.

Ebenso war das Ergebnis der Patientenstudie vielversprechend. Die mittleren ELISA-Signale der mit AITP diagnostizierten Patienten waren signifikant höher als die der gesunden Kontrollpersonen, obwohl die Patientengruppe wahrscheinlich Proben mit und ohne Autoantikörper gegen GPIIb/IIIa enthielt. Bei Proben von AITP-Patienten, die gemäß ihrer vorherigen Untersuchung mit einem anderen Assay auf anti-GPIIb/IIIa-Autoantikörper in positive und negative Gruppen eingeteilt wurden, war der Mittelwert der positiven Proben ebenfalls signifikant höher als der der negativen Proben. Die Ergebnisse dieser Vorstudie belegen die grundsätzliche Eignung und das hohe Potenzial des neu entwickelten Assays zur Diagnose von AITP.

Abstract

Autoimmune thrombocytopenia (AITP) is an acquired autoimmune disease, in which mature platelets as well as their progenitor cells are destroyed by immunological processes. This accelerates platelet clearance and impairs platelet production, leading to reduced platelet numbers. Symptoms are petechia, prolonged bleeding times, easy bruising, and in rare cases even life threatening intracerebral hemorrhage. Most therapeutic approaches either suppress the immunological response or increase the platelet production. However, the appropriate treatment of AITP is often impeded by an initial misdiagnosis of patients.

The main reason for this is that diagnosis of AITP is predominantly a process of exclusion, and thus dependent on the clinical experience of the treating physician. Although there have been different attempts to establish platelet-specific autoantibodies as biomarkers for AITP and to develop assays for their detection in the blood serum, none of those assays are currently used in routine diagnostics. This is partly a result of the complicated nature of most of these assays, which are mostly dependent on fresh donor or patient platelets as an antigen source. However, the more severe obstacle is their poor performance. The latter is generally reflected by an acceptable specificity but low sensitivity of the tests. This is mostly due to the difficult immobilization of intact platelet receptors on assay surfaces, as they tend to denature upon separation from the platelet membrane.

The aim of this PhD thesis was to develop a new assay format for the detection of autoantibodies against platelet receptors in AITP. This novel format should circumvent the disadvantages of previous assays, especially their need for intact human platelets and their complicated and time-intensive designs. For this purpose, the platelet glycoprotein (GP) receptors GPIIb/IIIa and GPIb/IX were recombinantly expressed in HEK-293 cells, which allowed to overcome the limited availability of human donor platelets and to modify the proteins of interest for an easier assay development. The correct expression, assembly and structure of those GP receptors in HEK-293 cells was verified by Western Blot, flow cytometry and adhesion assays.

In order to enable their application in most standard technologies developed for soluble proteins, the platelet GP receptors were reconstituted in nanodiscs. Nanodiscs are round slices of phospholipid bilayer with a diameter of 7 to 17 nm, which are stabilized by a belt of a so-called membrane scaffold proteins. The native three-dimensional structure and functionality of the GPIIb/IIIa and GPIb/IX receptors was preserved by their incorporation into nanodiscs, as shown by enzyme-linked immunosorbent assay (ELISA) with complex-specific antibodies as well as surface plasmon resonance (SPR) spectroscopy experiments with their respective ligands, fibrinogen and von Willebrand factor.

The GP receptor-containing nanodiscs were used as ligands in an ELISA-based procedure for the detection of GP receptor autoantibodies in human serum samples. The setup of this ELISA was designed for an easy operation and expandability for high throughput analyses. It was optimized for the differentiation of serum samples with and without specific antibodies against the GP receptors. Finally, the assay with GPIIb/IIIa nanodiscs

was validated with human serum samples. In total, 150 samples were measured, of which 69 were from AITP patients and 81 from healthy controls. The determined inter-assay and intra-assay coefficients of variation were well below generally acceptable limits. Also, the outcome of the patient study was promising. The mean ELISA signals of patients diagnosed with AITP were significantly higher than those of healthy controls, although it was likely that the patient group contained samples with and without autoantibodies against GPIIb/IIIa. In addition, samples from AITP patients, which were divided into positive and negative groups according to their prior testing for anti-GPIIb/IIIa autoantibodies with a different assay, showed again significantly higher mean signals in the positive group when compared to the negative group. The results of this preliminary study demonstrated the basic suitability and the high potential of the newly developed assay for the diagnosis of AITP.

Contents

1 Introduction

1.1 Platelets and hemostasis

In an adult person, about five liters of blood containing a multitude of coagulation factors, blood clotting proteins and regulatory elements constantly traverse the body. This process happens mostly without complications, without undue blood coagulation and arterial occlusion. At the same time, a small injury to a vessel wall is enough to induce a complex network of pathways which close the breach and prevent blood loss within minutes (Hoffman et al., 2012).

1.1.1 Hemostasis

The process responsible for this tight regulation is called hemostasis (from Greek haíma = blood and stasis = stagnation). The haemostatic system relies on the interplay between blood vessels, blood plasma, and blood cells, especially blood platelets. Platelets (also called thrombocytes) are the smallest type of blood cells, only a fraction of the size of erythrocytes or leukocytes (see figure 1.1 A). They are key mediators of hemostasis, involved in every step of the process (see fig. 1.1 B), either directly via adherence and aggregation at sites of injury or indirectly via secretion of pro-coagulant factors, attraction of other cells, or providing a surface and a starting point for the plasma coagulation cascade (Hiller, 2007).

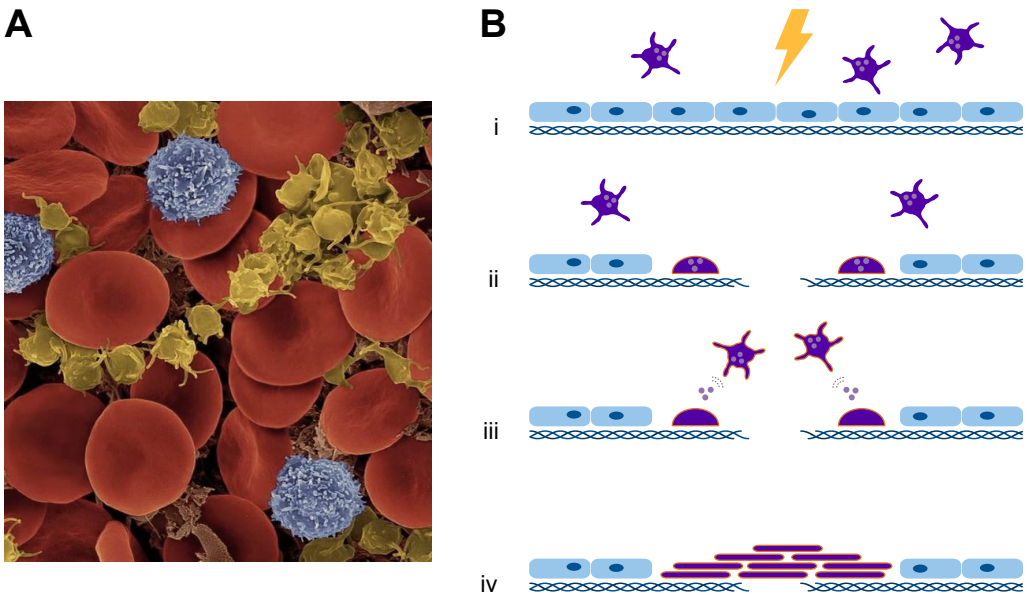

Figure 1.1: (A) Composite colored scanning electron micrograph (SEM) of red blood cells (red), T-lymphocytes (blue) and activated platelets (yellow), 800x magnification (Credit: Dennis Kunkel microscopy Inc./Visuals unlimited/Corbis). (B) Platelet activation, adherence and aggregation. Blood vessel injuries (i) lead to platelet adherence and shape change (ii), secretion of platelet-activating factors (iii) and the formation of a stable platelet plug (iv).

1.1.2 The platelet life cycle

On average, the human body produces and eliminates around 10^{11} platelets per day, maintaining a concentration of 150,000 to 400,000 platelets per microliter blood (Li et al., 2016). The platelet life cycle starts with thrombopoiesis from megakaryocytes in the bone marrow. Those polynuclear cells shed platelets into the bloodstream from protruded extensions in the blood vessels, the so-called proplatelets (Stegner et al., 2017).

Thrombopoietin (TPO) is the primary regulator of thrombopoiesis, the key hormone responsible for platelet production. It induces bone marrow megakaryocytes to survive, proliferate and produce platelets (Varghese et al., 2017). Newly synthesized TPO is released into the blood vessels by hepatocytes in the liver, and partly incorporated into circulating platelets. Thus, the platelet number is inversely proportional to the concentration of free TPO present in the blood stream, which is necessary for stimulation of megakaryocytes. This inhibitory feedback loop in which platelet counts inversely correlate with the amount of TPO is crucial for maintenance of a constant number of platelets (de Sauvage et al., 1996).

Platelets circulate for approximately 7 to 10 days, slowly undergoing age-related changes in morphology, activation, and surface receptor density (Rijkers et al., 2017). The life span of individual platelets is controlled by an internal apoptosis regulating pathway. As platelets age, sialic acid is gradually lost from the surface, which exposes the underlying galactose residues. This enables their clearance by the spleen and liver, triggers hepatic TPO release and thus promotes generation of new platelets (Grozovsky et al., 2015).

1.1.3 Thrombocytopenia

A low platelet count, defined as less than 100,000 platelets per microliter, leads to symptoms such as hematomas, petechiae, prolonged bleeding times or even spontaneous bleeding without external trigger (Kiefel and Müller-Eckhardt, 2010). This condition is called thrombocytopenia, and can be induced by a variety of causes. Most common are genetic disorders, liver diseases, malignancies, infections, inflammation, side effects of drugs, or excessive blood loss (Nebe, 2014).

Thrombocytopenia can also be caused by immune destruction of platelets. Either homologous platelets are destroyed, such as in drug-induced or autoimmune thrombocytopenia (AITP), or the immune reaction can be directed against heterologous platelets, like in neonatal or alloimmune immune thrombocytopenia (ITP).

- **Drug-induced thrombocytopenia:** Antibodies are produced against a combined epitope developing in drug-target-complexes on platelets, which leads to platelet destruction. The most common type is heparin-induced thrombocytopenia, wherein the patient develops a thrombocytopenia when under treatment with heparin. After discontinuation of the drug administration the symptoms disappear (Aster and Bougie, 2007).

- **Neonatal immune thrombocytopenia:** Maternal antibodies directed against fetal platelet antigens cross the placenta and destroy fetal platelets (Kiefel and Müller-Eckhardt, 2010).
- **Alloimmune thrombocytopenia:** The patient's immune system destroys transfused donor platelets such as contained in platelet concentrates. Those platelets have different antigens than their own platelets and are thus recognized as foreign (Heimpel, 2010).

1.2 Autoimmune thrombocytopenia (AITP)

1.2.1 Definition and historical overview

Autoimmune thrombocytopenia is an acquired autoimmune disease in which the patient's own platelets are destroyed by immunologic processes in the absence of other conditions known to cause thrombocytopenia. It is also known by its former names "idiopathic thrombocytopenic purpura" or "Morbus Werlhof".

It was named after the German physician Paul Gottlieb Werlhof (1699-1767), who in 1735 provided the classic clinical description of AITP (Werlhof, 1735). He wrote a complete initial report describing two patients with corresponding symptoms. However, the disease was probably known even before. Other physicians have described patients with similar symptoms, such as the Portuguese physician Amato Lusitano (1556) and the French Lazarus de la Rivière (1658).

The association between purpura, the typical rash of red or purple spots on the skin, and thrombocytopenia was not discovered until nearly 150 years after Werlhof. Different physicians in the late 19th century (Brohm, 1883; Denys, 1887; Hayem, 1889) observed that the platelet number was diminished in the active phase of purpura. The first experiments to gather insights into the mechanisms of AITP were conducted by Marino (1905) and Ledingham (1914), who could produce anti-platelet antisera by inoculating rabbits or guinea pigs with platelets from the other species respectively. A further proof for the involvement of an immunologic agent in AITP was the recovery of patients after successful splenectomy (Kaznelson, 1916). After removal of the spleen, immunologic destruction of platelets was inhibited and the platelet count increased.

The autoimmune origin of AITP was confirmed by experiments from Harrington et al. (1951) and Shulman et al. (1965). Blood plasma from AITP patients was transfused into healthy recipients, resulting in the rapid onset of severe thrombocytopenia. The effect was transient, dose-dependent, and the presence of the immunoglobulin G (IgG)-rich fraction was essential. Those experiments provided convincing evidence for the theory of platelet destruction by circulating antibodies. Subsequent studies revealed that those antibodies were of the IgG subtype and reactive against platelet surface glycoproteins (Kashiwagi and Tomiyama, 2013).

1.2.2 Epidemiology

AITP was separated into primary (idiopathic) and secondary forms (Liebman, 2008) after the recognition that a number of other medical conditions can also induce formation of anti-platelet auto-antibodies. In contrast, the primary form does not have any discernible cause. Around 80 % of AITP cases are primary (Cines and Blanchette, 2002).

The estimated incidence of primary AITP is between 2 and 4 per 100,000 adults per year, with a prevalence of 9 to 26 per 100,000 adults (Abrahamson et al., 2009; Terrell et al., 2008; Segal and Powe, 2006). It subsequently fulfills the definition of a rare or orphan disease (Heemstra et al., 2008). In Germany there are about 2400 new cases of AITP per year and 16,000 chronic patients (Matzdorff et al., 2018). In the population older than 65 years, the prevalence is similar in male and female patients, whereas in the younger population about twice as many women than men are affected (Lambert and Gernsheimer, 2017).

While AITP has formerly been defined as "chronic" if it lasted for more than 6 months and "acute" if it was self-limited and transient, by now three distinct phases of the disease are distinguished (Cines and Blanchette, 2002):

- "newly diagnosed" from the time of diagnosis up to 3 months,
- "persistent" between 3 and 12 months from diagnosis, and
- "chronic" if the disease lasts more than 12 months.

When the disease has become chronic, a spontaneous remission becomes less likely (Sailer et al., 2006). In Germany it is estimated that about 60% of adult patients develop chronic AITP (Matzdorff et al., 2018).

1.2.3 Symptoms of AITP

Symptoms of AITP differ widely in severity, from barely noticeable to life-threatening. Typical symptoms for platelet counts between 10,000 and 50,000 per microliter are shown in figure 1.2, such as petechia on the lower extremities, more rarely on the body and arms, prolonged menses, prolonged bleeding from wounds, and bruises associated with minimal or no trauma (Lambert and Gernsheimer, 2017). Only in rare cases with less than 10,000 platelets per microliter, more severe symptoms like mucocutaneous bleeding, epistaxis, hematuria, or internal bleeding can be present. Life threatening bleeding such as intracerebral hemorrhage is rare. Platelet function testing appears successful in predicting bleeding risk in patients (Frelinger et al., 2015). The bleeding predispositions are, however, very heterogeneous, and it is still unclear why patients with similar platelet counts can present with different clinical bleeding manifestations (Zufferey et al., 2017).

A systematic review by Neunert et al. (2015) summarized findings of 147 studies examining the frequency of bleeding events in AITP. Rates of severe bleeding (extensive mucosal bleeding as the minimum criterion) occurred in 9.6 % of patients, whereas 1.4 % of adults with chronic AITP showed intracerebral hemorrhage. Predictors of severe bleeding were

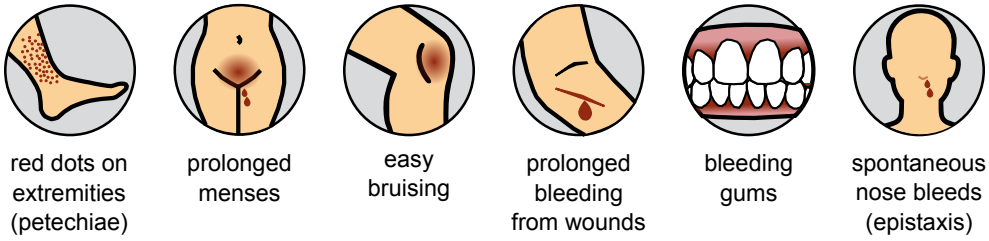

Figure 1.2: Common symptoms of AITP. Severe symptoms such as internal bleeding are rare.

not readily identified in primary studies, but platelet counts below 10,000 - 20,000 per microliter and previous minor bleeding were frequent associations. Other retrospective studies have suggested that increased patient age, use of medications, and male sex are associated with increased bleeding risk (Cohen et al., 2000; Lambert and Gernsheimer, 2017).

Interestingly, for a given platelet count symptoms are milder in AITP than in other thrombocytopenias. It is hypothesized that platelets in AITP patients are younger on average and more reactive, compensating in part the lower overall number (Matzdorff 2018).

1.2.4 Pathophysiology of AITP

The number of functional platelets in the blood stream is normally regulated by the balance between production and clearance of platelets. In AITP, both processes are affected (see fig. 1.3). Platelet clearance is accelerated and platelet production is impaired by immunological processes (Kashiwagi and Tomiyama, 2013), which leads to a lower overall number of platelets.

Normally, the immune system is carefully regulated since it must protect the body from outside invasion, and, at the same time, not over-react to self-antigens (McMillan, 2007). This fragile equilibrium is disrupted in AITP. However, the fundamental abnormality leading to the autoimmune response is unknown and probably differs among patients.

1.2.4.1 Autoantibodies against platelet antigens

Autoantibody-mediated labeling of platelets for phagocytotic breakdown was suggested as early as the 1960s (Harrington et al., 1951; Shulman et al., 1965). Autoantibodies bind to the platelets, which are then recognized by Fcγ receptors on tissue macrophages, predominantly in the spleen and liver. In addition to Fc-mediated phagocytosis, autoantibodies accelerate platelet clearance by complement deposition (Najaoui et al., 2012) and induction of platelet apoptosis (Goette et al., 2016). Furthermore, platelet opsonisation by autoantibodies can affect platelet reactivity by modulating agonist stimulation and platelet secretory granule release (Weiss et al., 1980).

Since the expression levels of platelet antigens increase during the maturation process of megakaryocytes (Lepage et al., 2000), anti-platelet autoantibodies can attack megakaryocytes as well. Antibodies bound to megakaryocytes may induce apoptosis, in addition to

antibody- and complement-dependent cytotoxicity (Perdomo et al., 2013). Morphological abnormalities in megakaryocytes of AITP patients showed extensive apoptotic and para-apoptotic changes. Increase of immature megakaryocytes, decrease of platelet production, and degenerative change of nucleus and cytoplasm, can be observed by optical microscopy (Houwerzijl et al., 2004; McMillan, 2007).

Autoantibodies are produced by antigen-specific B cells. Differentiation of B cells into antibody-secreting plasma cells is induced by T helper (Th) cells, which are in turn stimulated by splenic macrophages and dendritic cells presenting peptide fragments from destroyed platelets (Kashiwagi and Tomiyama, 2013; Catani et al., 2006). The number of autoantibody secreting plasma cells is increased in patients with AITP (Kuwana et al., 2006). Additionally, memory B cells are activated in the spleen and released into the circulation (Kuwana et al., 2002).

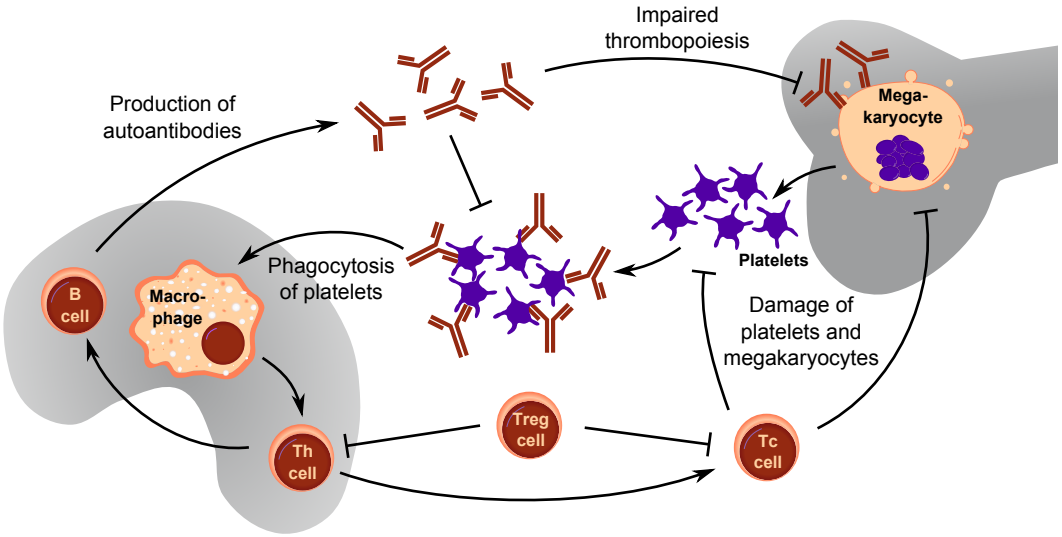

Figure 1.3: Schematic illustration of pathophysiology of AITP. Macrophages in the spleen destroy platelets labeled with autoantibodies and present their peptide fragments to T helper cells (Th cells), which in turn activate autoreactive B cells and cytotoxic T cells (Tc cells). Autoantibodies and Tc cells also suppress megakaryocytopoiesis. Impaired regulatory T cells (Treg cells) fail to suppress the self-reactive immune response.

1.2.4.2 Platelet-specific T cells

Not only is the production of abnormal helper T-cells reported in AITP (Olsson et al., 2003), other T-cell populations are linked to the pathogenesis of AITP as well. Platelet antigen-reactive cytotoxic T-cells attack both mature platelets and megakaryocytes (Li et al., 2007), thus leading to both platelet destruction and inhibition of platelet production. Platelet-reactive T-cells have been found in the blood samples of AITP patients (Olsson et al., 2003; Nomura, 2016).

The function of regulatory T cells (Treg) in AITP has been extensively examined, as emergence of platelet-specific B cells and cytotoxic T cells is an expected consequence of the loss of immunological tolerance to self-antigens. Tregs play an essential role in self-

tolerance by suppression of cell- and antibody-mediated immune responses (Sakaguchi, 2005). Several reports demonstrated reduction in Treg numbers and/or impairment of Treg function in AITP patients (Sakakura et al., 2007; Yu et al., 2008).

1.2.5 Platelet receptors involved in AITP

Autoantibodies in AITP bind to platelet surface antigens, predominantly to membrane glycoproteins (GPs). The first antigen was identified by van Leeuwen et al. (1982), who discovered that AITP antibodies did not bind to platelets that were genetically deficient in the glycoprotein IIb/IIIa (GPIIb/IIIa) complex. Antibodies that react with glycoprotein Ib/IX (GPIb/IX) are also quite common, around 75 % of platelet autoantibodies bind to either GPIIb/IIIa or GPIb/IX complexes (see fig. 1.4). Only 25 % recognize other membrane glycoproteins such as GPIa/IIa, GPIV, and GPV (McMillan et al., 2001; Hamidpour et al., 2006). GPIIb/IIIa and GPIb/IX are the most abundant of all platelet glycoprotein receptors (Saboor et al., 2013), which could probably explain their dominant role in AITP pathogenesis.

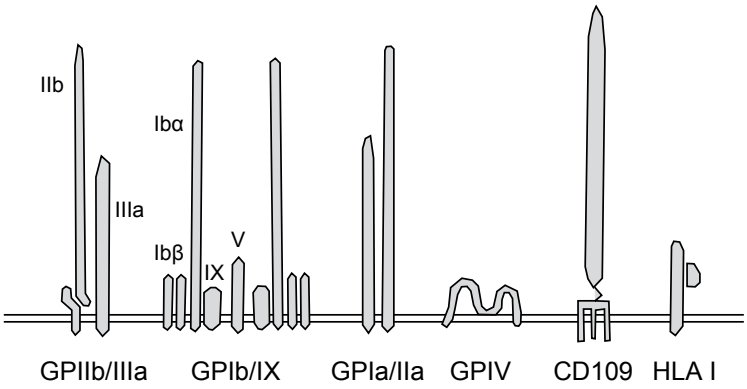

Figure 1.4: Schematic illustration of platelet surface antigens involved in AITP. About 75 % of autoantibodies bind to either GPIIb/IIIa or GPIb/IX.

1.2.5.1 GPIIb/IIIa

GPIIb/IIIa is an integrin receptor specific to platelets and its interaction with fibrinogen leads to outside-in signals that result in platelet shape change and granule secretion (Coller, 2015; Hagemeyer and Peter, 2010). The GPIIb/IIIa receptor consists of the two non-covalently bound subunits GPIIb and GPIIIa (also known as αIIb and β3, respectively), which are encoded by the genes ITGA2B and ITGB3. It represents the most abundant type of platelet receptor with 80,000 to 100,000 copies in the outer membrane (Saboor et al., 2013), covering about 15 % of the membrane surface and 20 % of the membrane mass (Rodriguez Bueno, 2011).

1.2.5.2 GPIb/IX

The leucine-rich repeat receptor GPIb/IX is not only an adhesive protein, but also assists in platelet activation and regulates the platelet cytoskeleton. It is a highly integrated,

stable membrane protein complex consisting of the subunits GPIbα, GPIbβ, and GPIX (encoded by the genes GP1BA, GP1BB, and GP9, respectively) in a ratio of 1:2:1 (Luo et al., 2007). Two copies of GPIb/IX are weakly linked by GPV (Li and Emsley, 2013). This complex is the second most abundant platelet membrane receptor with about 50,000 copies per cell (Saboor et al., 2013). Although GPIb/IX can bind to many different ligands, its crucial role in primary hemostasis relies on its ability to interact with von Willebrand factor (vWF) in areas of high shear stress. This interaction mediates binding of platelets to the injured endothelium. While the presence of GPIb/IX is sufficient for vWF binding, this interaction is further stabilized by GPV (Canobbio et al., 2004).

1.2.5.3 Antigen epitopes

There is evidence that only a limited number of antigen epitopes is involved in AITP. It was shown that IgG fractions from many different patients react with the same peptide sequences from GPIb/IX (He et al., 1995) or GPIIb/IIIa (Bowditch et al., 1996). Additionally, antibodies from two different patients often compete for the same binding sites (Hou et al., 1995), or different patient antibodies and the same monoclonal antibodies, respectively (Varon and Karpatkin, 1983; Escher et al., 1998). This leads to the conclusion that epitopes in AITP are often either identical or closely grouped rather than spread widely over the glycoprotein complexes.

In general, antigen epitopes can be linear, consisting of sequential amino acids, or non-linear, emerging during protein folding from amino acids that do not lie closely together. Many AITP antibodies bind to cation-dependent epitopes (Fujisawa et al., 1993; Kosugi et al., 1996), which implies that correct protein folding and complex formation is crucial for autoantibody binding.

The exact localization of epitopes could be determined with different experiments: binding studies with synthetic peptides from GPIIb/IIIa (Bowditch et al., 1996) or chimeric glycoproteins (McMillan et al., 2001) showed that most epitopes on the GPIIb/IIIa complex are localized on very restricted regions in the N-terminal ligand-binding site (amino acid 1-459) of GPIIb. Similar experiments for the GPIb/IX complex localized most of the epitopes on amino acids 333-341 on the GPIbα chain (He et al., 1995).

1.2.6 Management of AITP

Since the symptoms of AITP are directly caused by the low platelet count, most therapeutic approaches follow one of two paths: either immunologic platelet destruction is to be reduced, or platelet production enhanced. The goal of all treatment strategies for AITP is to achieve a platelet count that is associated with adequate hemostasis, rather than a normal platelet count (Semple, 2002). The decision to treat is dependent on bleeding severity, bleeding risk, patient activity level, and patient preferences. It involves weighing the risk of hemorrhage against the side effects of each form of therapy.

For platelet counts above 20,000 per microliter and absence of heavy bleeding, medication is usually not recommended according to different German, Austrian and Swiss soci-

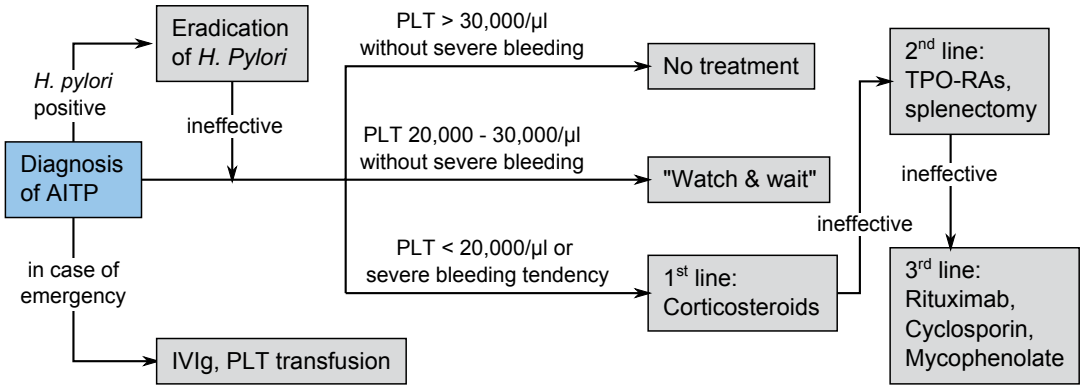

Figure 1.5: Treatment options for AITP. The sequence of treatment possibilities is along the lines of recommendations from different German, Austrian and Swiss societies for hematology. PLT = platelet, IVIg = intravenous Ig therapy, TPO-RA = thrombopoietin receptor agonist.

eties for hematology (Matzdorff et al., 2018). Only in severe cases, the first-line therapy consists of immune suppression with corticosteroids such as Prednisolone, Methylprednisolone or Dexamethasone. Approximately two-thirds of patients achieve a complete or partial response with this kind of treatment, and 10 - 30 % attain durable remission, which is defined as platelet counts higher than $100 \times 10^3/\mu l$ without medication (Rodeghiero and Ruggeri, 2014). Additionally, probable causes for a secondary AITP should be eliminated, for example by antibiotic eradication of *Helicobacter pylori* infections. Only patients requiring rapid or urgent elevation of platelet numbers receive intravenous immunoglobulin (IVIg) therapy, which accelerates the elimination of anti-platelet antibodies (Hansen and Balthasar, 2004). Platelet transfusions are usually reserved for life-threatening situations and used in conjunction with other therapies, as the patients' autoantibodies can clear donated platelets within minutes.

If those treatments do not show any improvement of the symptoms, the platelet production can be increased by thrombopoietin receptor agonists (TPO-RAs). Alternatively, splenectomy (spleen removal) is an option. The spleen is important for the clearance of antibody-coated platelets, as well as for the presentation of platelet autoantigens to immune cells (Nomura, 2016; Kuwana et al., 2002). Therefore, removal of the spleen can help in more than one way to keep more platelets in the circulation and to reduce the immune reaction.

There are different options for the third line treatment, if prior interventions were not successful. Selective B cell depletion with rituximab, a chimeric monoclonal antibody that targets B-cell surface antigens, leads to lower overall antibody production and has been shown to be effective in the treatment of AITP. Other immune-suppressant drugs such as cyclosporine or mycophenolate have the same effect. However, the side effects of those treatment options include an increased risk of infection (Shih et al., 2014).

1.3 Diagnosis of AITP

The appropriate treatment of thrombocytopenias is strongly dependent on their exact origin. However, diagnosis of AITP is mostly one of exclusion. The patient's history, physical examination, complete blood count, and peripheral blood smear must be characteristic of AITP, and other causes of thrombocytopenia must be excluded as much as possible (McMillan, 2003). Additional diagnostic measures such as bone marrow examinations may be necessary. The duration of bleeding helps to distinguish acute from chronic AITP, whereas the absence of systemic symptoms helps to rule out secondary forms and other diagnoses (Cines and Blanchette, 2002). Possible differential diagnoses that have to be eliminated include:

- other autoimmune diseases such as systemic lupus erythematosus or antiphospholipid syndrome
- immune dysregulation syndromes like common variable immunodeficiency
- malignancies such as leukemia and lymphoma
- bacterial infections (for example by *Helicobacter pylori*)
- viral infections (human immunodeficiency virus or hepatitis C virus)
- drugs such as heparin or quinidine
- single nucleotide polymorphisms in immunity-related genes

Thus, the diagnosis is strongly dependent on the clinical experience of the physician in charge (Arnold et al., 2017). On the one hand, possible cases of AITP can be overlooked and the symptoms attributed to a different cause. On the other hand, patients can be wrongly diagnosed, and treated unnecessarily for AITP while the true cause for their thrombocytopenia remains unclear (Cherif et al., 2018). As the disease is rare enough to be classified as orphan disease (Heemstra et al., 2008), most physicians are not experienced with its diagnosis and treatment. This is why patients are advised to seek out medical centers specialized in ITP (Matzdorff et al., 2018).

In order to support the clinical diagnosis of AITP and prevent misdiagnosis, a clear-cut diagnostic tool would be desirable, a biomarker specific for AITP. Ideally, this biomarker would be easily detectable and distinctly different in AITP patients and in the healthy population or in patients with other forms of thrombocytopenia. Additional benefits would be a correlation with the severity of the symptoms and a prediction for responsiveness to different treatment options (Porcelijn et al., 2017).

1.3.1 Antigen-specific tests

The obvious candidates for such a biomarker are the autoantibodies responsible for platelet destruction in AITP. Antibodies are present in the blood stream, so that sample preparation would be easy and standardized. They are well characterized and often used for diagnostic purposes, so that existing methods developed for other diseases could be adapted.

Table 1.1: Antigen-specific tests for the detection of platelet-specific antibodies.

Year	Author	Test
1978	Borne	platelet suspension immunofluorescence test (PSIFT)
1981	Schneider	platelet adhesion immunofluorescence test (PAIFT)
1984	Woods	microtiter well assay (Woods et al., 1984)
1987	McMillan	immunobead assay
1987	Kiefel	monoclonal antibody immobilization of platelet antigens (MAIPA)
1994	Kaye	antigen capture ELISA (ACE)
1995	Koksch	simultaneous analysis of specific PLT antibodies (SASPA)
1996	Kosugi	modified antigen capture ELISA (MACE)
2006	Meyer	antigen-specific particle assay (ASPA)
2007	Bakchoul	gel antigen-specific assay (GASA)
2009	Fujiwara	bead array technology for detection anti-platelet antibodies
2011	Chong	fluorescently labeled beads with recombinant β3 integrin fragments
2013	He	flow cytometric immunobead assay (FCIA)
2013	Skaik	single-antigen magnetic bead assay (SAMBA) with β3 integrin
2014	Porcelijn	luminex bead-based platelet antibody detection method (PAKLx)
2017	Metzner	platelet antibody bead array (PABA)
2017	Zhai	quantitative FCIA

Although diagnostic tests have been developed that directly determine anti-platelet autoantibodies, none of them is applicable in clinical routine testing yet (Neunert et al., 2011).

The examination of platelet autoantibodies for diagnostic purposes started around the year 1970 (Sachs, 2008), shortly after the significance of autoantibodies in the pathogenesis of AITP had been discovered. Different studies identified elevated levels of platelet-associated IgGs (PAIgGs) in nearly all AITP patients (Hegde, 1992), and they were soon thought to be the causative factor of the autoimmune response. However, it was found that PAIgGs also bound nonspecifically to platelets and were also present in healthy subjects (George, 1990), likely because platelets themselves can bind circulating IgG with their Fc receptors. The amount of PAIgGs thus proved to be a poor predictor of the disease.

In 1982, van Leeuwen et al. found that PAIgGs from many AITP patients did not bind to thrombasthenic platelets with reduced levels of GPIIb/IIIa. Since then various assays were developed to detect platelet-specific autoantibodies either bound to the platelet surface (direct tests) or free in plasma or serum (indirect tests) (Vrbensky et al., 2019). An overview over these assays is given in table 1.1.

Most tests are based on sandwich enzyme-linked immunosorbent assay (ELISA) methodologies (Heikal and Smock, 2013). They capture platelet glycoproteins from detergent lysates of whole platelets using specific monoclonal antibodies attached to a solid support (a microtiter plate or polystyrene beads). This setup is then used for the indirect detection of autoantibodies either directly from serum or plasma or eluted from the patient's

washed platelets (Lochowicz and Curtis, 2011).

The most popular among these are the antigen capture ELISA (ACE), modified ACE (MACE), and monoclonal antibody immobilization of platelet antigens (MAIPA), which use different methods for immobilization of platelet antigens (see fig. 1.6). In ACE, glycoproteins from platelet lysates are bound to the plate by specific monoclonal antibodies. Patient serum is added and bound antibodies are detected by a secondary enzyme-labeled anti-human antibody (Heikal and Smock, 2013). In the MACE (Kosugi et al., 1996) and MAIPA (Kiefel et al., 1987) methods, platelets are incubated with patient serum before detergent lysis, and thus antigen-autoantibody complexes are captured on the microtiter plate. The MAIPA method differs from MACE in that the platelets are also incubated with a glycoprotein-specific monoclonal antibody, in addition to patient serum, prior to detergent lysis. This complex is then captured onto the solid support for antibody detection. In recent years, these principles have been transferred to other more sensitive and less tedious detection methods, such as gel particle assays (Meyer et al., 2006; Bakchoul et al., 2007) or flow cytometry with fluorescent beads (He et al., 2013; Zhai et al., 2017).

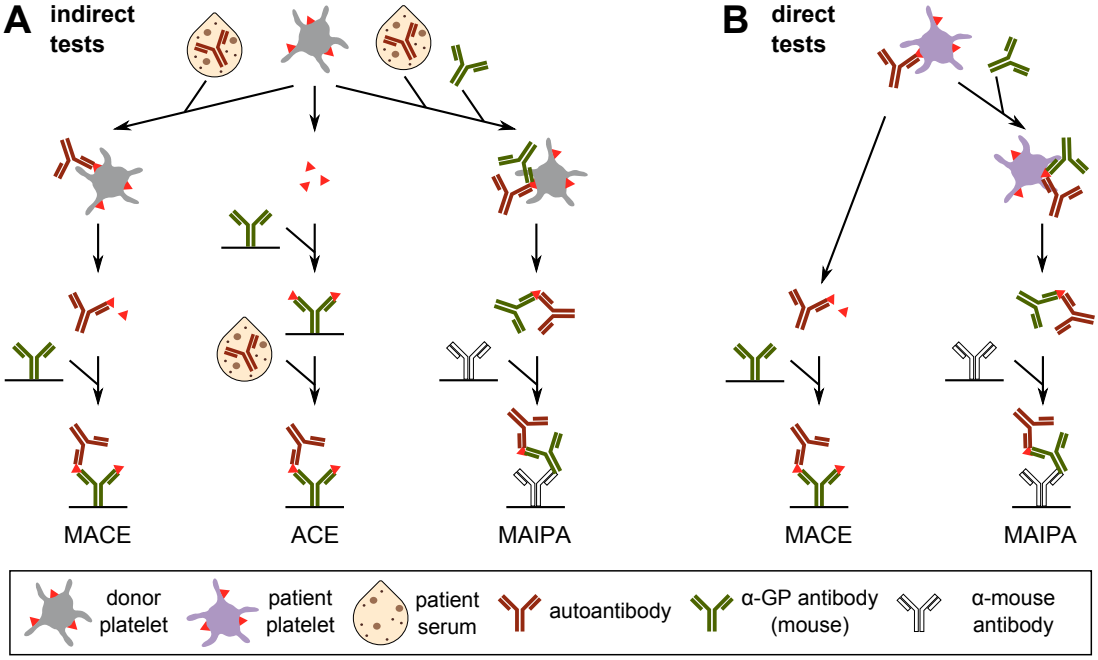

Figure 1.6: Schematic illustration of antigen capture assays. (A) Indirect assays measure the interaction of patient autoantibodies with antigens on platelets from healthy donors, whereas in (B) direct assays, autoantibodies already bound to patient platelets are determined. All assays use a labeled anti-human antibody (with fluorescence or radioactivity) as the last step for detection of bound autoantibodies. ACE = antigen capture ELISA, MACE = modified ACE, MAIPA = monoclonal antibody immobilization of platelet antigens.

Nearly all of those methods can be used for the direct detection of platelet-associated autoantibodies as well. Here, instead of donor platelets pre-incubated with patient samples, patient platelets with bound autoantibodies are used lysed and used as analyte. Direct testing is more sensitive and specific for autoantibody detection in AITP than indirect methods (Berchtold et al., 1997), but in severe thrombocytopenia it is difficult to obtain sufficient numbers of platelets.

However, some antibodies against low-density antigens or against labile epitopes that are destroyed by detergent lysis may be detected only in assays using intact platelets. A popular example is flow cytometric immunofluorescence detection (Curtis and McFarland, 2009), where patient serum is incubated with intact donor platelets, unbound antibody is washed away, and platelet-bound antibody is detected with fluorescent labeled anti-human antibodies by flow cytometry. Results indicate whether there are platelet-associated antibodies, but not the specific antibody target. These methods demonstrate superior sensitivity compared to methods using platelet lysates, but specificity is negatively impacted by the ability to detect non-pathogenic antibodies already bound to the platelets. Alternatively, some more recent assays use recombinant platelet antigen β3 integrin for capturing of autoantibodies (Bakchoul et al., 2007; Skaik et al., 2013) instead of platelet lysates.

Despite many recent developments in this field, only older tests are at least semi-routinely used. ACE, MACE and MAIPA are used for differential diagnosis of patients with unclear symptoms, whereas the other tests are not widely used (Matzdorff et al., 2018).

1.3.2 Challenges of diagnostic test development

The diagnosis of AITP faces various challenges, which inhibit the development of a universally applicable diagnostic test. As most autoantibodies recognize epitopes that are dependent on the correct folding and complex formation of the membrane antigens, it is very difficult to base the test on denatured or solubilized membrane proteins. Instead, whole platelets from either healthy donors (indirect tests) or the patients themselves (direct tests) are mostly used so far, with very few exceptions for specific platelet antigens (Bakchoul et al., 2007; Skaik et al., 2013).

However, nearly 20 % of samples from patients with AITP do not contain enough platelets for direct tests of platelet-associated antibodies (Porcelijn et al., 2017) due to their extremely low platelet count. Nevertheless, the use of platelets from healthy donors presents difficulties as well. Those platelets need to be isolated from fresh whole blood, which means that each laboratory uses a different set of platelets. Although healthy people are generally used as donors, antibody binding may be influenced by polymorphisms of platelet antigens, which can never be excluded except by genetic testing of volunteers. A study comparing eight laboratories in seven countries found acceptable reproducibility between laboratories for direct tests measuring platelet-associated autoantibodies against GPIIb/IIIa and GPIb/IX. However, poor agreement was found in detecting plasma autoantibodies to the same glycoproteins (Berchtold et al., 1997).

Furthermore, the execution of the ACE, MACE and MAIPA assays is technically demanding and time-consuming. Those procedures take one to two whole working days and are only performed in specialized reference laboratories.

Finally, even though those assays do have a good specificity, their sensitivity is quite low. The sensitivity is defined as the percentage of patients with AITP having a positive assay, whereas the specificity is the percentage of patients with "non-immune" thrombocytopenia

having negative results. This means that while a positive assay provides strong evidence for the presence of AITP, a negative assay does not necessarily rule it out (McMillan, 2003).

Recently, a systematic review and meta-analysis of different direct and indirect antiplatelet autoantibody tests evaluated their performance characteristics based on 18 preselected studies (Vrbensky et al., 2019). It found that the pooled estimates for the sensitivity of direct antiplatelet autoantibody testing for either anti-GPIIb/IIIa or anti-GPIb/IX was as low as 53 %, whereas the specificity of these tests was quite high at 93 %. For indirect testing, specificity was even higher at 96 %. However, sensitivity of indirect tests was only 18 %, which makes them inferior to direct assays. In as many as 30 to 40 % of the patients, no autoantibodies could be found at all (Cines et al., 2014).

There are many possible explanations for the poor performance of current antigen-specific tests (McMillan, 2003). Other platelet antigens or immunoglobulin subtypes than the examined may be involved in the pathogenesis, or no autoantibodies at all but other immunologic mechanisms. All studies used a process of exclusion for diagnosis, therefore there might be different reasons altogether for the low platelet count. As many as one in seven thrombocytopenic patients are initially misdiagnosed (Vrbensky et al., 2019). Finally, even if the initial diagnosis of AITP had been correct, patients could have received therapy prior to the blood collection that would suppress autoantibody levels.

Technical or sensitivity problems with existing assays can never be excluded, but one factor is common to all of the presented assays: all examined platelet antigens are membrane proteins, which have to be removed from their native environment for detection of bound autoantibodies. Whether by detergent lysis of whole platelets or by isolation of recombinant protein, the protein structure is likely to be impaired. In order to improve testing for anti-platelet autoantibodies, it would be necessary to find a way to substitute the whole platelet cells either from the patients themselves or from healthy donors, while maintaining the advantage of presenting a native-like structure for antibody binding.

1.4 Examination of membrane proteins

All platelet glycoprotein receptors are transmembrane proteins. In order to fulfill their task of connecting the intracellular and extracellular spaces of platelets, they span the plasma membrane and are thus amphipathic in nature. The combination of hydrophilic intra- and extracellular domains with hydrophobic transmembrane domains makes them vulnerable upon isolation from their native membranes. They tend to unfold and aggregate in aqueous solutions, which makes them incompatible with most standard laboratory methods developed for soluble proteins. Additionally, like most membrane proteins they need the interaction with the lipid bilayer for proper protein structure, folding, aggregation, dynamics, stability, orientation, and function (Dürr et al., 2012).

1.4.1 Membrane model systems

Transmembrane proteins are strongly underrepresented regarding biophysical investigations, structure determination and other *ex vivo* studies. Different solutions to this problem have been developed over the years, from very simple to more complex, in order to mimic the membrane environment and stabilize membrane proteins isolated from their cellular origin. Common examples are detergent micelles, bicelles or liposomes, as well as solid-supported planar phospholipid bilayers (see fig. 1.7). All of these techniques have their own advantages and limitations (Seddon et al., 2004).

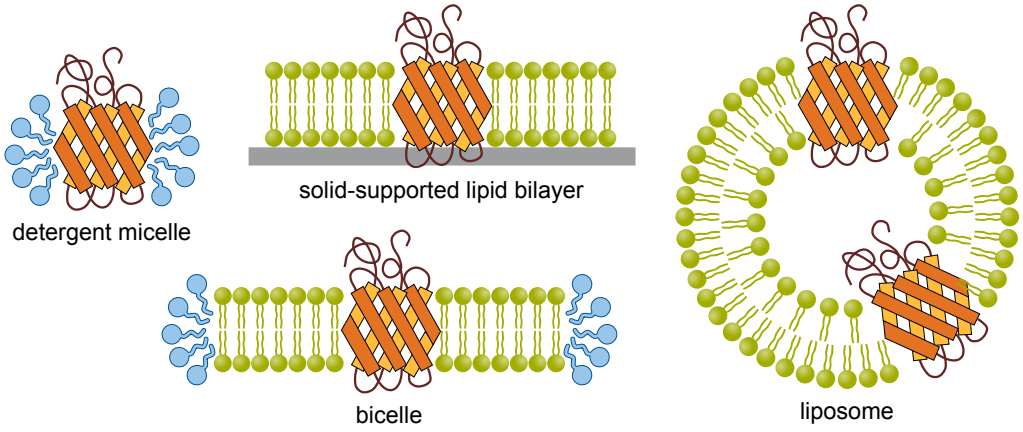

Figure 1.7: Schematic representation of established membrane model systems. Detergent molecules are shown in blue, phospholipids in green, and transmembrane proteins in orange.

The simplest way to protect the hydrophilic parts of transmembrane proteins from the aqueous environment is by addition of detergents in a high enough concentration for micelles to develop. While their hydrophilic heads are exposed to solvent, their hydrophobic tails are directed towards the protein. However, membrane proteins are only rarely functional in detergent solutions, mostly the contact with detergent leads to at least partial unfolding (Garavito and Ferguson-Miller, 2001). Additionally, the micellar phase absorbs and scatters light, which makes them unsuitable for many optical methods.

Liposomes are bigger particles consisting of phospholipid bilayers, which resemble the cellular membrane more closely. However, their membrane is curved, in contrast to the nearly planar plasma membrane on whole cells. Besides, they are unstable and difficult to synthesize in a reproducible manner, and either the intra- or extracellular domain of the inserted membrane protein is not accessible for analysis (Seddon et al., 2004).

Bicelles are small phospholipid bilayers encapsulated and solubilized by a detergent micelle, which shields the hydrophobic center of the bilayer from surrounding solvent molecules. They are much smaller than liposomes, and can be used in experiments where the larger vesicles are not an option. The generation of bicelles is quite complicated and depends on the exact ratio of phospholipid, detergent and protein as well as temperature and hydration level. They are unstable and can dissociate easily if the conditions change (Dürr et al., 2012).

Solid-supported lipid bilayers are planar structures sitting on a solid support. Because

of this, only the upper side of the bilayer is exposed to the surrounding solution. In contrast, the lower face is separated only by a very small hydrophilic gap from the support (Richter et al., 2006). For this reason, membrane proteins with larger hydrophilic domains do not find enough space and tend to denature. The advantages of supported bilayers however include their stability and the formation of a planar surface ideal for example for microscopy (Castellana and Cremer, 2006).

Taken together, none of these established techniques provides a native-like lipid bilayer with easy handling, reliable protein stabilization, full accessibility to both intra- and extracellular protein domains and compatibility with common analytical methods used in routine diagnostics (Mak et al., 2017).

1.4.2 Nanodisc technology

Around the year 2000, a new model membrane system was developed, which overcomes many of the limits of previous systems (Bayburt et al., 1998). In their studies of high-density lipoproteins (HDL), Stephen Sligar and his group stumbled upon a unique property of the protein Apolipoprotein A-1 (ApoA-1). This protein is involved in the transport of cholesterol esters in the blood plasma (Atkinson and Small, 1986). During synthesis, HDL particles first have a discoidal configuration which is then transformed into a spheroidal shape as cholesterol esters are inserted. The group found a way to arrest this process in the discoidal phase by genetic modification of ApoA-1. They called the resulting synthetic construct membrane scaffold protein (MSP), and the resulting particles nanodiscs (NDs) (Denisov et al., 2004).

1.4.2.1 Structure of nanodiscs

Nanodiscs are round slices of phospholipid bilayer, similar to bicelles, but overcoming their problems in matters of stability and ease-of-handling. Figure 1.8 shows a schematic illustration, clearly showing the stabilizing double belt of MSP around the discs. The scaffold protein is an amphipatic protein with a mostly α-helical structure (Nath et al., 2007). The hydrophobic amino acid residues on the inside of this belt interact with the fatty acid residues of the phospholipid bilayer, whereas the hydrophilic outside of the α-helices is in contact with the surrounding solvent. The thickness of the phospholipid bilayer is about 5.7 nm (Bayburt and Sligar, 2002), which corresponds to the dimensions of natural bilayers in the cellular plasma membrane (Shaw et al., 2004).

The nanodisc diameter depends on the MSP variant used. The longer the scaffold protein, the bigger the resulting nanodisc will be (Hagn et al., 2013; Ritchie et al., 2009). Usually, nanodiscs with a diameter between 7 and 17 nm are used, into which many different kinds of membrane proteins can be integrated. Their size ranges from small proteins with only one transmembrane domain (Tzitzilonis et al., 2013) via G-protein coupled receptors (Sun et al., 2019; Leitz et al., 2006) and beta-barrel proteins (Raschle et al., 2009; Hagn et al., 2013) to complete protein complexes (Yan et al., 2011) and even whole reaction chains (Duan et al., 2004; Morrissey et al., 2008).

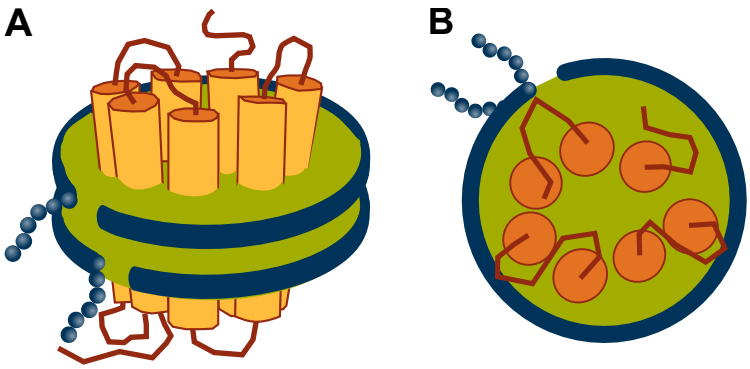

Figure 1.8: Structure of nanodiscs. Schematic illustration of nanodisc in (A) side view and (B) top view. The phospholipid bilayer is shown in green, the two copies of MSP (with 6x-His-tags) in blue, and an inserted transmembrane protein in orange.

1.4.2.2 Nanodisc applications

Publications involving nanodiscs have increased considerably since the early 2000s. The initial focus on structural studies of nanodiscs with and without incorporated membrane proteins has been complemented by functional and interaction studies in recent years. Manipulation and examination of membrane proteins is possible by all methods developed for soluble proteins, such as the following examples:

- **Protein isolation and purification:**
  - size exclusion chromatography (SEC) (Kawai et al., 2011; Hagn et al., 2018)
  - affinity chromatography (Akkaladevi et al., 2013; Cai et al., 2017)
  - density gradient centrifugation (Bayburt et al., 2006)
- **Structural studies:**
  - nuclear magnetic resonance spectroscopy (Raschle et al., 2009; Tzitzilonis et al., 2013)
  - negative stain / cryo-electron microscopy (Sheng et al., 2010; Katayama et al., 2010)
  - atomic force microscopy (Bayburt et al., 2002)
  - circular dichroism (Bayburt et al., 2006)
  - dynamic light scattering (Inagaki et al., 2012)
  - sedimentation velocity (Inagaki et al., 2012)
  - small angle x-ray scattering (Ishchenko et al., 2017)
  - analytical ultracentrifugation (Inagaki et al., 2012; Johnson et al., 2014)
  - electron paramagnetic resonance spectroscopy (Gao et al., 2012)
  - single-molecule force spectroscopy (Roos et al., 2012)
- **Interaction studies:**
  - mass spectrometry (Marty et al., 2013)
  - peptide fingerprinting (Roy et al., 2015)
  - surface plasmon resonance (SPR) spectroscopy (Proverbio et al., 2013; Trahey et al., 2015; Ritchie et al., 2011)

  - co-immunoprecipitation (Borch et al., 2011)
  - fluorescence correlation spectroscopy (Gao et al., 2012; Ly et al., 2014)
  - bio-layer interferometry (Sharma and Wilkens, 2017)
  - enzyme-linked immunosorbent assay (ELISA) (Sheng et al., 2010; Yan et al., 2011)
  - total internal reflection fluorescence (Raschle et al., 2015)
- **Protein functionality:**
  - ATPase assay (Taylor et al., 2001; Ritchie et al., 2011)
  - kinase activity assay (Roy et al., 2015)
  - radioligand binding assay (Leitz et al., 2006)
  - NADPH consumption assay (Duan et al., 2004)

The application spectrum of nanodiscs has been further broadened by the development of nanodisc libraries (Marty et al., 2013; Roy et al., 2015; Shirzad-Wasei et al., 2015). Here, the whole membrane proteome of a cell is incorporated into nanodiscs without prior protein isolation, and is thus available for proteomic studies. Other novel applications include the development of vaccines based on nanodiscs (Kuai et al., 2017), drug discovery (Wilcox et al., 2015) as well as their use as a therapeutic for the *in vivo* antigen-specific reduction of pathogenic autoantibodies in the mouse model (Sheng et al., 2010).

The structure and behavior of nanodiscs themselves have been extensively studied as well. The molecular dynamics and phase transitions of the lipid bilayer in nanodiscs were examined, for example by solid-state NMR, and found to closely resemble those in the original plasma membrane (Mörs et al., 2013). The lipid composition of the nanodiscs can be adapted as desired, which allows the investigation of the interplay between membrane proteins and their surrounding lipids (Morrissey et al., 2008).

1.4.2.3 Nanodiscs for diagnostic assays

The special characteristics of nanodiscs allow the examination of membrane proteins with an unprecedented simplicity and practicability, and make them especially suitable for diagnostic purposes. As nanodiscs are completely compatible with hydrophilic solutions, methods developed for soluble proteins can easily be adapted to nanodiscs. Their uncomplicated generation and handling, as well as their stability under different conditions (Denisov et al., 2004), makes them convenient for routine applications.

In the context of AITP diagnosis, a native-like protein structure is of utmost importance. This is ensured by an authentic imitation of the natural phospholipid bilayer of the cellular plasma membrane, in a planar configuration with typical phase transitions (Shaw et al., 2004). The native structure of many incorporated membrane proteins has been demonstrated (Bayburt and Sligar, 2010), amongst others that of the two platelet GP receptors GPIIb/IIIa and GPIb/IX (Ye et al., 2010; Yan et al., 2011). Figure 1.9 shows schematic illustrations of those receptors incorporated into nanodiscs.

The nanodisc technology facilitates assay development mostly due to two characteristics of nanodiscs. Firstly, proteins that are incorporated into nanodiscs are accessible from both

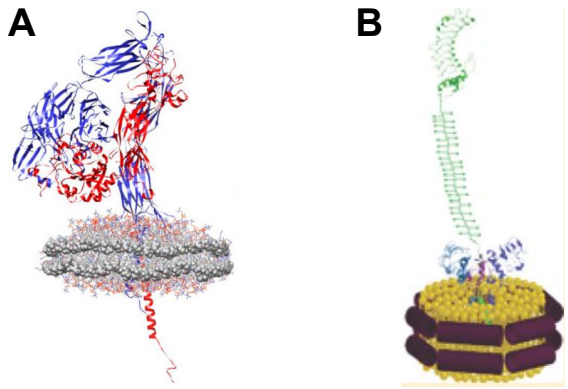

Figure 1.9: Schematic illustration of platelet GP receptors incorporated into nanodiscs. (A) GPIIb/IIIa from Ye et al. (2010) and (B) GPIb/IX from Yan et al. (2011).

sides. This allows for example capturing of target proteins at the intracellular domains, while the extracellular domains remain free for analyte binding. Secondly, the membrane scaffold proteins can be easily modified in different ways, for example by addition of affinity tags, which allows the use of methods developed for modified proteins without alteration of the target protein itself (Schuler et al., 2013).

1.5 Aim of this thesis

The aim of this PhD thesis was to develop a new assay format for the detection of autoantibodies in AITP. The disadvantages of previous assays, most of all the need for whole platelet cells, should be circumvented and the assay made less complicated and time-intensive. The new assay should be easy to perform, stable, reliable, while performing at least as well as comparable methods. As most relevant platelet antigens in AITP, the glycoprotein receptors GPIIb/IIIa and GPIb/IX were chosen as example antigens in this project.

As a source for platelet antigens not only human donor platelets were given consideration, but recombinant expression of both glycoprotein complexes in human embryonic kidney (HEK)-293 cells should be established as well. Here, the aim was production of the respective membrane proteins in large amounts, while maintaining a native-like protein structure. At the same time, the proteins should receive fluorescent tags for easier handling and to facilitate later assay development. Characterization of the cells should be conducted mostly in respect to protein expression and functionality.

The glycoprotein receptors should be reconstituted and stabilized with the nanodisc technology in a native-like membrane environment. As raw material for the generation of nanodiscs, both human platelets and cultured cells expressing the recombinant proteins were to be used and compared. Protein incorporation into nanodiscs should be based on established protocols. However, the process should be optimized for gentle protein treatment, efficient protein incorporation and ease of handling. The hands-on-time was another important factor, especially in regard to a possible further application as a routine test. The resulting nanodiscs should be characterized in respect to their size, uniformity and protein content. The correct functionality of incorporated proteins was to be verified in order to ensure that proteins showed in fact native-like behavior.

A diagnostic assay principle for the detection of AITP-autoantibodies should be established in a sandwich ELISA format, with optimization of all crucial steps and extensive testing with monoclonal antibodies. A low limit of detection was of importance, as autoantibodies are present at low concentrations, as well as stability and possible storage of ELISA plates. The best assay set-up should be evaluated by proof-of-concept experiments with a small number of patient samples, as well as adapted for maximal signal difference between positive and negative samples. Finally, the optimized assay should be used to compare a patient cohort with AITP to healthy subjects. The results should be evaluated statistically and discussed for plausibility and correlation with prior characterization of the samples.

2 Material and methods

2.1 Material, equipment and software

Antibodies and nanobodies

Primary antibody [clone]	host species	supplier
anti-basigin/CD147 [109403]	mouse	R&D Systems MAB972-SP
anti-GFP [E385]	rabbit	Abcam ab32146
anti-GPIbα [EPR6995]	rabbit	Abcam ab134087
anti-GPIbβ	rabbit	Abcam ab96565
anti-GPIX [EP52494]	rabbit	Abcam ab133573
anti-GPIb/IX complex [SZ-1]	mouse	Beckman Coulter IM0538
anti-GPIIb [EPR4330]	rabbit	Abcam ab134131
anti-GPIIIa [ERP17507]	rabbit	Abcam ab179473
anti-GPIIb/IIIa complex [AP-2]	mouse	Kerafast EBW105
anti-histidine	mouse	GE Healthcare 28-9950-56
anti-PEG tag + HRP	mouse	GenScript A01795
anti-Penta-His	mouse	Qiagen 34660
anti-RFP	rabbit	GenScript A00682
GFP VHH nanobody	alpaca	ChromoTek gt-250
RFP VHH nanobody	alpaca	ChromoTek rt-250
Secondary antibody	**host species**	**supplier**
anti-human IgG + HRP	rabbit	Dako P0214
anti-human IgG + HRP	rabbit	Acris R1333HRP
anti-mouse IgG H&L + HRP	goat	Abcam ab97023
anti-rabbit IgG H&L + HRP	donkey	Abcam ab16284
anti-rabbit IgG + HRP	donkey	GE Healthcare NA934V

Other proteins and enzymes

Name of protein / enzyme	purpose	supplier
AvaI	restriction enzyme	NEB R0152
Bovine serum albumin (BSA)	blocking reagent	Merck A3059

FastAP Alkaline Phosphatase	inhibition of re-ligation	Thermo EF0654
HindIII	restriction enzyme	Thermo ER0501
Human serum albumin (HSA)	blocking reagent	Merck A1653
Fibrinogen	GPIIb/IIIa ligand	Merck 341576
MSP1E3D1	Membrane Scaffold Protein	Merck M7074
MSP1E3D1	Membrane Scaffold Protein	own production
peqGOLD Taq polymerase	DNA polymerase	VWR PEQL01-1000
Skim milk powder	blocking reagent	Merck 70166
SspI	restriction enzyme	Thermo ER0771
T4 DNA Ligase	fusion of DNA ends	Thermo EL0011
von Willebrand factor reagent	GPIb/IX ligand	Roche Dynabyte

Lipids and detergents

Detergent	supplier
n-Dodecyl-β-D-Maltoside (DDM)	Thermo 89903
n-Dodecyl-phosphocholine (FC-12)	Cube 16021
Octyl-β-D-glucopyranoside (OG)	Merck 09882
Sodium Dodecyl Sulfate (SDS)	Merck 71725
Triton X-100	Merck 93426
Tween 20	Merck P1379

Lipid	supplier
L-α-Phosphatidyl-choline (PC)	Merck P2772
1,2-dioleoyl-sn-glycero-3-phosphoethanol-amine-N-[methoxy(polyethylene glycol)-2000] (PEG-PE)	Avanti 880120C

DNA plasmids

Name of plasmid	GP inserts	supplier
pEF1-alpha-IIb	GPIIb	Addgene 27288
pcDNA3.1-beta-3	GPIIIa	Addgene 27289
pcDNA3.1+/C-(K)DYK:GPIBA	GPIbα	Genscript NM-000173.6

pcDNA3.1+/C-(K)DYK:GPIBB	GPIbβ	Genscript NM-000407.4
pcDNA3.1+/C-(K)DYK:GP9	GPIX	Genscript NM-000174.4

Name of target vector	fluorescence tag	supplier
pcDNA3 mCherry LIC cloning vector	mCherry	Addgene 30125
pcDNA3 GFP LIC cloning vector	mCherry	Addgene 30127

Cell lines

E. coli cell strains	genotype	supplier
DH5α	*fhuA2 lac(del)U169 phoA glnV44 ϕ80' lacZ(del)M15 gyrA96 recA1 relA1 endA1 thi-1 hsdR17*	Addgene
NEB5α	*fhuA2 (argF-lacZ)U169 phoA glnV44 fhuA2 (a80a(lacZ)M15 gyrA96 recA1 fhuA2 (relA1 endA1 thi-1 hsdR17*	NEB C2987I

Human cell lines	recombinant expression of	supplier
HEK-293 (wt)	-	DSMZ ACC-305
HEK-293 IIb/IIIa	GPIIb-mCherry + GPIIIa-eGFP	see section 3.2.3
HEK-293 Ib/IX	GPIbα-mCherry + GPIbβ-eGFP + GPIX	see section 3.2.3

Cell culture media, antibiotics and other medium supplements

Substance	purpose	cell lines	supplier
Agar	for agar plates	*E. coli*	MP 194615
Ampicillin	antibiotic	*E. coli*	Roth HP62.1
Tryptone	amino acid source	*E. coli*	VWR J859
Yeast extract	nutrient source	*E. coli*	VWR J850
Dimethyl sulfoxide	freezing supplement	HEK-293	Serva 20385
DMEM, high glucose, GlutaMAX^{TM}, pyruvate	basic medium	HEK-293	Thermo 31966021

DPBS	wash buffer	HEK-293	Merck D8537
EDTA 0.5 M	for cell sorting	HEK-293	Thermo 25200
FBS "Good Forte"	nutrient source	HEK-293	Pan Biotech P40-47500
G418	antibiotic	HEK-293	Roth CP11.1
HEPES 1 M	for cell sorting	HEK-293	Thermo 15630
Penicillin-Streptomycin	antibiotic	HEK-293	Thermo 15140
Trypan blue (0.4%)	cell counting	HEK-293	Thermo 15250061

Chemicals

Name of chemical	supplier
Acetic acid 100 %, p.a. (glacial)	Merck 1.00063
Acrylamide/Bis Solution 40 %, 37.5:1	Bio-Rad 161-0148
Ammonium persulfate (APS) $\geq$ 98 %, p.a.	Roth 9592.2
Ethanol gradient grade	Merck 1.11727
Ethidium bromide 1%	Roth 2218.2
Glycerol, p.a.	Merck 1.04092
Glycine	Merck 1.04169
Guanidine hydrochloride $\geq$ 99 %	Merck G4505
Hydrochloric acid (HCl) 37 %, p.a.	Roth 4625.1
Imidazole $\geq$ 99 %, p.a.	Roth 3899.4
Magnesium chloride hexahydrate $\geq$ 99 %, p.a.	Roth 2189.2
Methanol hypergrade for LC-MS	Merck 1.06035
Paraformaldehyde 4 %	Merck 1.00496
Poly(ethylene glycol) 3,350	Merck P4338
Polyvinylpyrrolidone 10,000	Merck PVP10
Potassium phosphate (KH_2PO_4), p.a.	Merck 104877
Potassium chloride (KCl) $\geq$ 99.5 %, p.a.	Roth 6781.3
Sodium chloride (NaCl) $\geq$ 99.5 %, p.a.	Merck 1.06404
Sodium hydroxide (NaOH), p.a.	Merck 1.06498
Disodium hydrogen phosphate (Na_2HPO_4), p.a.	Merck 30435
Sulfuric acid (H_2SO_4) 95-97 %, p.a.	Merck 1.00731
Tetramethylethylenediamine (TEMED)	BioRad 161-0800
Tricine (N-Tris-(hydroxymethyl)-methyl-glycin)	Roth 6977.2
Tris (Tris(hydroxymethyl)aminomethane), p.a.	Merck 1.08382
Trisodium citrate 3.2 %	Sarstedt 05.1071

Kits, reagents and stains

Name of product	supplier
3,3',5,5'-Tetramethylbenzidine (TMB)	Merck T8665
6x DNA gel loading dye	Merck G7654
Amine coupling kit	GE Healthcare BR100050
Bromophenolblue	Merck 108122
High MW gel filtration calibration kit	GE Healthcare 28403842
His capture kit	GE Healthcare 28995056
Monarch DNA Cleanup kit	NEB T1030
Monarch Miniprep Kit	NEB T1010
Protease Inhibitor Mini Tablets, EDTA free	Thermo A32955
Quick Start Bradford 1x Dye Reagent	Bio-Rad 500-0205
Quick Start BSA standard set	Bio-Rad 500-0207
Rainbow Molecular Weight Marker	GE Healthcare RPN800E
Rot-Blue Quick Gel stain	Roth 4829.2
SuperSignal West Dura WB substrate	Thermo 34075
TBE buffer 10x	Thermo 15581044

Consumable materials

Product	supplier
6-well cell culture plate	TPP 92406
96-well PolySorp flat bottom plate	VWR 735-0131
96-well tissue culture test plate	TPP 92696
Amicon ultra centrifugal filters (MWCO 10+30kDa)	Merck UFC5030
Bio-Beads SM-2 Adsorbent	Bio-Rad 152-8920
Cryo-Tubes	Greiner 122263
Fluorescence spectroscopy cuvettes	Perkin Elmer
HisPur Ni-NTA Spin Columns, 0.2 ml	Thermo 88224
Immobilon-P PVDF Membrane	Merck IPVH00010
Mini Trans-Blot Filter paper	Bio-Rad 170-3932
Neubauer counting chamber	Brand 717805
SPR Sensorchip CM5	GE Healthcare 29149604
Superdex 200 10/300 GL column	GE Healthcare 28990944
T25 cell culture flask	TPP 90026
T75 cell culture flask	TPP 90076

T125 cell culture flask	TPP 90151
Reaction tubes 1.5 ml	Sarstedt 72.690.001
Reaction tubes 2 ml	Sarstedt 72.695.500
Reaction tubes 15 ml	Greiner 188271
Reaction tubes 50 ml	Greiner 227261

Instruments

Instrument	supplier
agarose gel chamber	Eurogentec Mupid-exU
agarose gel imager	LTF Labortechnik
ÄKTA FPLC system	GE Healthcare
- Fraction collector	- Frac-900
- UV monitor	- UPC-900
- pump system	- P-920
analytic balance	Sartorius AC 120S
automated hematology analyzer	Sysmex XT 2000i
centrifuges	Thermo Megafuge 1.0R
	Hettich Rotina 360R
	Hettich Rotina 420R
	Eppendorf 5415 R
cell culture microscope	Leica Microsystems DM IL LED
cell culture workbench	Envair eco safe comfort
CO_2 incubator	Binder C150 (E2)
cryo freezing container	Thermo Mr. Frosty
ELISA plate reader	BioTek ELx 808
fluorescent microscope	Thermo EVOS FL
luminescence spectrometer	Perkin Elmer LS 50 B
magnetic stirrer	IKA Combimag RCH
PCR thermocycler	Thermo GeneAmp PCR System 9700
pH meter	Sartorius PB-11-P11
power supply	Bio-Rad PowerPac HC
SDS PAGE system	Bio-Rad Mini-PROTEAN tetra
spectrophotometer	Thermo NanoDrop 2000
SPR instrument	GE Healthcare Biacore X100
Thermomixer	Eppendorff comfort
ultrasound sonicator	Bandelin Sonorex Super 10P
water bath	Memmert WNB 10

Western Blot system	Bio-Rad Mini trans tank
Western Blot imager	INTAS Advanced

Software

Software	purpose	supplier
ApE 2.0.53c	editing of DNA sequences	W. Davis (Utah University)
Biacore X100 control	control of Biacore X100	GE Healthcare
Biacore evaluation	evaluation of SPR experiments	GE Healthcare
ChemoStar Imager	control of INTAS WB imager	INTAS Science Imaging
FL Winlab	control of spectrofluorometer	Perkin Elmer
FlowJo V10	evaluation of flow cytometry	Becton Dickinson
Gimp	generation of figures	Free Software Foundation
Inkscape	generation of figures	Free Software Foundation
Microsoft Excel 2010	data analysis	Microsoft
MiKTeX 2.9	manuscript composition	Free Software Foundation
NanoDrop 2000 software	control of NanoDrop 2000	Thermo
R i386 3.5.0	data analysis	Free Software Foundation
R Studio	data analysis	Free Software Foundation
Texmaker 4.5	manuscript composition	Free Software Foundation
Unicorn 4.0	control of ÄKTA FPLC system	GE Healthcare
Zotero	literature management	Roy Rosenzweig Center

Suppliers

All materials, equipment, instruments and software were purchased from the following suppliers:

- Abcam (Cambridge, MA, USA)
- Acris (Rockville, MD, USA)
- Addgene (Watertown, MA, USA)
- Avanti Polar Lipids (Alabaster, AL, USA)
- Bandelin (Berlin, Germany)
- Beckman Coulter (Brea, CA, USA)
- Becton Dickinson (Franklin Lakes, NJ, USA)
- Binder (Tuttlingen, Germany)
- Bio-Rad (Hercules, CA, USA)
- Biotek (Bad Friedrichshall, Germany)
- Brand (Wertheim, Germany)

- ChromoTek (Planegg-Martinsried, Germany)
- Cube Biotech (Monheim, Germany)
- Dako (Glostrup, Denmark)
- DSMZ - German Collection of Microorganisms and Cell Cultures, Leibniz Institute (Braunschweig, Germany)
- Eppendorf (Hamburg, Germany)
- Eurogentec (Lüttich, Belgium)
- Free Software Foundation (Boston, MA, USA)
- GE Healthcare (Little Chalfont, GB)
- GenScript (Piscataway, NJ, USA)
- Greiner Bio-One (Kremsmünster, Austria)
- Hettich (Tuttlingen, Germany)
- IKA (Staufen im Breisgau, Germany)
- Intas Science Imaging Instruments (Göttingen, Germany)
- Kerafast (Boston, MA, USA)
- Leica Microsystems (Wetzlar, Germany)
- LTF Labortechnik, (Wasserburg, Germany)
- Memmert (Schwabach, Germany)
- Merck (Darmstadt, Germany)
- Microsoft (Redmond, WA, USA)
- MP Biomedicals, LLC (Santa Ana, CA, USA)
- New England Biolabs (Ipswich, MA, USA)
- Pan Biotech (Aidenbach, Germany)
- Perkin Elmer (Waltham, MA, USA)
- Qiagen (Hilden, Germany)
- R&D Systems (Minneapolis, MN, USA)
- Roche(Basel, Switzerland)
- Roth (Karlsruhe, Germany)
- Sarstedt (Nümbrecht, Germany)
- Sartorius (Göttingen, Germany)
- Serva (Heidelberg, Germany)
- Thermo Fisher Scientific (Waltham, MA, USA)
- TPP (Trasadingen, Switzerland)
- VWR (Radnor, PA, USA)

2.2 Methods for nanodisc generation from platelets

2.2.1 Platelet isolation from whole blood

The platelet isolation protocol was modified from Crawford et al. (1992). Approximately 30 ml of human blood were collected into 5-ml monovette tubes (Sarstedt) containing 0.5 ml of a trisodium citrate solution. The first few milliliters of blood had to be discarded because they could be contaminated with tissue factor and thrombin, which can activate platelets.

The citrate blood was transferred to two 15-ml tubes and centrifuged immediately at 100 x g for 30 min at 20 °C (soft spin) to obtain platelet-rich plasma (PRP, see fig. 2.1). The PRP was transferred to a new tube, then a second soft spin was applied. The PRP should not be red any more at this stage. It was then split into 1-ml fractions into new 1.5 ml-tubes and mixed with 500 µl of platelet preparation buffer.

PBS (pH 7.4)	2.6 mM	KCl
	138 mM	NaCl
	10 mM	Na_2HPO_4
	1.8 mM	KH_2PO_4
platelet preparation buffer	10 ml	PBS
	1 ml	trisodium citrate
	1x	protease inhibitor mini tablet
platelet storage buffer	4.5 ml	platelet preparation buffer
	0.5 ml	glycerol

To obtain a platelet pellet, the PRP was centrifuged at 1800 x g for 10 min at 20 °C (hard spin). The pellet was then washed in 500 µl of platelet preparation buffer and a second hard spin was applied. The resulting pellet was resuspended in 200 µl of platelet storage buffer and stored at -80 °C.

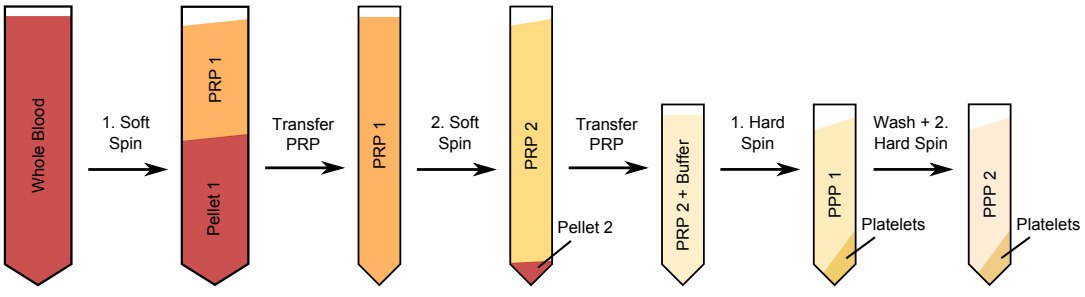

Figure 2.1: Schematic illustration of the platelet preparation, from whole blood to the final platelet pellet, which was then resuspended and frozen. PRP = Platelet Rich Plasma; PPP = Platelet Poor Plasma.

The cell content of whole blood and platelet fractions was examined by flow cytometry with a XT 2000i Automated Hematology Analyzer (Sysmex). In a complete blood count,

numbers of red blood cells, white blood cells and platelets as well as the hematocrit were determined automatically.

2.2.2 Nanodisc generation from purified lipids or human platelets

The preparation of nanodiscs from different kind of raw material follows a common principle: the purified Membrane Scaffold Protein (MSP) is mixed with a detergent solution containing phospholipids, membrane proteins, membrane lysate, whole cell lysate, or a mixture of those. By removal of the detergent, self-assembly of nanodiscs is induced. The resulting nanodiscs can be purified by different techniques or used directly without prior purification. Nanodiscs can be stored up to one week at 4 °C.

For all experiments in this thesis, nanodiscs prepared from 250 µg of MSP1E3D1 (with a molecular weight of 32.6 kDa) were filled up to 1000 µl final volume. As for each nanodisc two copies of MSP are necessary, this resulted in 3.8 nmol nanodiscs, or a final concentration of about 4 µM. Only for nanodiscs that were subjected to purification, the final volume was reduced to 500 µl, and the concentration thus 8 µM.

2.2.2.1 Preparation of purified phospholipids

The phospholipid species used in this thesis are L-α-phosphatidylcholine (PC) and the stabilizing agent 1,2-dioleoyl-sn-glycero-3-phosphoethanolamine-N-[methoxy(polyethylene glycol)-2000] (PEG-PE). Both had to be dissolved in a detergent solution of octyl-β-D-glucopyranoside (OG) in order to allow incorporation into nanodiscs. The different substances were prepared as follows:

- **PC:** 50 µl of PC (100 mg/ml in chloroform) were dried in a glass tube first with nitrogen and then under vacuum. The resulting milky layer in the tube was then dissolved in 250 µl of detergent solution(6 % (w/v) OG in H_2O) by heating in a water bath to 37 °C and sonification. The resulting 20 mg/ml phosphatidylcholine solution could be stored for one week at 4 °C or frozen at -80 °C.
- **PEG-PE:** PEG-PE (25 mg/ml in chloroform) was dried first with nitrogen and then under vacuum, then dissolved in 6 % (w/v) OG in H_2O to a final concentration of 25 mg/ml. The PEG-PE solution was stored at -80 °C and could be thawed and frozen repeatedly.

2.2.2.2 Nanodiscs from purified lipids

Nanodiscs containing only purified lipids and MSP were used as negative control, as they do not contain any platelet membrane proteins. For their generation, 175 µg of dissolved PC were mixed with 250 µg of MSP1E3D1, corresponding to a molar ratio of 227 nmol PC to 7.8 nmol MSP. This mixture was filled up with PBS to a final volume of 300 µl and added to 50 mg of prepared Bio-Beads SM-2 (Bio-Rad), which had been soaked in 700 µl PBS for at least 30 min under gentle agitation. After incubation for 1 hour at

room temperature (RT) while shaking, the assembled nanodiscs were removed from the Bio-Beads and filled up with PBS to 1000 µl.

2.2.2.3 Platelet nanodiscs for protocol comparison

Frozen platelets prepared from 900 µl whole blood (prepared as described in section 2.2.1) were thawed and centrifuged (2000 x g, 10 min, 20 °C) in order to remove the storage buffer. The resulting cell pellet was then used for nanodisc generation with and without prior membrane isolation. For membrane purification, the pellet was resuspended in 1 ml of cold sonication buffer. The platelet suspension was then sonicated on ice for 10 s at maximum power. The suspension was centrifuged (1200 x g, 15 min, 4 °C), the supernatant was removed and saved and the pellet of unlysed cells and large cell fragments was resuspended in cold sonication buffer. A further 10 s sonication was applied and, after centrifugation, the two supernatants were pooled and centrifuged at 1200 x g for 10 min at 4 °C to deposit any larger aggregates. This pooled homogenate was transferred to polycarbonate centrifuge tubes and ultracentrifuged at 100,000 x g at 4 °C for 45 min. The membrane pellet was resuspended with 100 µl of sonication buffer and stored at 4 °C overnight.

sonication buffer (pH 7.2)	340 mM	Sorbitol
	10 mM	HEPES
	1x per 10 ml	protease inhibitor tablet

For nanodisc generation, whole platelets or platelet membranes prepared from 900 µl whole blood were lysed with 100 µl PBS with 1 % (v /v) Triton X-100 and then mixed with 250 µg of MSP1E3D1 and 40 µg of PEG-PE. The reaction mixture was incubated with 30 mg of Bio-Beads (pre-equilibrated with 800 µl PBS at RT for at least 30 min) for 60 min at RT while shaking. The resulting nanodiscs were purified by immobilized metal ion affinity chromatography (IMAC) with Ni-NTA columns and analyzed by size-exclusion chromatography (SEC).

2.2.2.4 Nanodiscs from whole platelets

After protocol optimization, the following approach was considered best for generation of nanodiscs from whole platelets (see fig. 2.2). During the optimization process, different steps were adapted as described in the results section.

Frozen platelet fractions were thawed and centrifuged (2000 x g, 10 min, 20 °C). The resulting cell pellet was lysed in 200 µl of a 1 % (v/v) OG solution in PBS and mixed until it became clear. The cell suspension was incubated at room temperature for 10 min while shaking, then centrifuged (30 min, 16,100 x g, 20 °C) to remove remaining cell debris.

The protein concentration of the 1:10 diluted supernatant was determined by Quick-Start Bradford protein assay (Bio-Rad) according to the manufacturer's instructions. All

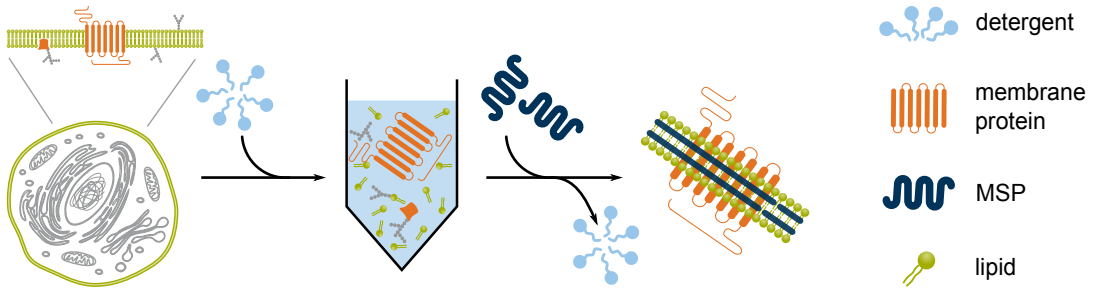

Figure 2.2: Schematic illustration of general nanodisc generation protocol from whole cells. Cells used as raw material are solubilized in a detergent solution. After addition of MSP, the self-assembly of nanodiscs is induced by removal of detergent.

samples were measured in duplicates. The color change was quantified with a ELx808 plate reader (BioTek) at 595 nm and compared to a BSA calibration curve.

PEG-PE and MSP1E3D1 were added to the supernatant at a ratio of 250 µg MSP1E3D1 and 40 µg PEG-PE per 125 µg of cell lysate and filled up to 300 µl with PBS. Self-assembly of nanodiscs was then induced by detergent removal with 50 mg Bio-Beads SM-2 (Bio-Rad) for one hour at room temperature while shaking (see fig. 2.2). Finally, the assembled nanodiscs were removed from the Bio-Beads and filled up with PBS to 1000 µl.

2.2.3 Nanodisc purification

Nanodiscs could be purified by immobilized metal ion affinity chromatography (IMAC) with Ni-NTA columns and / or by size-exclusion chromatography (SEC) with agarose-based columns in order isolate the nanodiscs from unwanted species. Additionally, SEC could be used for analytical purposes. All purification steps were performed at room temperature.

2.2.3.1 IMAC

HisPur Ni-NTA spin columns (Thermo Scientific) were used to purify nanodiscs by specifically binding the His-Tag of MSP. The spin columns were used according to the manufacturer's instructions, with all buffers based on PBS and adjusted to pH 7.4. As high amounts of imidazole were used for elution, it had to be removed by subsequent SEC.

equilibration buffer (pH 7.4)	PBS with 10 mM imidazole
wash buffer (pH 7.4)	PBS with 25 mM imidazole
elution buffer (pH 7.4)	PBS with 250 mM imidazole

2.2.3.2 SEC

SEC with a Superdex 200 Increase 10/300 GL column (GE) in an ÄKTA FPLC System was used to separate nanodiscs, lipid and protein aggregates as well as other molecules by

size. First, the column was equilibrated with PBS until a stable baseline was attained. A sample volume of 500 µl was applied with a Hamilton syringe first into a sample loop and then onto the column. The different components contained in the sample were eluted according to their size with PBS at a flow rate of 0.75 ml/min. The absorbance of eluting proteins was monitored at 280 nm with an integrated UPC-900 detector. Fractions were collected according to the elution volume if desired. For calibration and estimation of molecular weights, a high molecular weight gel filtration calibration kit (GE Healthcare) was used.

2.2.4 SDS polyacrylamide gel electrophoresis and Western Blot

2.2.4.1 SDS polyacrylamide gel electrophoresis (PAGE)

The existence of proteins in different samples was analyzed with SDS PAGE. If the protein concentration was too low, the samples were concentrated with spin columns (MWCO 10 kDa or 30 kDa). Then the samples were mixed with 3x loading buffer at a 2:1 ratio and heated to 95 °C for 5 minutes.

3x loading buffer (pH 6.8)	187.5 mM	Tris base
	150 mM	DTT
	6 %	SDS
	30%	glycerol
	0.03 %	bromophenol blue
SDS stacking gel (4 %)	3.5 ml	H_2O
	0.83 ml	1.5 M Tris pH 6.8
	50 µl	10 % SDS
	0.5 ml	40 % Acrylamide/Bis 37.5:1
	10 µl	TEMED
	100 µl	10 % APS
SDS separating gel (12 %)	2.6 ml	H_2O
	1.65 ml	glycerol
	2.5 ml	1.5 M Tris pH 8.8
	100 µl	10 % SDS
	3.0 ml	40 % Acrylamide/Bis 37.5:1
	10 µl	TEMED
	100 µl	10 % APS
SDS running buffer	25 mM	Tris-HCl
	192 mM	glycine
	0.1 %	SDS

The prepared samples were applied to discontinuous SDS gels. As a molecular weight standard, 5 µl of Full-Range Rainbow Molecular Weight Marker were used. The gels were run in SDS running buffer, first at 100 V for about 10 min, then at 200 V until the blue front reached the bottom of the gels.

The proteins could be detected by different methods, depending on the desired result. Staining with Roti-Blue Quick Solution according to the manufacturer's instruction revealed all proteins present on the gel. For a more specific protein detection, Western blotting was used.

2.2.4.2 Protein transfer for Western Blot (WB)

For detection of protein bands with specific antibodies, the proteins were transferred from the SDS gel to a polyvinylidene difluoride (PVDF) membrane. The membrane was first incubated in 100 % ethanol for about 3 min, then put into WB transfer buffer until it was used. The blotting staple was assembled into the transfer cassette in the following order (see fig. 2.3): first a fiber pad, then one sheet of Whatman paper, then the gel and the PVDF membrane, last another Whatman paper and fiber pad. The whole staple was soaked in WB transfer buffer and air bubbles were rolled out gently with a plastic tube.

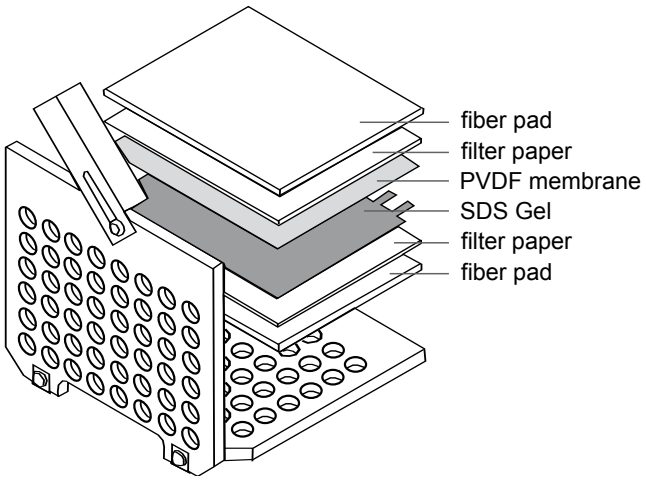

Figure 2.3: Schematic illustration of the composition of the Western Blot staple.

Finally the transfer cassette was closed and placed into the blotting module filled with transfer buffer. A cooling unit and a stir bar were added to keep the buffer temperature low and the ion distribution even in the tank. The transfer was carried out at 0.3 A for 90 min.

WB transfer buffer	25 mM	Tris base
	192 mM	glycine
	0.0001 %	SDS
	20 %	ethanol

2.2.4.3 Antibody incubation

After protein transfer, the membrane was blocked in 10 ml of blocking solution (5 % skim milk powder in TBS-T) for either 1 hour at room temperature or at 4 °C over night. The primary antibody was then applied and incubated at 4 °C over night or at room temperature for 2 hours. It was diluted according to the manufacturer's instructions into 2 to 5 ml of blocking solution. The PVDF membrane and the antibody solution were put into a 15-ml or 50-ml tube according to the size of the membrane and incubated under rotation.

TBS-T	15.3 mM	Tris-HCl
	4.7 mM	Tris base
	150 mM	NaCl
	0.1 %	Tween-20

Afterwards, the membrane was washed three times for 10 min in TBS-T and incubated with the corresponding secondary antibody for 1 hour at room temperature. After another three washing steps in TBS-T, the membrane was incubated with the SuperSignal West Dura Extended Duration Substrate (Thermo) for a few minutes and the chemiluminescence was detected with an Intas Advanced Western Blot Imager.

2.2.5 Surface plasmon resonance spectroscopy with platelet nanodiscs

SPR experiments were performed with a Biacore X100 instrument (GE Healthcare) equipped with a sample and a reference flow cell. All SPR experiments were performed using a CM5 sensor chip at 25 °C with PBS-T (PBS containing 0.05 % Tween-20) as running buffer at a flow rate of 10 µl/min unless otherwise specified.

For determination of binding characteristics of nanodiscs from human platelets, anti-His antibody was immobilized as ligand on both flow cells. For this purpose, amine-coupling chemistry was used. All reagents were provided by the His Capture Kit (GE Healthcare) and used exactly according to the manufacturer's instructions. Both flow cells, the measurement flow cell Fc2 and the reference flow cell Fc1, were treated this way. All following experiments were executed with platelet nanodiscs on Fc2 and with PC nanodiscs as negative control on Fc1.

After the immobilization, the chip regeneration was tested with different standard solutions (10 mM glycine with pH 3.0, 2.5, 2.0 and 1.5, 50 mM NaOH, 2 M $MgCl_2$ and 0.1 % SDS with pH 2.0). In each cycle, nanodisc solutions with a concentration of 4 µM were injected for 5 min onto both flow cells (PC nanodiscs on Fc1, platelet nanodiscs on Fc2), followed by a 30 sec injection of the corresponding regeneration solution at 30 µl/min. Each regeneration condition was repeated three times.

Binding characteristics of nanodiscs were then examined by injection of different concentrations (0 to 4 µM) of nanodiscs onto the flow cells. Each cycle was concluded by

injection of a 10 mM glycine solution (pH 1.5) for 12 sec at 30 µl/min.

For detergent dissolution of nanodiscs bound to the flow cells, 4 µM nanodisc solutions were injected for 5 min onto both flow cells, followed by rising concentrations of the respective detergent in PBS (either Triton X100 or Tween-20) from 0 % to 0.25 % for 1 min each. At the end of each cycle, the flow cells were regenerated with a 10 mM glycine solution (pH 1.5), which was injected for 12 sec at 30 µl/min.

Finally, antibody binding to the nanodiscs was determined for different antibodies. Again, 4 µM nanodisc solutions were injected for 5 min onto both flow cells, followed by 33 nM antibody solutions of anti-GPIX, anti-GPIIb, anti-PEG and anti-procalcitonin as negative control. Afterwards, the flow cells were regenerated as described above with a 10 mM glycine solution at pH 1.5.

2.3 Cloning and expression of platelet glycoprotein receptors

2.3.1 Cloning protocol

DNA coding sequences for the glycoprotein subunits were isolated from purchased plasmids, amplified by PCR and cloned into the target vectors. This process was checked after each step by control digest, and the end products were verified by Sanger sequencing.

2.3.1.1 Amplification and storage of plasmids

Plasmids containing the coding sequences of the single glycoprotein subunits were purchased from either Addgene or GenScript: GPIIb (Addgene: 27288) and GPIIIa (Addgene: 27289) for the GPIIb/IIIa complex, GPIbα (GenScript: OHu21772), GPIbβ (GenScript: OHu18618), and GPIX (GenScript: OHu18917) for the GPIb/IX complex. The gene sequences were chosen according to the UniProt canonic sequence, which corresponds to the most common isoform for the respective GP (see table 2.1).

Table 2.1: Protein subunits for GPIIb/IIIa and GPIb/IX. The most common isoform of each protein was chosen for expression in HEK-293 cells.

Glycoprotein	CD antigen	Gene	sequence identifier
GPIIb	CD41	*ITGA2B*	P08514-1
GPIIIa	CD61	*ITGB3*	P05106-1
GPIbα	CD42b	*GP1BA*	P07359-1
GPIbβ	CD42c	*GP1BB*	P13224-1
GPIX	CD42a	*GP9*	P14770-1

Plasmids from Addgene were delivered in the form of *E. coli* DH5α bacterial stabs, whereas GeneScript delivered purified plasmids, which were transformed into *E. coli* NEB5α for amplification and storage (see section 2.3.1.4.

Bacteria containing the plasmids were cultivated in LB medium with 100 µg/ml ampicillin at 37 °C under gentle agitation. Glycerol stocks for long-term storage were prepared

from 500 µl overnight culture mixed with an equal volume of sterile 50 % glycerol in H_2O and frozen at -80 °C. For inoculation of fresh medium, a sterile pipette tip was scratched over the frozen cells and thrown into a tube containing LB with ampicillin.

For isolation of plasmid DNA from overnight cultures, the Monarch Plasmid Miniprep kit (NEB) was used according to the manufacturer's instructions, followed by a second purification step with the Monarch PCR & DNA Cleanup Kit (NEB). Purified DNA was stored short-term at 4 °C and long-term at -20 °C.

LB medium	2.5 g	NaCl
	2.5 g	Tryptone
	1.25 g	yeast extract
	ad 250 ml	H_2O

LB medium was autoclaved at 123 °C for 30 min.

2.3.1.2 PCR

The purified plasmids served as templates for PCR reactions using a peqGOLD Taq DNA Polymerase 'all inclusive' (VWR) according to the manufacturer's recommendations. The respective primers for all GP constructs are shown in table 2.2.

Table 2.2: Primers used for GP amplification. Given are the annealing temperatures and sequences of the primers used for the amplification of GPs. All sequences are shown in 5' to 3' direction. Extensions of 5 bp 5' of the restriction site are written in lower cases, restriction sites are written in underlined lower cases, whereas coding sequences of the TEV site and P2A site are written in italic upper and those of GP subunits are written in bold upper cases.

Primer	T (°C)	Sequence (5' → 3')
GPIIb fw	52	gcgttaagcttATGGCCAGAGCTTTGTGT
GPIIb rv (+TEV)		aacgcaatatt*GCCTTGGAAGTATAGATTTTC* CTCCCCCTCTTCATCATCTTC
GPIIIa fw	52	gcgttaagcttATGCGAGCGCGGCCG
GPIIIa rv (+TEV)		aacgcaatatt*GCCTTGGAAGTATAGATTTTC* AGTGCCCCGGTACGTGATATTG
GPIbA fw	57	gcgttaagcttATGCCTCTCCTCCTCTTGCTGC
GPIbA rv (+TEV)		aacgcaatatt*GCCTTGGAAGTATAGATTTTC* GAGGCTGTGGCCAGAGTACCTAATG
GPIX fw	60	gcgttaagcttATGCCTGCCTGGGGAGCC
GPIX rv (+P2A)		aacgcctcgag*AGGTCCAGGGTTCTCCTCCACGTCTCC AGCCTGCTTCAGCAGGCTGAAGTTAGTAGCTCCGCTTCC* ATCCAGGGCCTCTGTGGTGG
GPIbB fw	60	gcgttctcgagATGGGCTCCGGGCCGC
GPIbB fw (+TEV)		aacgcaatatt*GCCTTGGAAGTATAGATTTTC* GGACTCGTCGGTTCCGGCTC

All denaturation steps were executed at 95 °C, followed by annealing at the indicated temperature for 30 s and extension at 68 °C for 1 min per 1000 bp. A total of 30 cycles were ended by a final extension step at 68 °C for 7 min. The PCR reactions were purified using the Monarch PCR & DNA Cleanup Kit (NEB) and the DNA concentration and yield determined with a NanoDrop 2000 instrument.

2.3.1.3 Cloning

The cloning of the resulting PCR products is depicted schematically in figure 2.4. The PCR products for GPIIb, GPIIIa, or GPIbα were directly cloned into the eukaryotic expression vector pcDNA3 via the HindIII and SspI restriction sites, whereas GPIX and GPIbβ PCR products were first ligated via their XhoI sites and then cloned into pcDNA3 via the HindIII and SspI restriction sites. For this purpose, the PCR products as well as the target vectors were digested with HindIII and SspI (or with XhoI respectively) according to the manufacturer's instructions, and then mixed and ligated by incubation with a T4 DNA ligase. Re-ligation of the target vectors was inhibited by removal of 5'- and 3'-phosphate groups from digested vectors with FastAP thermosensitive alkaline phosphatase (Thermo) prior to ligation.

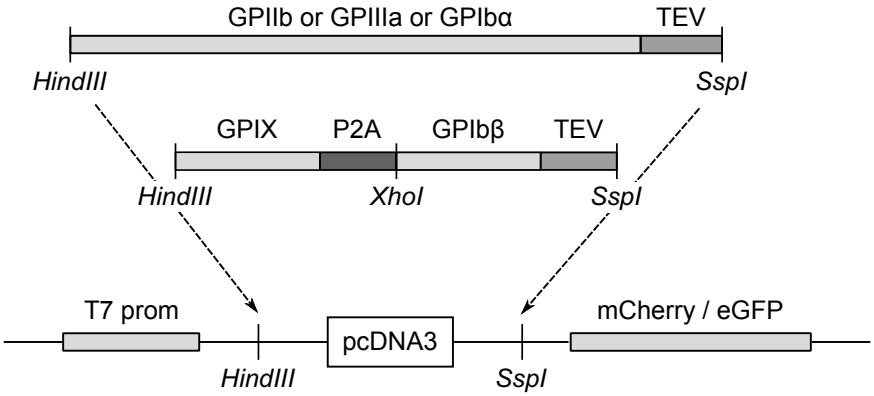

Figure 2.4: Schematic illustration of the cloning strategy for GP expression plasmids.

The target vectors contained either a C-terminal eGFP fluorescent tag (Addgene: 30127) or mCherry tag (Addgene: 30125), resulting in the following vectors: (#1) pcDNA3-GPIIb-mCherry, (#2) pcDNA3-GPIIIa-eGFP, (#3) pcDNA3-GPIBA-mCherry and (#4) pcDNA3-GPIX-P2A-GPIBB-eGFP.

2.3.1.4 Transformation of *E. coli*

Plasmids were transformed into *E. coli* NEB5α for amplification and storage. For this purpose, 50 µl of chemically competent cells were thawed on ice and mixed with 10 - 50 ng of DNA. Incubation on ice for 30 min allowed the DNA to adhere to the cell membranes, before a 30 sec heat shock at 42 °C enabled DNA transfer into the cells. After a further 5 min incubation step on ice, 950 µl of SOC medium were added to the cells, and after 1 hour incubation at 37 °C the bacteria were plated on LB-agar plates containing 100 µg per ml ampicillin and grown at 37 °C over night.

Only cells that had taken up a complete plasmid were able to grow on these plates. Colonies were picked the next day into 5 ml of fresh LB medium with ampicillin and incubated for 24 hours at 37 °C. Plasmid DNA was isolated by Miniprep and analyzed for correct assembly. Before transfection, the DNA was purified from remaining bacterial endotoxins with the Monarch PCR & DNA Cleanup Kit (NEB).

LB agar plates	2.0 g	NaCl
	2.0 g	Tryptone
	1.0 g	yeast extract
	3.0 g	agar
	ad 200 ml	H_2O
SOC medium	4.0 g	Tryptone
	1.0 g	yeast extract
	0.1 g	NaCl
	0.038 g	KCl
	ad 200 ml	H_2O
	3.6 ml	20 % glucose (sterile)
	1.0 ml	2 M $MgCl_2$

LB agar was autoclaved at 123 °C for 30 min. After cooling to about 55 °C, ampicillin was added and agar plates were poured.
For SOC medium, all components except glucose and $MgCl_2$ were mixed and autoclaved at 123 °C for 30 min. After cooling, the remaining ingredients were added.

2.3.1.5 DNA analysis

In order to control PCR products or assembled DNA fragments for correct size and sequence, agarose gel electrophoresis with or without prior control digest was used. Certain restriction enzymes cut DNA fragments at exactly defined sequences, which led to a characteristic pattern of differently sized DNA bands after agarose electrophoresis.

For this, the DNA samples were mixed with an appropriate volume of 6x loading-dye and loaded on agarose gels containing 0.01 % (v/v) ethidium bromide solution. Depending on the size of DNA fragments and purpose, 0.75 - 1.5 % (w/v) agarose gels in 1x TBE buffer were used. The gels were run in a horizontal electrophoresis chamber filled with 1x TBE buffer at 100 mA for 20 - 60 min. Afterwards, the separated DNA was visualized by UV illumination.

In order to exclude critical point mutations that could alter the protein sequence, the generated plasmids were verified by Sanger sequencing in a final step.

2.3.2 HEK-293 culture and transfection

2.3.2.1 Cultivation of HEK-293 cells

Human Embryonic Kidney (HEK-293) cells (ACC-305, DSMZ) were cultured in DMEM+++ under 5 % CO_2 at 37 °C. For the selection and maintenance of stably transfected cell lines the culture medium contained additionally 150 µg/ml geneticin disulphate (G418).

DMEM+++	500 ml	DMEM
	50 ml	FBS
	5 ml	Pen/Strep

HEK-293 cultures were were subcultured by splitting three times a week after reaching about 80 - 90 % confluency, estimated by light microscopy: on Mondays and Wednesdays in a 1:4 ratio, and on Fridays in a 1:8 ratio. For this purpose, the old medium was poured out and the cell layer carefully washed with DPBS. The cells were then resuspended in fresh DMEM+++ by pipetting up and down, thus detaching the cells from the coated surface of the flask by shear forces. Trypsin was not used to detach cells in order to avoid proteolysis of membrane proteins. Required volume of the cell suspension, according to the splitting ratio, was transferred to a new cell culture flask with fresh DMEM+++.

To examine the morphology as well as the expression level of transfected cell lines, cells were routinely checked under light microscope and fluorescence microscope. Cell numbers were determined using a Neubauer counting chamber. Cells were diluted if necessary, stained with 0.4 % Trypan Blue and pipetted into the counting chamber. Four of the big squares were counted using the light microscope. The total cell number in the sample was calculated under consideration of the dilution rate and the chamber volume.

For nanodisc generation, cells left over after routine splitting were used. The cell suspension was centrifuged (400 x g for 5 min), the supernatant removed and the cells frozen in PBS containing 10 % glycerol at -20 °C.

2.3.2.2 Storage of HEK-293 cells

Cryopreservation of cells allowed long-term storage and regular rejuvenation of the cell lines. After splitting of the cells, left-over cell suspension was harvested by centrifugation at 400 x g for 5 min and resuspended in DMEM+++ at 20 × 10^6 cells per ml. 250 µl of this cell suspension was mixed carefully with an equal volume of ice-cold freezing medium in a labeled cryo tubes (Nunc). The tubes were placed into a pre-cooled cryo freezing container and frozen at -80 °C for at least 5 hours before being transferred into liquid nitrogen for long-term storage.

For setting up new cultures, cryopreserved cultures were rapidly thawed in a water bath at 37 °C, resuspended in 1 ml DMEM+++ and transferred to a 15-ml tube containing 4 ml of pre-warmed DMEM+++. After centrifugation at 400 x g for 5 min, the supernatant

containing DMSO was removed, the pellet resuspended in DMEM+++ and transferred into a new T75 flask. The medium was exchanged 24 hours later, for transfected cell lines G418 was added at this point.

freezing medium	3 ml	DMEM+++
	1 ml	FBS
	1 ml	DMSO

2.3.2.3 Stable transfection of HEK-293 cell lines

For chemical transfection of HEK-293 cells the TransIT®-LT1 Transfection Reagent from Mirus Bio LLC was used according to the manufacturer's instructions. The day before transfection, cells were split in a 1:4 ratio. Cells from a confluent T75 flask were resuspended with 8 ml DMEM+++, of which 2 ml were diluted with 10 ml fresh medium. The resulting cell suspension was distributed into a 12-well plate with 1 ml per well and incubated at 37 °C and 5 % CO_2 over night. The plasmids used for co-transfection (either GPIIb-mCherry and GPIIIa-eGFP, or GPIBA-mCherry and GPIX-P2A-GPIBB-eGFP) were mixed in a molar 1:1 ratio, and pre-incubated with the LT1 reagent. The resulting complexes were added drop by drop to the now about 80 % confluent cell layer, and incubated at 37 °C and 5 % CO_2 for 24 hours, before the medium was changed. After 48 hours, transfected cells were transferred to selection medium (containing 150 µg/ml G418) and cultured for about two weeks.

Double positive cells highly expressing both eGFP and mCherry fusion proteins were then selected by fluorescence-activated cell sorting (FACS). For this purpose, the transfected cells were grown to confluence in a T75 flask, harvested, and resuspended in 3 ml Sorting buffer.

Sorting buffer	100 µl	0.5 M EDTA
	1.25 ml	1 M HEPES
	0.5 ml	FBS
	ad 50 ml	DPBS

The cells were sorted using a FACSAria III cell sorter (Becton Dickinson) for HEK-293 IIb/IIIa and a FACSAria Fusion cell sorter (Becton Dickinson) for HEK-293 Ib/IX. Of each cell line, 300,000 cells with the highest signal in the FITC channel for eGFP and the PE-A or PE-Texas Red channel for mCherry were bulk sorted into 2 ml pure FCS, and subsequently cultivated in a new T25 flask until confluency.

2.3.3 Analysis of HEK-293 cells

2.3.3.1 Flow cytometry

Surface expression and conformational integrity of the GP complexes on stably transfected HEK-293 cells were examined by flow cytometry. Expression of these complexes could be observed without prior staining as fluorescent protein tags were fused directly to the intracellular C-terminus of the GP subunits. Those were visible in the FITC channel and the PE-Texas red channel for eGFP and mCherry, respectively.

In addition, cells were stained with complex-specific primary monoclonal antibodies anti-GPIIb/IIIa (clone AP2; Kerafast EBW105) and anti-GPIb/IX (clone SZ1; Beckman Coulter IM-0538). Those antibodies bind only to intact GP complexes, not to the single subunits.

In brief, suspensions of detached cells left over after splitting were centrifuged at 400 x g for 5 min and washed with DPBS. The cells were distributed into the wells of a 96-well V bottom plate (500,000 cells per well). After staining of dead cells with 50 µl of Zombie NIR Fixable Viability Kit (BioLegend) 1:1000 in DPBS for 10 min on ice, the cells were washed with DPBS containing 2 % FBS. This washing step was repeated between each two subsequent staining steps.

The cells were incubated with 3.33 µg/ml primary antibody for 30 min on ice, washed, and then incubated with an AF350–conjugated anti–mouse secondary antibody (Thermo A-11045) for 15 min on ice. This antibody could be detected in the Indo-1 (violet) channel, and did not interfere with either eGFP or mCherry. After a final washing step the cells were resuspended in DPBS with 2 % FBS and analyzed on an LSRFortessa cell analyzer (Becton Dickinson).

2.3.3.2 Determination of glycoprotein copy number

HEK-293 cells stably transfected with either GPIIb/IIIa or GPIb/IX were lysed in 1 % (w/v) OG in PBS at a concentration of 20,000 cells/µl and centrifuged at 16,100 x g for 15 min. The eGFP fluorescence in the resulting supernatant cell lysate was determined with a Perkin Elmer LS50B spectrofluorometer with a quartz cuvette. The excitation wavelength was 475 nm, and the emission spectrum was recorded from 495 nm to 595 nm. The emission maximum at 509 nm was used for further analysis.

In order to calculate the GP copy number per cell (N_{GP}) from the eGFP fluorescence intensity in the lysate, a standard curve was generated with purchased eGFP protein (OriGene: TP790050) in dilutions from 0 to 280 nM. Thus, the eGFP concentration (c_{eGFP}) and subsequently the number of fluorescent protein molecules per cell (N_{eGFP}) could be determined from the standard curve according to equation 2.1. Finally, the number of GP complexes per cell (N_{GP}) was calculated by dividing N_{eGFP} by the number of eGFP tags per GP complex ($N_{eGFPperGP}$) (equation 2.2). Hereby it has to be kept in mind that GPIb/IX complexes contain two copies of eGFP instead of a single one present in GPIIb/IIIa complexes.

$$N_{eGFP} = c_{eGFP} \times \frac{N_A}{20 \times 10^9 \times \frac{1}{l}} \tag{2.1}$$

$$N_{GP} = \frac{N_{eGFP}}{N_{eGFPperGP}} \tag{2.2}$$

2.3.3.3 Cell adhesion assay

In order to examine binding of whole HEK-293 cells to different pre-treated surfaces, 8-well culture slides (Falcon 354108) were coated with 150 µl of either fibrinogen or von Willebrand factor at 100 µg/ml or 1 % BSA as negative control. After incubation at 4 °C over night, the wells were blocked with 1 % BSA for 1 hour at room temperature.

The wells were then washed twice with PBS, and 100,000 HEK-293 cells of different cell strains (HEK-293 IIb/IIIa, HEK-293 Ib/IX or HEK-293 wt as negative control) were added in 300 µl PBS. Unbound cells were removed after 1 hour at 37 °C, and remaining cells were fixated with 4 % paraformaldehyde for 5 min at room temperature in the dark. After two last washing steps with PBS, the walls of the chambers were removed and the resulting slides were preserved by covering with mounting medium and cover slips. The specimens could now be observed by transmission light microscopy at a 10,000x magnification.

2.4 Generation and analysis of nanodiscs with recombinant GP receptors

2.4.1 Nanodiscs from whole HEK-293 cells

Nanodiscs were generated similar to the description above (see section 2.2.2). In brief, HEK-293 cells were lysed in a 1 % (w/v) OG solution in PBS. The protein concentration in the lysate was determined using the Quick-Start Bradford protein assay (Bio-Rad) as described above.

Cell lysate corresponding to 100 µg of total protein was mixed with 250 µg MSP1E3D1 and 200 µg PEG-PE as stabilizing agent (corresponding to 20 PEG-PE molecules per nanodisc). This mixture was incubated with 50 mg Bio-Beads at room temperature (RT) for 1 h under gentle agitation, thereby removing the detergent and inducing the self-assembly of the nanodiscs. The nanodisc containing supernatant was immediately used in the experiments.

2.4.2 Enzyme-linked immunosorbent assay

A sandwich ELISA was used to measure the amount of antigen between two layers of antibodies (capture and detection antibody) which detect different epitopes of the antigen. The different layers of the ELISA sandwich were added in consecutive steps. In each step, the appropriate amount of diluted material was added to each well, then the plate was

covered and incubated. After each step, any material that had not bound to the plate was washed away. For this purpose, the wells were filled with washing buffer, then the liquid was removed by flicking the plate over a sink and patting the plate on a stack of paper towels. After each incubation step in the described protocol three washing steps with 300 µL PBS-T (PBS containing 0.05 % Tween-20) per well were inserted.

Wells of a Nunc PolySorp flat-bottom 96 well plate were coated with 100 µl of PBS containing GFP-binding protein, RFP-binding protein (Chromotek) or a mixture of both in a concentration of 0.5 - 1 µg/ml, by incubating them at RT for 2 h. Remaining protein-binding sites of the coated wells were blocked with 5 % skim milk powder or 1 % BSA in PBS at RT for 1 h, before 100 µl of nanodisc fractions were added to each well and incubated at 4 °C over night.

The next day, the wells were incubated with 100 µl/well of primary antibody in an appropriate dilution at RT for 2 h, and subsequently for 1 h with the corresponding horseradish peroxidase-conjugated secondary antibody. For detection and quantification of bound antibodies, 100 µl of the substrate solution TMB (3,3',5,5'-tetramethylbenzidine) were dispensed into each well and incubated for 10 min in the dark, or until a color change from clear to blue could be observed. The reaction was stopped by adding 50 µl of 1 M sulfuric acid and the absorbance of each well was measured at 450 nm using a BioTek ELx808 Absorbance reader. Results were determined in duplicates and given in absorbance units (AU).

2.4.3 Surface plasmon resonance spectroscopy

SPR experiments were performed similar to the description above (see section 2.2.5). Again, a Biacore X100 instrument (GE Healthcare) was used with CM5 chips. As above, the running buffer was PBS-T, at a flow rate of 10 µl/min.

Here, 100 µg/ml fibrinogen (Merck) or 100 µg/ml anti-vWF antibody (Dako: A0082) for GPIIb/IIIa or GPIb/IX nanodiscs, respectively, were immobilized as ligands using an amine-coupling chemistry as above. The ligands were diluted in 10 mM sodium acetate, pH 4.6 and immobilized for 7 min on the sample flow cell Fc2. The second flow cell (Fc1) served as a reference surface and was treated with non-binding proteins (BSA for GPIIb/IIIa or HSA for GPIb/IX). The chips were regenerated with a 30 s injection of 10 mM glycine, pH 1.5 at a flow rate of 30 µl/min at the end of each cycle. All samples were injected in duplicates in random order.

For SPR experiments with GPIIb/IIIa nanodiscs, the nanodiscs were injected in different concentrations over both flow cells. This injection was carried out for 5 min, while the subsequent dissociation was monitored for further 2 min. In contrast, SPR experiments with GPIb/IX nanodiscs contained two injection steps. In a first injection, von Willebrand factor (Dynabyte) at a concentration of 150 U/µL was injected in order to prepare a binding surface, before, in a second step, the nanodiscs were injected for 5 min and the dissociation was monitored for further 2 min. Nanodiscs resulting from wild type HEK-293 cells served as negative controls in both SPR experiment set-ups.

2.5 Patient study

2.5.1 Patient assignment

Left-over blood serum samples of 69 AITP patients were supplied in an anonymized form by the Institute for Transfusion Medicine at the university hospital in Tübingen by Prof. Dr. med. Tamam Bakchoul. Included were male and female patients with the diagnosis of AITP, diagnosed by a process of exclusion. Age, sex and platelet count were available for most of the patients. Additionally, 31 blood samples from healthy donors were provided, but without any clinical information. A second group of negative control samples consisted of 50 anonymous left-over patient samples from the orthopedic unit of the Klinikum rechts der Isar in Munich, who had normal platelet counts and were thus considered to be healthy in regard to AITP.

Because of the rareness of the disease, a retrospective evaluation of patient data produced for the initial diagnosis has been approved by the ethics committee of the university hospital in Tübingen. Only left-over material was used for this study, so that no additional blood drawing was necessary. No new information was produced during this study. Either data was used that had been generated during normal diagnosis of patients (age, sex, platelet count, MAIPA results), or laboratory results were re-determined with the new assay (autoantibody levels). The data protection regulations according to the EU General Data Protection Regulation (DSGVO) were complied with.

2.5.2 Study setup

All serum samples (69 patient samples and 81 healthy controls) were measured in random order on 12 ELISA plates with the set-up described above in section 2.4.2. The only adaption was exchange of the primary antibody against serum in a 1:100 dilution in PBS-T, incubated for two hours at 37 °C.

All samples were measured in duplicates, and the results given as A_{450nm} values. Samples with an intra-assay Coefficient of Variability (CV) higher than 10 % were discarded and the measurement repeated. Additionally, half of all samples were repeated randomly in order to determine the inter-assay CV.

2.5.3 Statistical analysis

Four well-characterized serum samples were measured repeatedly on each ELISA plate, two positive and two negative samples. In order to obtain a correction factor for each ELISA plate for comparison with the first plate, all four samples were normalized relative to plate #1, and resulting values were averaged for each plate. This resulted in correction factors between 0.61 and 1.48, which were multiplied with all A_{450nm} values from the respective plate.

All data were analyzed with R version 3.5.0, with help of the graphical user surface RStudio version 1.1.463. The results were presented as mean ± standard deviation if not stated otherwise. Statistical significance between the mean values of two independent

groups was analyzed using the t-test, if normal distributions of the underlying values was assumed.

3 Results and discussion

3.1 Generation of nanodiscs from whole human platelets

In the scope of this thesis, a novel assay principle for the detection of autoantibodies in AITP based on the nanodisc technology should be developed. The crucial prerequisite for this assay is the incorporation of platelet membrane glycoprotein receptors into nanodiscs. After separation from their original membrane and transfer into the nanodisc membrane, the protein structure still has to be native-like. Only then optimal binding and detection of the autoantibodies is possible.

Different raw materials have been used for the production of membrane proteins for incorporation into nanodiscs, from cell-free expression to bacteria, insect and mammal cells (Rouck et al., 2017). The protein source depends on the kind of protein and the planned application. As platelet antigens are the desired membrane proteins here, extraction of proteins directly from human platelets was the first step of this project.

3.1.1 Platelet isolation

Platelets were isolated from human blood samples, taken freshly from voluntary donors. Anticoagulation was achieved by addition of sodium citrate. The blood components were separated by a series of different centrifugation steps, adapted from Crawford et al. (1992). The first step, the so-called soft spin, removes red and white blood cells due to their bigger size. The remaining platelet-rich plasma (PRP) is then centrifuged at higher velocity in order to harvest the smaller platelets. The platelet isolation protocol has been established previously (Mak et al., 2017) and optimized in the beginning of this thesis. The main improvements were the introduction of a second soft spin step as well as a slight adaption of centrifugation times and speeds.

During platelet isolation, variation of the amount of supernatant PRP allows for adaption of purity versus yield. The more carefully the PRP is separated from the pellet, the purer the resulting platelet fraction will be, at the expense of the recovery rate. The described protocol is optimized for platelet purity rather than yield. Typically, only around 30 to 40 % of the platelets present in whole blood can be recovered. In return, more than 99 % of white blood cells are removed, and nearly all of the red blood cells (more than 99.9 %).

3.1.2 State of the art of nanodisc generation

A basic protocol for nanodisc generation from whole platelets was developed previously (Mak et al., 2017). Isolated human platelets or platelet membranes were solubilized with Triton X-100, then remaining cell debris was removed by centrifugation, and the protein concentration in the supernatant was determined by Bradford assay. 500 µg of the supernatant were mixed with 250 µg MSP1E3D1 and 40 µg PEG-PE, and nanodisc assembly

was induced by incubation with Bio-Beads for three hours at room temperature or over night at 4 °C. Resulting nanodiscs were purified first by IMAC with a Ni-NTA column, then by size exclusion chromatography with a Superdex 200 column.

During SEC, the protein concentration was monitored constantly by measuring the light absorption at 280 nm. Together with calibration of the column with a high molecular weight calibration kit, this allowed analysis of nanodisc formation according to the size distribution of particles contained in the reaction mixture. SEC of unprocessed platelet lysates resulted in a distinct peak at about 8 ml elution volume, directly after the void volume of the column. This indicates the formation of large aggregates after removal of the detergent by the SEC column. In contrast, application of the purified scaffold protein MSP1E3D1 without any added lipids or cell material resulted in a peak at about 15 ml, which is equivalent to a molecular weight of approximately 60 kDa, corresponding to a MSP1E3D1 dimer (data not shown).

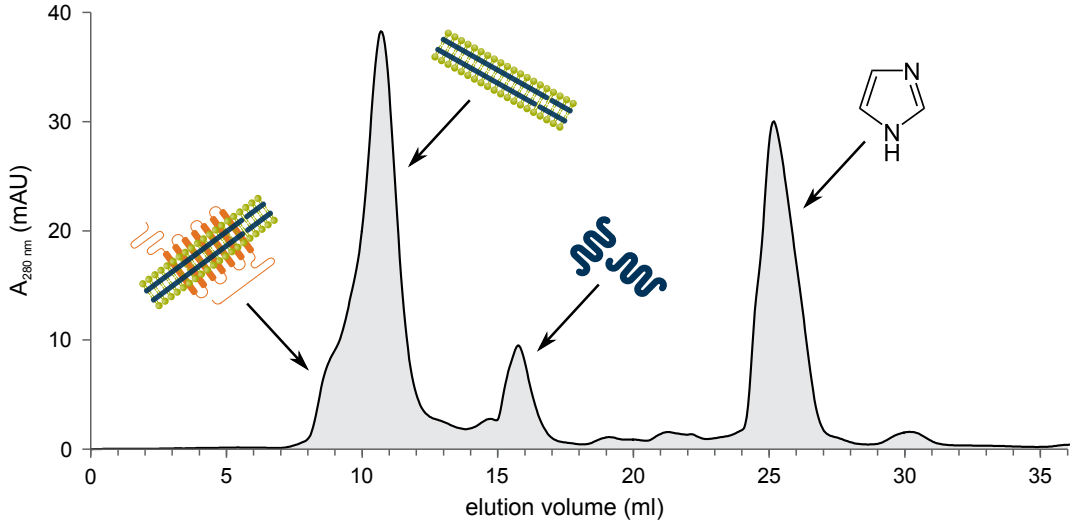

Figure 3.1: SEC diagram of nanodiscs generated according to the previously developed protocol. Identified species are depicted as images. From left to right: nanodiscs with and without membrane proteins included, left-over scaffold protein and imidazole.

Only if MSP and cell material were combined to form nanodiscs, the characteristic peak pattern was clearly visible (see fig. 3.1): The main peak spanning an elution volume between 9 ml and 12 ml consisted of nanodiscs. The maximum of this peak was between 11.0 and 11.5 ml, consistent with published results (Grushin et al., 2017; Denisov et al., 2004). On the right side of this peak, "empty" nanodiscs without incorporated membrane proteins could be found, whereas nanodiscs containing one or multiple proteins eluted at lower volumes and thus formed a shoulder or sometimes a separated peak. The molecular weight of empty nanodiscs, consisting only of two copies of MSP1E3D1 filled with about 120 molecules of membrane phospholipids (Denisov et al., 2004) and 20 molecules of PEG-PE, was calculated as about 200 kDa, matching the right end of the peak. At about 15 ml to 16 ml, a small amount of left-over MSP1E3D1 was visible, and the high peak at about 25 ml consisted of imidazole used for elution from the IMAC Ni-NTA column.

This newly developed approach was quite different from previously published protocols.

Before, the application of nanodiscs had been limited almost exclusively to previously isolated membrane proteins. According to the most commonly used protocol (see for example Leitz et al. (2006), Yan et al. (2011) or Taylor et al. (2001)), membrane proteins are produced in an overexpression system and isolated from the membrane fraction. This rather complicated process involves solubilization and centrifugation steps that lead to a reduced yield and potential protein damage, as the natural phospholipid environment is completely removed. Only after solubilization and purification, membrane proteins are incorporated into nanodiscs made from lipids that have been isolated previously from a different source than the membrane protein itself.

Even the rare exceptions from this procedure still used the plasma membrane fraction instead of whole cells as raw material (Marty et al., 2013; Roy et al., 2015; Shirzad-Wasei et al., 2015). The natural phospholipids of the cell membranes were not removed from the proteins in these cases, but incorporated into the nanodiscs together with an excess of additional lipids. However, these methods still rely on the time-consuming and complicated separation of the cytoplasmic membrane from all other cell components. In contrast, the improved express protocol works without membrane isolation and purification steps, making the whole process both faster and easier (see fig. 3.2).

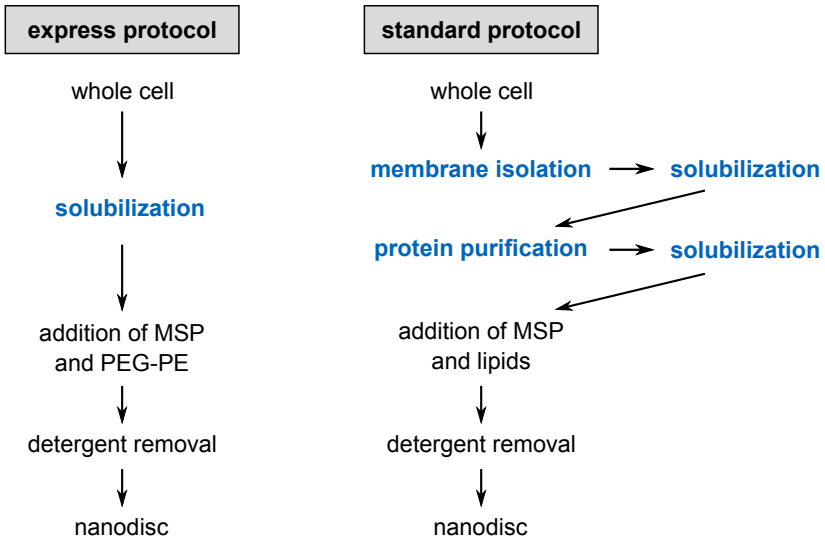

Figure 3.2: Comparison of standard and express nanodisc preparation protocols. Main differences are highlighted in blue.

For this project, the express protocol would be better suited, especially in regard to a possible routine application. However, it should not perform worse than the standard protocol for the proteins of interest, GPIIb/IIIa and GPIb/IX. In order to compare both approaches, platelet nanodiscs were prepared with and without membrane isolation. After purification by IMAC, size and content of resulting nanodiscs were analyzed by SEC and WB, respectively. It could be shown that the yield of nanodiscs containing the desired proteins was even higher with the express protocol.

SEC of both kinds of nanodiscs resulted in a very similar peak pattern with both methods (fig. 3.3). The nanodisc and MSP peaks were at exactly the same position,

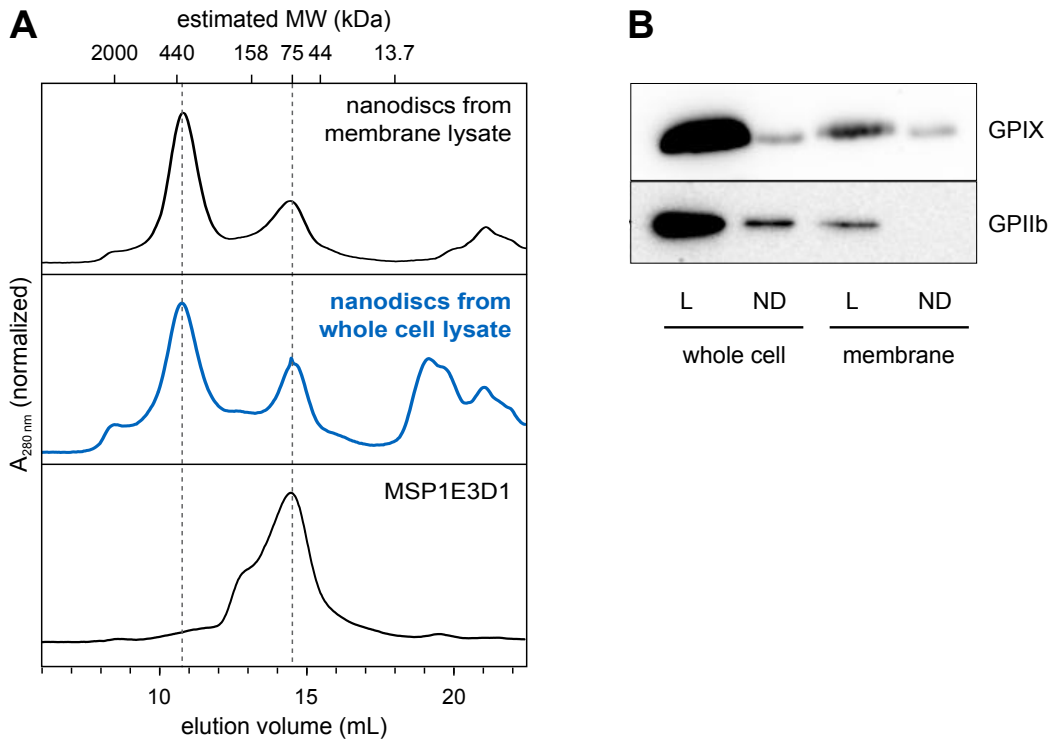

Figure 3.3: Comparison of nanodiscs from whole cells and lysate. (A) SEC of nanodiscs from membrane and whole cell lysates and MSP1E3D1 for comparison. Molecular weight (MW) was estimated by calibration with a gel filtration calibration kit. (B) Western Blot against GPIX and GPIIb of lysates and nanodiscs from whole cells and isolated membranes.

again similar to published results (Grushin et al., 2017; Denisov et al., 2004). The main difference was a higher protein signal at elution volumes bigger than 18 ml for whole cell nanodiscs, probably from remaining cell material that had bound unspecifically to the Ni-NTA material of the IMAC column. The whole nanodisc peak from 7.5 to 15.5 ml was collected and concentrated for SDS PAGE and WB analysis.

If the protein content of whole cell lysate and membrane lysate was compared for GPIIb and GPIX, a clear decrease in protein amount was visible after membrane isolation. Nanodiscs generated from the isolated membrane fraction as raw material thus also contained less GP receptors than those from whole cell lysates. This corresponded well to published experiments (Mak et al., 2017). Based on this result, whole cells instead of only the membrane fractions were used as raw material for nanodisc generation in all experiments in this thesis.

3.1.3 Optimization of nanodisc generation protocol

Although the express protocol was generally feasible, there were still some points to be optimized for this thesis. The main obstacle was the long preparation time, nanodisc generation still took at least seven hours with this protocol, or nearly a whole working day. The main steps to be shortened were the incubation time with Bio-Beads and the purification process. Another problem was the low yield of membrane protein after incorporation into nanodiscs, when compared to the raw material. This was most probably

due to the multiple purification steps.

3.1.3.1 Reduction of purification steps

Purification of nanodiscs by IMAC with a Ni-NTA column resulted in a very pure sample, but it had different drawbacks. It was time-consuming, and necessitated a second purification step in order to remove the high amounts of imidazole needed for elution. If this step was simply omitted, the resulting SEC diagram showed multiple additional peaks (see fig. 3.4). The pattern was quite different in the range from 18 ml to 30 ml elution volume, as soluble proteins were removed by IMAC. Here, the distinctive peak at 20 ml most likely consisted of hemoglobin impurities left over during platelet isolation from whole blood. Instead, an imidazole peak at 26 ml was added. Another difference without IMAC purification was the emergence of a separate peak at the exclusion volume of the column, here at about 8 ml, which consisted of protein and lipid aggregates. The peak pattern for elution volumes between 8 and 18 ml was similar with and without IMAC, with the main nanodisc peak at 11.5 ml being better separated without Ni-NTA purification. Additionally, nearly half of all material was lost after the additional purification step. In summary, the generation of nanodiscs without the additional Ni-NTA purification looked feasible, if only the separation of the different peaks were better.

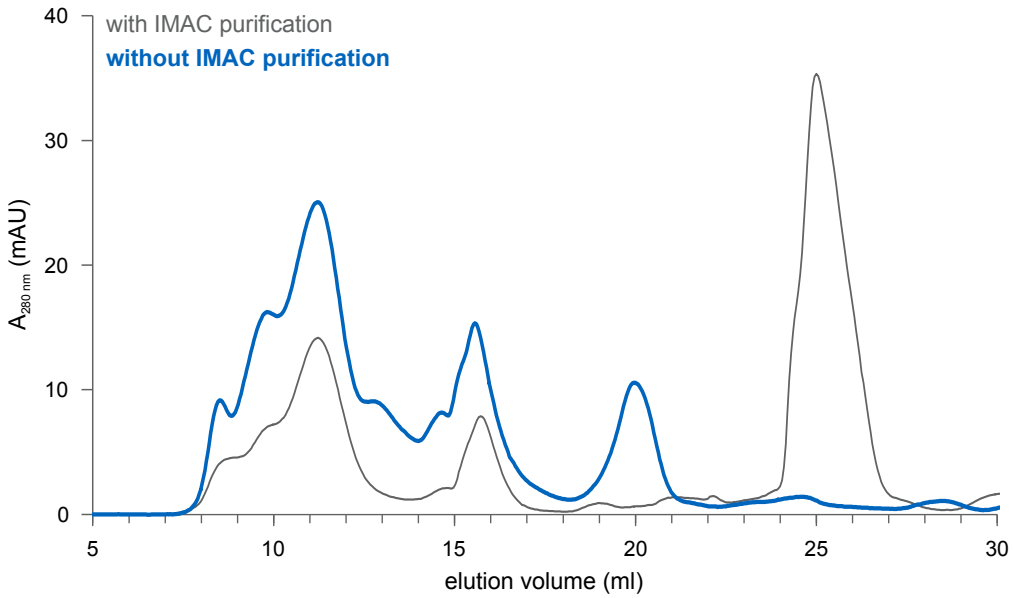

Figure 3.4: SEC diagrams of nanodiscs with and without purification by IMAC. The condition used for further experiments is highlighted in blue.

3.1.3.2 Ratio of scaffold protein to cell lysate

In order to circumvent the lengthy purification procedure, it would have been ideal to optimize the nanodisc protocol in order to achieve a single nanodisc peak, without any left-over MSP or aggregated cell material which led to additional peaks overlapping the nanodisc peak. Additionally, this optimization could lead to a better usage of the available

cell material.

For this experiment, the amount of platelet material was reduced down to 1/8 of the previous protocol, while the amount of scaffold protein remained unchanged. This resulted in ratios of MSP to platelet material from 1:0.25 to 1:2 (see fig. 3.5). The nanodisc peak got higher with rising amounts of platelet material. At ratios 1:0.5 and 1:1 the nanodisc peak was highest compared to other peaks. At a 1:0.25 ratio, the characteristic peak pattern was not clearly visible anymore. A 1:1 ratio of MSP to platelet material was considered best and used for further experiments.

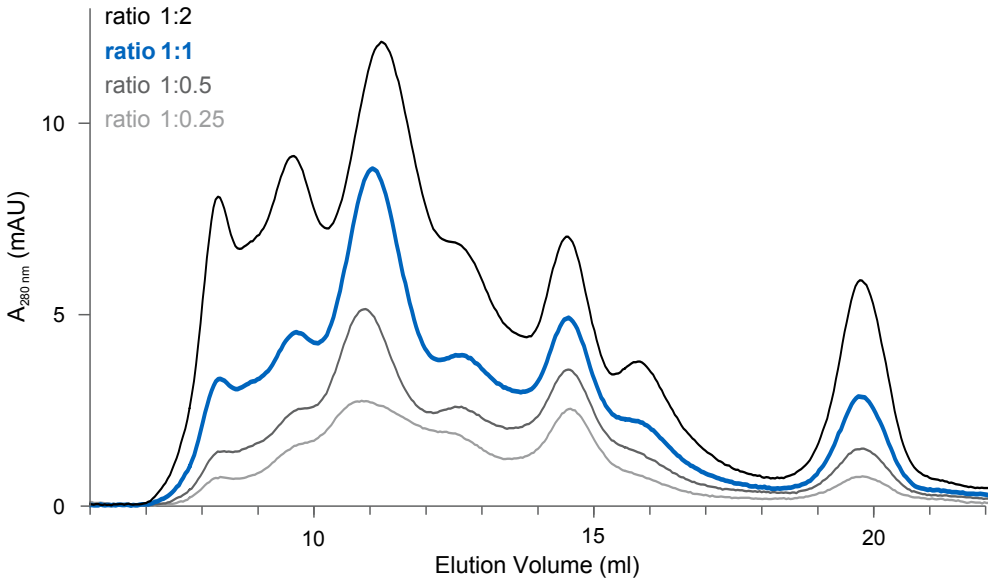

Figure 3.5: SEC diagrams of nanodiscs generated with a ratio of MSP to lysate from 1:0.25 to 1:2. The condition used for further experiments is highlighted in blue.

3.1.3.3 Shortening of incubation time

The next parameter to be optimized was the incubation time with Bio-Beads. Those beads consist of a nonpolar polystyrene adsorbent which can remove organic molecules with a molecular weight smaller than 2000 Da from aqueous solutions via hydrophobic interactions. Those beads are generally suited for use in chromatography columns, but here the bulk method was used. This means that the beads were simply incubated together with the nanodisc assembly mixture in a glass tube for a certain amount of time. Afterwards, the nanodisc solution was removed from the Bio-Beads and used for further experiments.

Different incubation times at room temperature were tested, from 15 min to 180 min (see fig. 3.6). As Triton X-100 absorbs light at 280 nm because of its aromatic molecular structure, it was visible as a peak at about 23 ml in the FPLC diagram. It was nearly completely removed after only 30 min incubation, and from 60 min on no further change was visible. The nanodisc peak, visible at about 11.5 ml, did not change much between 30 and 90 min. For all further experiments an incubation time of 60 min was chosen, as a compromise between time saving and complete detergent removal.

Those steps, optimization of nanodisc purification and shortening of incubation time,

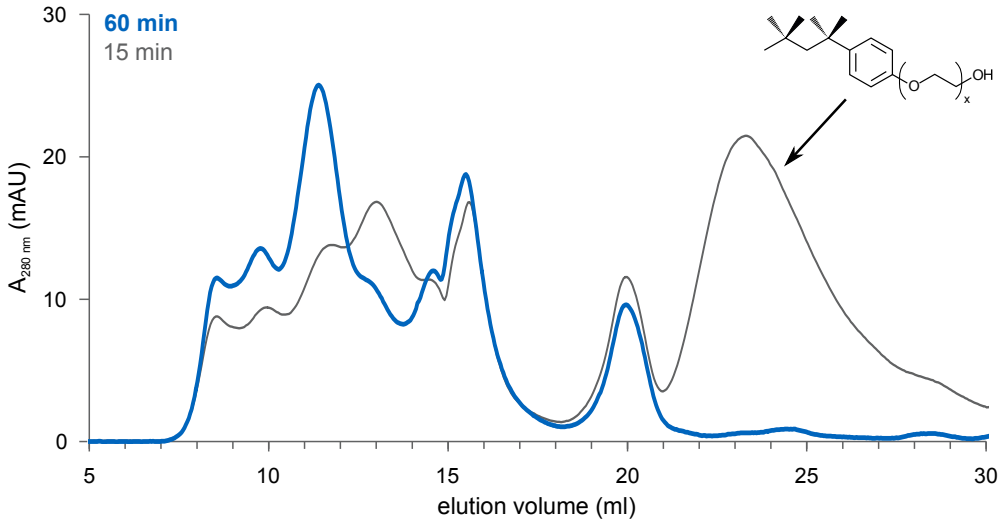

Figure 3.6: Comparison of SEC diagrams of nanodiscs generated by incubation times with Bio-Beads for either 15 or 60 min. Insufficient removal of Triton X-100 leads to an additional peak at about 23 ml. The condition used for further experiments is highlighted in blue.

reduced the total working time for nanodisc generation from about 7 hours to less than three hours. This enabled a better use of the working day, as nanodiscs could be generated in the morning, with subsequent analysis in the afternoon. Additionally, this abolished the need for nanodisc storage over night prior to the subsequent experiments.

3.1.3.4 Solubilization of membrane components

An important factor influencing the incorporation of a certain membrane protein into nanodiscs is the detergent used for solubilization of the cell material. During solubilization of the cells a crucial compromise has to be maintained: on the one hand, the membrane protein in question should be separated from membrane, kept in solution and be stabilized while in this sensitive state, while on the other hand the detergent should not bind too tightly or denature the protein (Garavito and Ferguson-Miller, 2001). There are many different types of detergent, varying in their structure and chemical properties. Nonionic or zwitterionic detergents as well as bile acid salts meet these requirements best (Seddon et al., 2004), whereas ionic detergents are less gentle and generally denature proteins. The ideal detergent for nanodisc generation should be able to solubilize cellular material and to incorporate the solubilized membrane protein into nanodiscs, without destroying the protein structure.

In order to quickly screen which detergents are suited for a more thorough examination, platelet cells were lysed with different nonionic and zwitterionic detergents at a concentration of 10 times their critical micelle concentration (see fig. 3.7 A). The resulting cell lysate was centrifuged at 16,100 rcf for 30 min in order to remove unsolubilized cell material, and the protein concentration of the supernatant was determined. Here it was important to pay attention to the compatibility of the Bradford assay with the different detergents, and to dilute the samples if necessary.

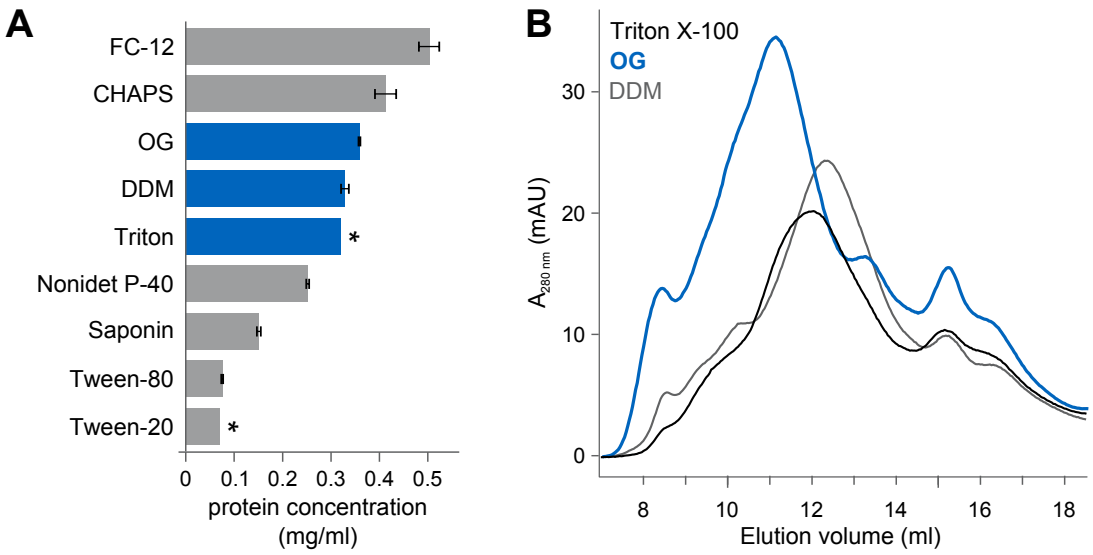

Figure 3.7: Platelet nanodiscs with different detergents. (A) Protein concentrations of platelet lysates generated with different detergents. Detergents chosen for nanodisc generation are shown in blue. Samples are measured in duplicates, except for samples marked with *. (B) SEC of nanodiscs prepared from the same amounts platelets solubilized with different detergents.

The nonionic detergents Tween-20 and Tween-80 as well as Saponin left a clearly visible cell pellet and solubilized nearly no protein. All other detergents solubilized the cell material to a certain degree. Although in this experiment, n-Dodecyl-phosphocholine (FC-12) and 3-[(3-cholamidopropyl)dimethylammonio]-1-propanesulfonate (CHAPS) resulted in the highest protein concentration in the supernatant, the much milder non-ionic detergents octyl-β-D-glucopyranoside (OG) and dodecylmaltoside (DDM) as well as Triton X-100 performed not much worse. Nonionic detergents break lipid-lipid and lipid-protein interactions without disrupting protein-protein interactions (Seddon et al., 2004). Thus they should be better suited for isolation of complete membrane protein complexes. The three detergents highlighted in blue in figure 3.7 A were further examined by generation of nanodiscs from the cell lysates.

The SEC curves in figure 3.7 B showed that all three detergents were generally suitable for the generation of nanodiscs. However, the use of OG for platelet solubilisation led to the highest nanodisc peak. Additionally, the shoulder at the left side of the main peak is most pronounced for the OG nanodiscs. As this shoulder likely contains nanodiscs with incorporated membrane proteins, OG was chosen as detergent for all subsequent experiments.

3.1.4 Verification of platelet GP receptor incorporation into nanodiscs

3.1.4.1 Western Blot

After a feasible nanodisc generation protocol had been established, the incorporation of GPIIb/IIIa and GPIb/IX complexes was examined. For this purpose, nanodiscs were prepared and separated by SEC. Resulting fractions were collected and subsequently examined by SDS-PAGE and Western Blot. Thus it could be determined which membrane

protein complexes were included, and in which fraction of the nanodiscs (see fig. 3.8). For the GPIIb/IIIa complex, GPIIb was examined, and GPIX for the GPIb/IX complex. Both proteins were clearly detectable in the nanodiscs peak.

While the amount of MSP1E3D1 corresponded quite clearly with the height of the peak, the glycoproteins were not found in the main peak, but at smaller elution volumes. Here, it has to be kept in mind that the proteins were detected by different methods. The GP receptors were detected by WB, which is able to make protein amounts as small as 100 fg visible. In contrast, MSP was stained on the gel by the much less sensitive Coomassie staining, which has a detection limit of about 50 ng according to the manufacturer's instructions. This means that there is still much more MSP in the 9 ml and 10 ml fractions than GPIIb or GPIX, indicating that those fractions consisted still of nanodiscs instead of undefined cellular aggregates.

This result is a further hint for the hypothesis that the highest peak consisted mainly of empty nanodiscs, while nanodiscs with incorporated membrane proteins had a higher molecular weight and thus eluted at smaller volumes. Whereas GPIIb is predominantly found in the 10 ml fraction, the amount of GPIX is higher in the 9 ml fraction. Based on this result, for further experiments the nanodisc peak was collected between 9 and 11 ml elution volume.

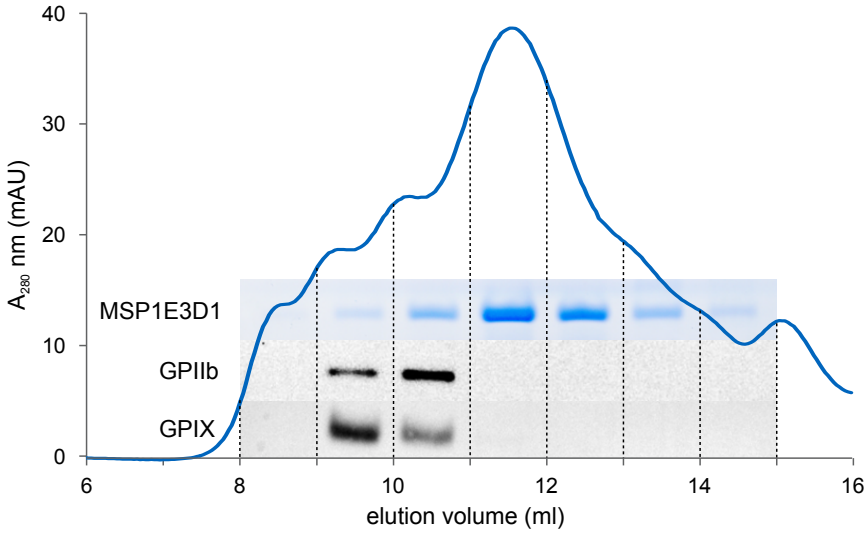

Figure 3.8: SEC of nanodiscs prepared according to the final protocol (blue line). Fractions were collected from 8 to 15 ml and analyzed by Western Blot against GPIIb and GPIX. For comparison, MSP1E3D1 was detected in the fractions by SDS-PAGE.

3.1.4.2 Surface plasmon resonance spectroscopy

As the general binding of different antibodies to platelet nanodiscs had been confirmed, it was tried to examine the binding behavior further by SPR. With SPR, binding can be visualized label-free in a time-dependent manner, which allows to draw conclusions about both thermodynamics and kinetics of antibody binding.

For the first experiments, a CM5 chip with a carboxymethylated dextran layer covalently

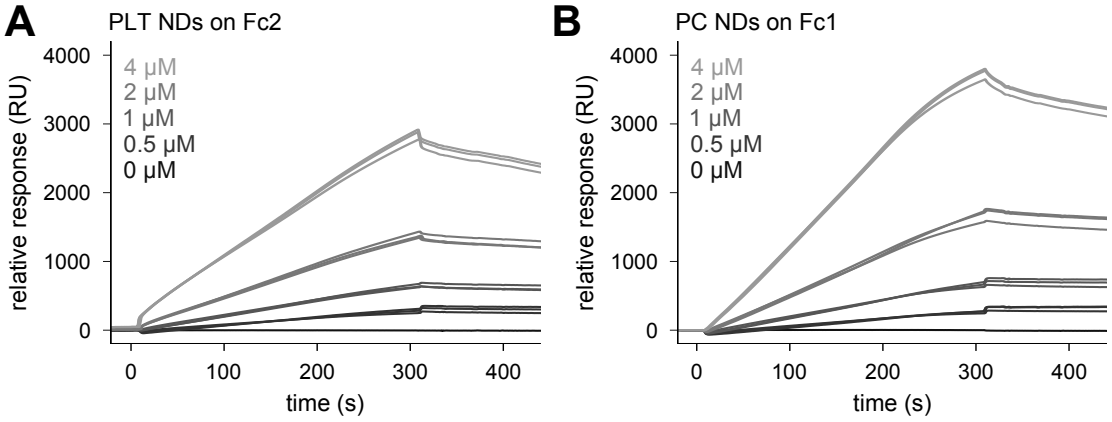

Figure 3.9: Binding of nanodiscs in different dilutions to CM5 chip coated with anti-His antibodies. (A) Platelet nanodiscs immobilized onto the measurement flow cell Fc2 and (B) control nanodiscs without incorporated membrane proteins on the reference flow cell Fc1. All measurements were conducted in triplicates.

attached to a gold surface was used for immobilization of anti-His antibodies via amine coupling with EDC and NHS . The anti-His antibody bound to the His-tagged MSP1E3D1 used for nanodisc generation, and thus to all kinds of nanodiscs. The SPR instrument used in these experiments, a Biacore X100, has two flow cells, one for the measurement itself and one as a reference. Platelet nanodiscs were bound to the measurement cell (called Fc2), and nanodiscs generated from bought PC without any membrane proteins onto the reference cell (called Fc1).

Both kinds of nanodiscs showed reproducible binding to the chip. The curves show the typical division into association and dissociation phases. Injections of nanodiscs with concentrations from 0.5 µM to 4 µM lead to SPR signals that increased with the nanodisc concentration. In contrast, injection of PBS as a blank solution showed no change in signal. A quantitative comparison of absolute binding levels between PC and PLT nanodiscs is not possible, as those nanodiscs were injected onto different flow cells. Additionally, the concentrations are only estimated, based on the assumption that the complete amount of MSP was incorporated during nanodisc assembly. In reality, the fraction of non-incorporated MSP might well be different between preparations, and therefore the final ND concentration.

Regeneration of the SAM chip was similar for the PC and platelet nanodiscs. Different regeneration solutions were tested, including different pH ranges (acidic to basic conditions), high ionic strength and the addition of detergents (see fig. 3.10). Acidic regeneration (10 mM glycine with pH 2.0 or 1.5) as well as high ionic strength (2 M $MgCl_2$) worked best. As glycine pH 1.5 showed slightly better results for PLT nanodiscs, it was used for further experiments.

As a proof for binding of nanodiscs, instead of for example just left-over MSP, dissolution of bound nanodiscs with different detergents was examined. This treatment should either not influence binding of his-tagged MSP to the anti-His antibody on the chip, or lead to a complete regeneration. Bound nanodiscs however should be dissolved, leading to

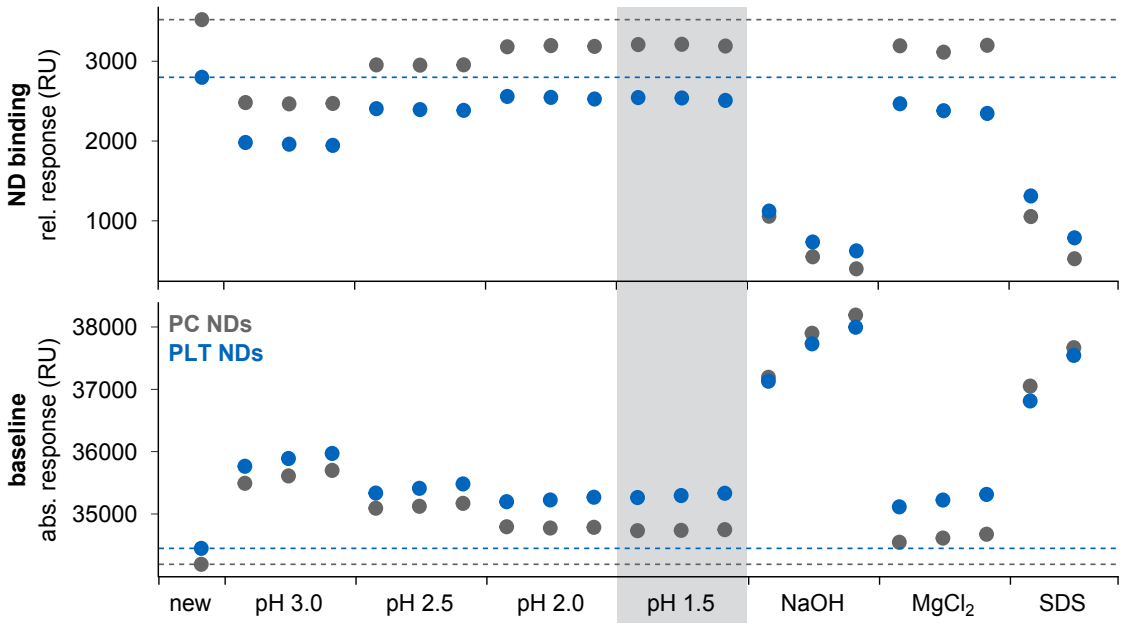

Figure 3.10: Regeneration of PC nanodiscs (grey) and platelet nanodiscs (blue) with 10 mM glycine pH 3.0, pH 2.5, pH 2.0, pH 1.5, 50 mM NaOH, 2 M $MgCl_2$, and 0.1 % SDS pH 1 (from left to right). Lower panel: baseline at the beginning of each cycle. Upper panel: nanodisc binding relative to the baseline. Dashed lines indicate the original levels attained on a new SPR chip.

an incomplete regeneration, as lipids and membrane proteins are washed away, while the MSP remains bound the anti-His antibody on the chip.

For this experiment, rising concentrations of either Triton X-100 or Tween 20 were injected (see figure 3.11). Injection of PBS or very low concentrations of Triton X-100 (0.002 or 0.01 %) led only to a slight bulk shift overlaying the extrapolated dissociation curve (dotted lines). However, at a concentration of 0.05 % Triton, the signal suddenly dropped, establishing a new baseline of only MSP bound to the chip. This new baseline was still much higher than the one before binding of the nanodiscs, which means that something must have remained bound to the chip. In contrast, Tween-20 did not seem to be able to dissolve NDs, even at high concentrations. Thus, it could be used as a buffer component to prevent unspecific binding in further experiments.

After binding of NDs to the chip could be shown, the next step was addition of antibodies against different parts of the nanodiscs. For this purpose, platelet nanodiscs in a concentration of 2 µM were first injected onto Fc2 for 5 min, followed by a second 5 min injection of antibody and finally regeneration with 10 mM glycine at pH 1.5.

The anti-PEG antibody recognized the stabilizing agent PEG-PE that had been integrated into the lipid bilayer. Thus it should bind to all nanodiscs, whether they contained membrane proteins or not. In contrast, antibodies against GPIIb and GPIX only showed a weak unspecific signal, that was comparable to the control antibody anti-procalcitonin (see fig. 3.12).

This negative result could be either due to a fault with the antibody, or with the nanodiscs. As ND binding to the chip had been proven, it could be assumed that too

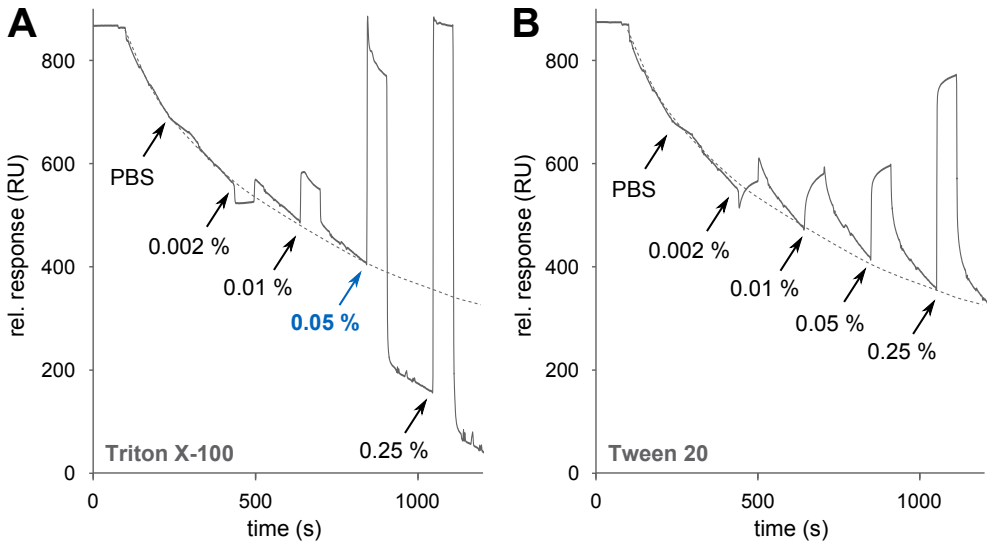

Figure 3.11: Dissolution of PC nanodiscs with rising concentrations of (A) Triton X-100 and (B) Tween 20. Nanodiscs were bound to a CM5 chip via anti-His antibodies and treated with rising concentrations of detergent. Dissolution of nanodiscs starts at 0.05 % Triton X-100 (blue arrow). Dashed lines indicate an extrapolation of the dissociation curve without detergent.

many nanodiscs without the required membrane protein were bound to the chip, and not enough containing the desired protein. In order to overcome this obstacle, and to enrich the desired nanodisc fraction, anti-GP receptor antibodies were immobilized on the chip instead of the anti-His antibodies. With this approach, only platelet nanodiscs containing those membrane proteins should be able to bind to the surface. Anti-GPIX antibodies were used for this purpose, as they possessed a higher binding affinity than anti-GPIIb. However, this approach did not lead to any nanodisc binding at all (data not shown).

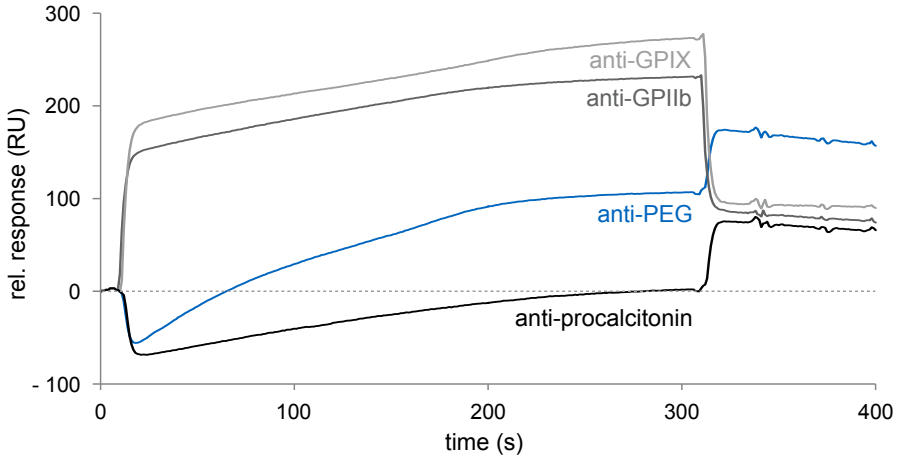

Figure 3.12: Different antibodies (anti-GPIX, anti-GPIIb, anti-PEG and anti-procalcitonin as negative control) were added to platelet nanodiscs immobilized via anti-His onto a CM5 chip. Only anti-PEG (blue line) showed any binding compared to the negative control anti-procalcitonin.

3.1.4.3 ELISA

Replication of these experiments with ELISA instead of SPR did not change the results, although ELISA is much more sensitive than SPR due to the signal amplification by an enzyme-linked secondary antibody. The set-up of the SPR experiments was replicated as exactly as possible. Anti-His antibodies were immobilized in the wells of a 96-well PolySorp plate, and remaining binding sites were blocked with 5 % skim milk powder. Platelet nanodiscs were bound to this surface, and finally incubated with the antibodies used in the SPR experiment above (anti-GPIIb and anti-GPIX) and a corresponding secondary antibody. However, no binding of those antibodies to nanodiscs could be observed, although all controls worked as expected (data not shown).

Even if the incorporation of membrane proteins GPIIb/IIIa and GPIb/IX from platelets into all nanodiscs used for SPR and ELISA experiments had been verified by Western Blot controls, those proteins could not be detected by either SPR or ELISA directly. This was most probably due to the lower sensitivity of those methods.

If literature estimates for the sensitivity of WB, SPR and ELISA are compared, WB needs by far the smallest sample amount for detection. For SPR, a rule of thumb suggests that binding of about 1 pg of protein per mm^2 of chip surface leads to a refractory change of 1 RU. As the dimensions of a flow cell have been determined to be 0.54×2.28 mm, this leads to a total surface area of 1.23 mm^2, and to a requirement of about 40 pg of bound protein for a signal change of 50 RU (Anderluh et al., 2005).

The detection limit of ELISA with HRP-coupled secondary antibodies and a TMB substrate can be as low as 10 pg of protein per well, if all parameters are adjusted optimally (Zhang et al., 2013).

By contrast, the detection limit of our WB system is estimated to be at about 100 fg protein per band according to the manufacturer's description. This is 100 times more sensitive than ELISA, and 400 times more sensitive than SPR. Additionally, the sample for Western Blot is applied completely, whereas both SPR and ELISA only detect proteins that are actually bound to the test surface. It can be assumed that not the entire amount of protein present in the sample will be captured, so the protein amounts given above are a very optimistic estimate. Thus, for the detection of membrane proteins integrated into nanodiscs, a much higher protein amount would be necessary for ELISA or SPR than for WB.

There are several different solutions for this problems. The lower sensitivity of SPR or ELISA could be compensated by different factors:

1. a higher total amount of nanodiscs could be immobilized to the surface
2. the number of receptor molecules per nanodisc could be increased
3. the fraction of nanodiscs containing the desired proteins could be enhanced
4. the nanodiscs containing the desired proteins could be selectively enriched
5. the sensitivity of either SPR or ELISA could be improved

Furthermore, all previous experiments were conducted with purified, mostly monoclonal

antibodies with excellent binding characteristics and in more or less unlimited amounts. In contrast, the aim of this project is detection of autoantibodies in serum samples, which are present in much lower concentrations and potentially show worse binding characteristics. This means that the sensitivity of for example the ELISA should be augmented by at least a factor 500 to 5000, in order to be able to differentiate clearly between samples with and without autoantibodies.

It is not realistic to increase the sensitivity of an ELISA or SPR assay with serum samples by that much only by optimization of the methods themselves. The easiest factors to adjust are for both methods the immobilization, suppression of unspecific signal, and improvement of the signal-to-noise ratio by ideal washing and blocking (Studentsov et al., 2002). All this will most probably not be enough, especially as serum samples lead to a higher unspecific signal than purified antibodies in buffer solutions.

Thus, the most promising factor remaining are the nanodiscs themselves. Generation of nanodiscs can certainly be optimized, as the technique is new enough that drastic increases in efficiency can certainly be expected. However, for this project a different approach has been chosen. The raw material for nanodisc generation and thus antigen isolation has been unmodified human platelets so far, which have both a limited expression rate and a limited total quantity. Therefore, it was tried to express the platelet antigens recombinantly in cultured cells.

3.2 Expression of GPIIb/IIIa and GPIb/IX in HEK-293 cells

Recombinant expression of platelet GP receptors in cultured cells could improve the planned assay on multiple levels at once: both the total number of cells and the number of glycoprotein molecules per cell could be increased by several orders of magnitude. Copy numbers of up to several million per cell are not uncommon for expression of membrane proteins (Andréll and Tate, 2013), in contrast to expression levels below 100,000 on platelets (Saboor et al., 2013). The total number of cultured cells can easily be up-scaled in contrast to platelet numbers isolated from the blood of voluntary donors. Most importantly, the membrane proteins can be modified in different ways (Wurm, 2004). Protein tags allow more efficient immobilization, purification and enrichment, while at the same time facilitating culturing of cells. The right choice of cloning and expression conditions allows for selection of cells and adjustment of the expression level.

3.2.1 Choice of overexpression system

Overexpression of proteins is most commonly done in bacterial cells, which are easy to modify and handle, and do not need special equipment for cultivation. However, expression of membrane proteins in bacterial systems remains challenging due to their unique physical properties and requirement for association with cellular membranes (Schlegel et al., 2010). Bacterial cells do in fact contain one or more membrane layers, but those are different from the eukaryotic plasma membrane. The lipid composition of the membrane is different in bacteria and can lead to incorrect folding and function of overexpressed membrane proteins (Freigassner et al., 2009).

Additionally, protein expression and intracellular transport differ widely between bacteria and eukaryotic cells. Eukaryotic membrane proteins are translated directly into the endoplasmatic reticulum (ER) membrane, which ensures their correct localization on the plasma membrane (Grisshammer, 2006). In bacteria, membrane proteins must be overexpressed in such a way that they properly insert into a membrane from which they can be purified after detergent extraction or wherein they can be studied directly. Otherwise, they are expressed in inclusion bodies, from which they have to be isolated and refolded to regain their native conformation (Thomas and Tate, 2014).

Additionally, most eukaryotic membrane proteins are glycosylated when inserted into the ER membrane, and for a considerable number of them this is essential for proper folding, stability and function (Freigassner et al., 2009). Glycosylation patterns are organism and cell type dependent, and are only rudimentary in bacteria.

All those challenges discourage the use of bacterial cells for a recombinant expression system. Instead, eukaryotic cells should be used, ideally mammal cells. The downsides of membrane protein expression in eukaryotic cells, the low yield of product in comparison to prokaryotic cells as well as the their complicated handling, are more than balanced by their more native-like expression of glycoproteins (Wurm, 2004). As the purpose of the expressed proteins is to serve as target for patient autoantibodies, the extracellular part should mimic the original platelet proteins as closely as possible. This can only be achieved by expression

in human cells, ideally derived from megakaryocytes, which are platelet progenitor cells. Cell lines derived from megakaryocytes express all platelet membrane proteins, and could be used directly as a protein source. This would allow production of an unlimited number of cells, but in order improve other assay characteristics, enhancement of the expression rate and modification of the proteins would be beneficial. Additionally, it would be useful to generate cell lines which express only one of the GP complexes, but not the others. Thus, subsets of autoantibodies against different targets could be differentiated.

With those conditions in mind, the human kidney cell line HEK-293 was chosen as the ideal expression system. It is a semi-adherent fibroblastoid cell line growing as a monolayer. It has a high transfection efficiency, the capacity to express transgenic receptor proteins with high fidelity (Thomas and Smart, 2005) and higher protein yields as compared to other mammalian cells (Wurm, 2004). These attributes together with the cell size, morphology, the ease of maintenance and a high growth rate with a doubling time of about 24 - 30 hours (Thomas and Smart, 2005) have established HEK-293 cells as a host of choice for heterologous expression of membrane proteins. The wild type cells do not express the glycoprotein complexes GPIIb/IIIa and GPIb/IX.

Stable, functional expression of GPIIb/IIIa complexes in HEK-293 cells has been published various times. Examples are generation of stable cell lines by electroporation (Abraham et al., 1997) or by chemical transfection (Filizola et al., 2004).

While transient transfection of GPIb/IX in HEK-293 is not uncommon, a completely stable cell line has not yet been published. Mostly, stable cell lines expressing only one or two of the subunits are supplemented by transient expression of the missing parts (Zhang et al., 2015; Lavenu-Bombled et al., 2016). However, stable expression of complete GPIb/IX complexes has been published in other cell types. López et al. (1992) generated stable CHO (Chinese Hamster Ovary) and L cell lines (mouse fibroblasts), which are derived from hamster and mouse cells respectively. Those cell lines have been used by many different groups mainly for structural studies, the receptors have been shown to be functional and to bind to von Willebrand factor. Another approach has been the generation of chimeric proteins, where a portion of the extracellular domain of GPIbα was grafted onto the transmembrane/intracellular domain of the single chain surface molecule ICAM-1 (Petersen et al., 1996).

3.2.2 Cloning of GPIIb/IIIa and GPIb/IX plasmids

3.2.2.1 Choice of vector

For this project, the vector backbone pcDNA3 has been chosen, that contains a complete eukaryotic operon as well as other other parts necessary for protein expression in HEK-293 cells (see fig. 3.13):

- a multiple cloning site (MCS) for insertion of the gene of interest
- human cytomegalovirus (CMV) immediate-early promoter/enhancer: binding site for RNA polymerase and transcription factors

- T7 promoter: for *in vitro* transcription in the sense orientation
- bovine growth hormone (BGH) polyadenylation signal: Efficient transcription termination and polyadenylation of mRNA
- neomycin resistance gene: G418 resistance for selection of stable transfectants

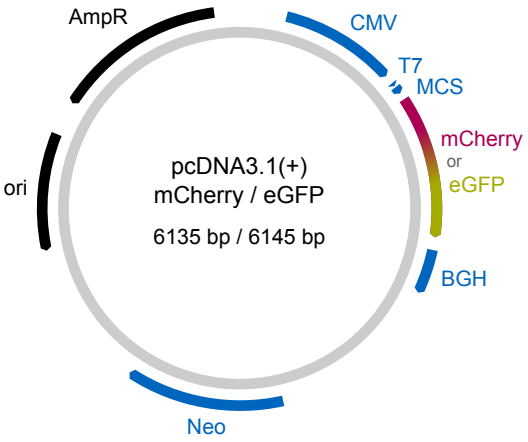

Figure 3.13: Plasmid map of pcDNA3(+) with mCherry / eGFP. Sequences for protein expression in HEK-293 cells are shown in blue, while bacterial elements are black. Fluorescent tags mCherry or eGFP are red and green. The protein of interest can be inserted into the multiple cloning site (MCS).

Additionally, the plasmid contains a bacterial origin of replication and an ampicillin resistance gene, which enable easy amplification, modification and storage of the plasmid in *E. coli*.

Two slightly modified versions of this plasmid were used, with fluorescent tags already included into the multiple cloning sites. In the plasmid # 30125, a mCherry fluorescent tag is added directly to the intracellular C-terminus of the protein of interest, in the plasmid # 30127 an eGFP tag.

3.2.2.2 Cloning strategy

The general approach for the generation of HEK-293 cells expressing a protein of interest consists of the following steps:

1. amplification of the gene of interest via polymerase chain reaction (PCR) and addition of necessary sequences to the DNA ends via PCR primers
2. generation of single-stranded, overlapping DNA ends with restriction enzymes
3. ligation into the desired, pre-digested plasmid
4. transformation into *E. coli*, selection and amplification
5. extraction from *E. coli* and purification
6. transfection of purified DNA into HEK-293 cells
7. selection of expressing cells

Both desired GP complexes contain multiple subunits each, so multiple gene sequences had to be transferred into the HEK-293 cells. Integration of DNA sequences into HEK-293 cells is a statistical process, with the success rate depending on different factors such as the length of the desired DNA sequence (Hornstein et al., 2016). Generally, co-transfection of two plasmids is difficult but possible, whereas co-transfection of three plasmids is very unlikely. Therefore two different strategies were used for GPIIb/IIIa and GPIb/IX.

For GPIIb/IIIa, which consists of only two subunits, a separate plasmid was used for each subunit. GPIIb was inserted into the vector # 30125, thus adding a mCherry fluorescent tag at its C-terminus. For GPIIIa the vector # 30127 was used, combining it with eGFP. Just in case those fluorescent tags might disturb downstream processing as well as further applications of the protein, a TEV cleavage site was added in between protein and tag (see fig. 3.14).

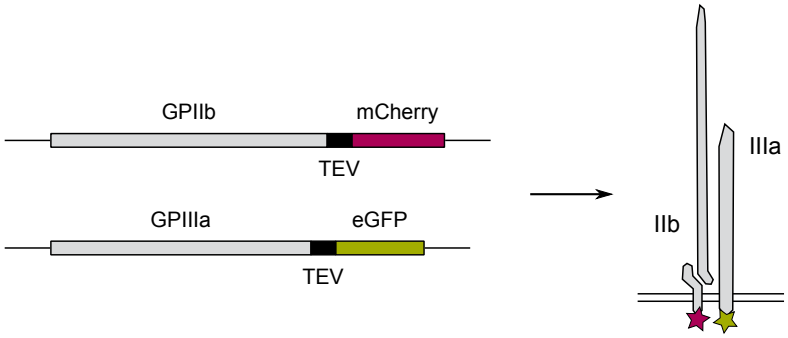

Figure 3.14: Schematic illustration of GPIIb/IIIa DNA sequences (left) and resulting protein complex (right).

In contrast, GPIb/IX consists of three different types of subunit, GPIbα, GPIbβ and GPIX. The biggest subunit, GPIBA, was inserted into the vector # 30125 with mCherry, analogous to the approach for GPIIb. The two smaller subunits were combined and inserted into the plasmid # 30127. In order to save space, the controlling regions for protein expression were not duplicated, instead a so-called P2A sequence was inserted between the proteins (Szymczak and Vignali, 2005; Kim et al., 2011). This sequence leads to an interruption of the translated amino acid chain, one peptide bond of this 19 amino acid sequence will not be generated. Thus, two amino acid chains exit the ribosome as separated proteins: The first protein (GPIX in this case) contains a 18 amino acid part of the P2A sequence at its C-terminus, and the second protein (GPIbβ in this case) contains a single additional proline residue at its N-terminus, and the eGFP tag added by the pcDNA3 plasmid at its C-terminus (fig. 3.15).

3.2.2.3 Amplification of coding sequences and insertion into the target vectors

The first step for cloning of the desired glycoprotein DNA constructs was amplification of the coding sequences by PCR. Aim of the amplification was both maximum yield and purity. The reaction conditions had to be optimized for each gene and primer pair concerning reaction buffer conditions and temperature. The resulting DNA was analyzed

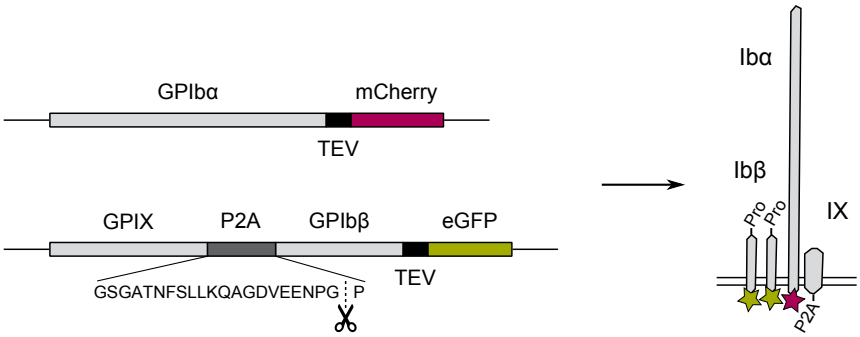

Figure 3.15: Schematic illustration of GPIb/IX DNA sequences (left) and resulting protein complex (right). The amino acid sequence and cleavage site of the P2A sequence is depicted underneath the DNA sequence.

by agarose gel electrophoresis of the unprocessed PCR reaction.

Only if a dominant band at about the correct size was visible, ideally without disturbing additional bands, a control digest with different enzymes was performed. The correct sequence was verified by comparison of the resulting pattern on the agarose gel with the theoretical pattern generated with the software ApE (A plasmid Editor). While the single constructs GPIIb, GPIIIa and GPIbα could be inserted directly into the corresponding vectors once their control digest pattern had been confirmed, the GPIX-P2A-GPIbβ-TEV construct took one extra step. The GPIX and GPIbβ PCR products were digested with XhoI, mixed, ligated and amplified by one more PCR step with the primers GPIX fw and GPIBB rv. The resulting sequence could be treated just like the single constructs and was also verified by control digest and agarose gel electrophoresis.

The resulting agarose gel electrophoresis pattern showed successful amplification of all GP coding sequences. Only GPIIIa and GPIbα showed weak secondary bands with lower molecular weights, which did not disturb further cloning steps. Otherwise, all sizes of DNA fragments before and after control digest with AvaI were exactly as expected.

Once the DNA fragments showed the correct total size and control digest patterns (see fig. 3.16), they were inserted into the target vector pcDNA3 with either mCherry or eGFP. The DNA was digested with both HindIII and SspI, and mixed with the corresponding pre-digested vector. The overlapping single-stranded DNA ends of matching sequences annealed and were connected by a T4 DNA ligase, which repaired single-strand nicks. Chemically competent *E. coli* NEB5alpha were transformed with the now complete vectors, and grown on agar plates with the selection medium ampicillin. Only if a bacterial cell took up and amplified a complete vector molecule without any strand breaks, it could express the antibiotic resistance genes and survive on medium supplemented with this antibiotic. Thus bacteria containing whole plasmids formed colonies that could be picked individually and analyzed further.

3.2.2.4 Analysis of final plasmids

The bacterial colonies were picked from the agar plates and grown as overnight cultures in LB medium containing ampicillin. Plasmid DNA isolated from those clones by Miniprep

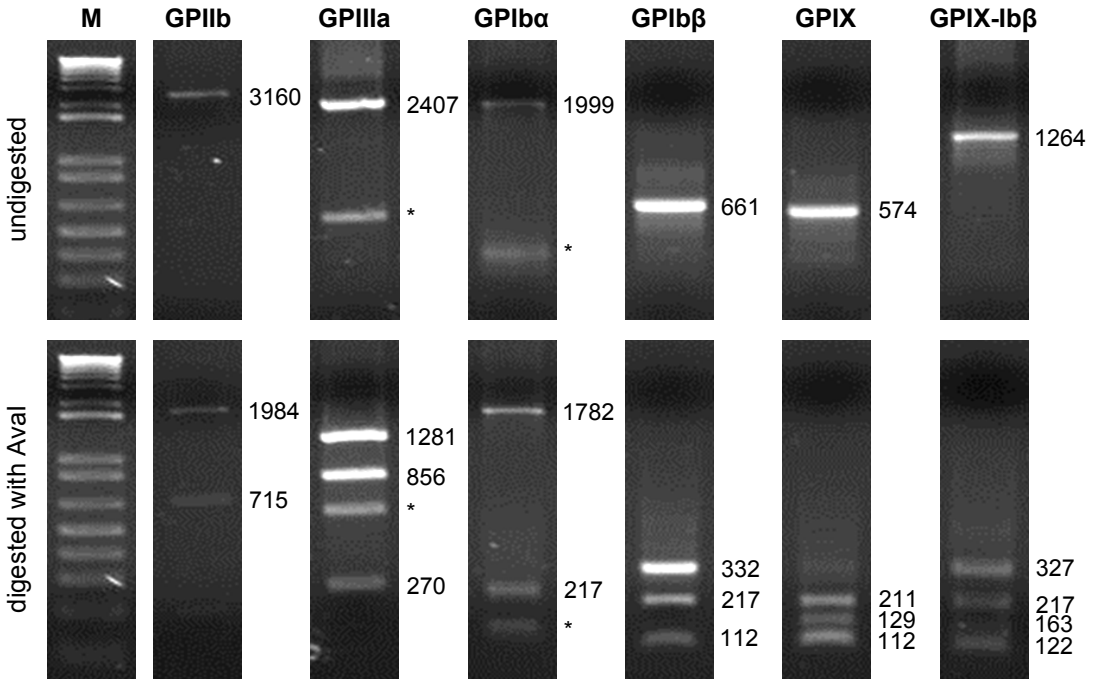

Figure 3.16: Agarose gel electrophoresis of all PCR products. Undigested DNA fragments (upper panel) and AvaI-digested DNA (lower panel) are shown with sizes of expected bands in bp. For size comparison, a 1 kb Plus DNA Ladder (Invitrogen) is shown on the left. Unexpected bands are tagged with a *.

was controlled for the correct insert by control digest. As there were always clones which took up some of the remaining undigested vector molecules, these had to be separated from the cells containing the correct vector with the desired insert. For this purpose, isolated plasmid DNA was digested with HindIII and SspI, resulting in an excision of the previously introduced GP insert.

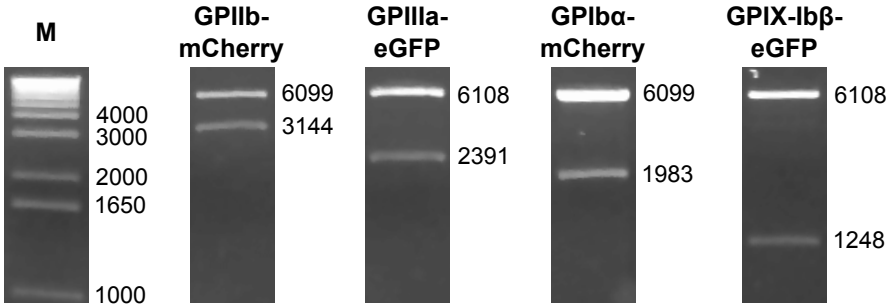

Figure 3.17: Agarose gel electrophoresis of final plasmids digested with HindIII and SspI. Calculated lengths of DNA fragments in bp are shown directly right of respective bands. For size comparison, a 1 kb Plus DNA Ladder is shown on the left.

Clones which showed the correct total plasmid size and digest pattern (see fig. 3.17) were then sequenced, in order to exclude critical point mutations that can not be detected by a mere control digest. The sequencing resulted in 100 % identity with the theoretical sequence for all constructs except GPIIIa-eGFP, which showed two silent point mutations. They changed the DNA sequence, but resulted in codons for the same amino acids as the

original sequence. Even though analysis of the codon usage in human cells showed a slightly decreased frequency for the mutated codons, in slowly growing organisms the codon usage is not crucial for the translation efficiency. Thus the mutations were ignored, and the sequence used as it was.

After the sequence had been verified, the selected *E. coli* clones were grown in bigger quantities. For transfection of HEK-293 cells, DNA was isolated by Miniprep and purified again with a DNA cleaning kit in order to remove remaining *E. coli* endotoxins, which can significantly affect cell proliferation and viability and decrease transfection efficiency in many eukaryotic cell lines (Butash et al., 2000). Once amount and purity of the DNA were sufficient, the DNA was ready for transfection into HEK-293 cells.

3.2.3 Expression of GPIIb/IIIa and GPIb/IX in HEK-293 cells

3.2.3.1 Transfection of HEK-293 cell lines

For chemical transfection of HEK-293 cells, the TransIT®-LT1 Transfection Reagent from Mirus Bio LLC was used. According to the manufacturer's description, this chemical consists of a lipid and protein/polyamine mixture that forms complexes with DNA, which can pass the plasma and nuclear membranes. In the nucleus, the DNA either remains in the original plasmid form and serves as template for mRNA before it will be gradually degraded (transient cell lines), or in some rare cases it will be integrated permanently into the chromosomal DNA (stable cell lines). Only if this happens, the DNA remains permanently in the cells and will be passed on during cell division (He et al., 2014).

After transient transfection, proteins are normally expressed for 48 to 96 hours. However, for this project the cells are needed as a constant source of protein, so a stable insertion into the genome was ensured by antibiotic selection for several weeks. In contrast to transient expression, stable expression allows long term, as well as defined and reproducible, expression of the gene of interest.

This was achieved by antibiotic selection for at least two weeks after transfection. Under selection conditions, all cells that had only taken up the vector transiently and not included it into their genome slowly died, until only stable transfectants were left. The resulting stable cell lines however still consisted of different cell populations, which expressed the proteins of interest in different combinations or in different degrees. As both vectors used together for the co-transfections contained the same antibiotic resistance for G418, cells expressing all of the GP subunits had to be isolated from those with only partial expression. For this purpose, the fluorescence of the fused eGFP and mCherry protein tags was used for flow cytometric analysis of stably transfected HEK-293 cells (see fig. 3.18).

Here, different cell populations could be clearly seen, which indicated different combinations of recombinant GP receptor subunits in the transfected cells. The double positive populations could be separated from the two single positive ones, expressing either the eGFP or the mCherry fluorescent fusion protein. Besides fluorescent cells, in both transfectants a double negative population could be observed. It had only acquired the antibiotic

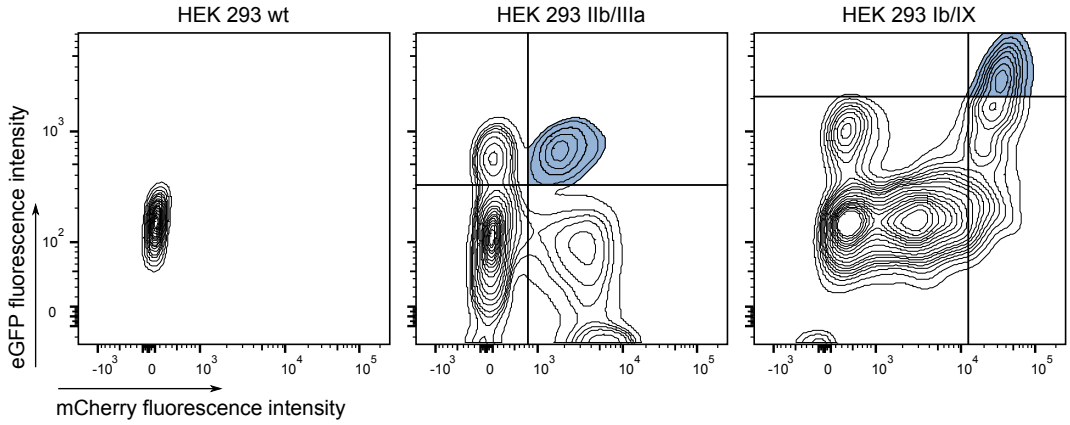

Figure 3.18: Sorting results (contour plots) of transfected HEK-293 cells showing eGFP and mCherry fluorescence. Cells depicted in blue were considered positive for both eGFP and mCherry. Untransfected wild type (wt) HEK-293 cells were used as negative control.

resistance, or lost the fluorescent fusion proteins during the integration into the genome. 5.2 % and 4.8 % of the GPIIb/IIIa and GPIb/IX transfectants, respectively, showed up as double positive cells, having both of the transfected plasmids integrated in their genome (highlighted in blue in fig. 3.18). The double positive transfectants were considered to express the complete GPIIb/IIIa or GPIb/IX complex. Hence, 300,000 cells of the double positive population were bulk sorted by FACS.

While for cells transfected with GPIIb/IIIa the intensity of eGFP or mCherry fluorescence was similar in single and double transfected cells, the fluorescence intensity was much higher in the double positive GPIb/IX transfectants when compared to the respective single expressing populations. A potential explanation is that efficient plasma membrane expression of the GPIb/IX complex requires the presence of all three subunits (López et al., 1992). In the absence of one of the subunits, the others are mostly degraded instead of transported to the plasma membrane.

Both HEK-293 IIb/IIIa and HEK-293 Ib/IX cell lines were propagated for their use in further experiments under permanent G418 antibiotic selection in order to prevent loss of the desired genes. Of each cell type, back-ups were frozen in liquid nitrogen, and could be revived as desired.

3.2.3.2 Analysis of gene expression

After expression of both fluorescent molecules in both HEK-293 IIb/IIIa and HEK-293 Ib/IX had been confirmed, the next step was to find out where the proteins were localized. Fluorescence microscopy clearly showed localization of the two fluorescent markers on the plasma membrane of both cell lines (see fig. 3.19). As soluble eGFP or mCherry would have been expressed in the cytoplasm, this result gave a first hint to the covalent bond between the fluorescent tags and the corresponding membrane proteins.

The next step was examination of the cells by Western Blot. Whole HEK-293 IIb/IIIa and HEK-293 Ib/IX cells were lysed with 1 % OG, centrifuged to remove cell debris, and the lysate was applied to a SDS PAGE. After transfer of the separated protein bands

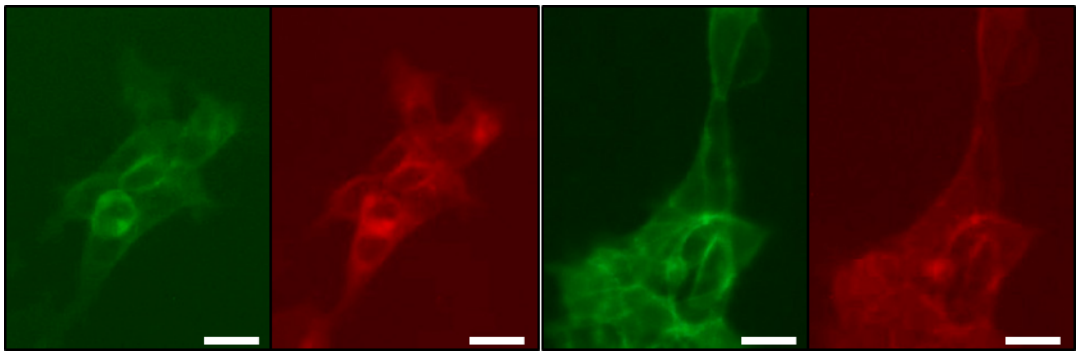

Figure 3.19: Fluorescence microscopy of HEK-293 IIb/IIIa (left) and HEK-293 Ib/IX (right). Images were taken in GFP (green) and RFP (red) channels with a 40x objective. The scale bar equals 20 µm.

onto a PVDF membrane, the presence of different proteins was examined by WB with the following antibodies: anti-GPIIb and anti-GPIIIa for the GPIIb/IIIa complex, and anti-GPIbα, anti-GPIbβ and anti-GPIX for the GPIb/IX. HEK-293 wt lysate and human platelet lysate were used as control samples.

All GP receptor components could be detected in the respective cell types, in contrast to the negative controls. For all HEK-293 proteins, the molecular weights were higher than for platelet proteins, due to the additional fluorescent tags, or the additional P2A amino acids in the case of GPIX. Interestingly, for HEK-293 IIb/IIIa cells both GPs showed double bands, whereas the platelet lysate only resulted in single bands at the appropriate size. As HEK-293 wt cells did not show GPIIb or GPIIIa expression, this was not due to native expression of those proteins in HEK-293 cells. Instead, it could be due to different glycosylation patterns. For very high expression rates, the cellular glycosylation machinery can be insufficient (Grisshammer, 2006), which would lead to incomplete glycosylation and thus the emergence of double bands.

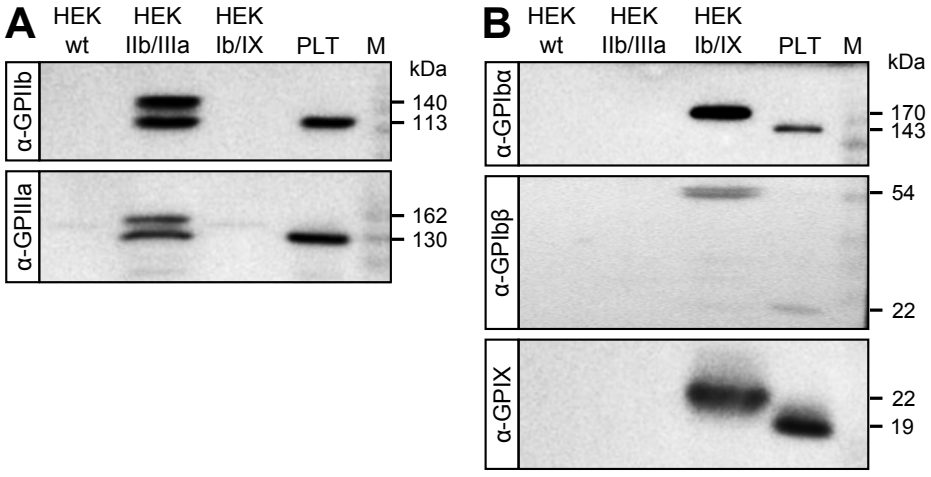

Figure 3.20: Western Blot of HEK-293 cell lysates (HEK-293 wt, HEK-293 IIb/IIIa and HEK-293 Ib/IX) as well as platelet lysates (PLT). (A) Antibodies against components of the GPIIb/IIIa complex. (B) Antibodies against components of the GPIb/IX complex. M = Full-Range Rainbow Molecular Weight Marker.

EGFP and mCherry co-expression on the plasma membrane as well as verification of proteins by WB already indicated that the recombinant GP receptors were present on the cellular plasma membrane. However, the correct folding and assembly of the GP receptors as well as their transport to and actual presence on the cell surface remained to be confirmed by receptor-specific methods. For this purpose, sorted HEK-293 transfectants were stained with complex-specific primary antibodies (IgG clones AP-2 and SZ1 for GPIIb/IIIa and GPIb/IX, respectively), combined with an AlexaFluor 350 (AF350) labeled secondary antibody and analyzed by FACS. Here it was necessary to chose a fluorescent label that did not interfere with either mCherry or eGFP, as those colors were already present on the cells. Importantly, the complex-specific antibodies only recognize the extracellular domains of correctly folded and assembled GP receptor complexes. Furthermore, as the cells had not been permeabilized prior to staining, the antibodies could not enter the cells and thus only bind to proteins expressed on the plasma membrane surface.

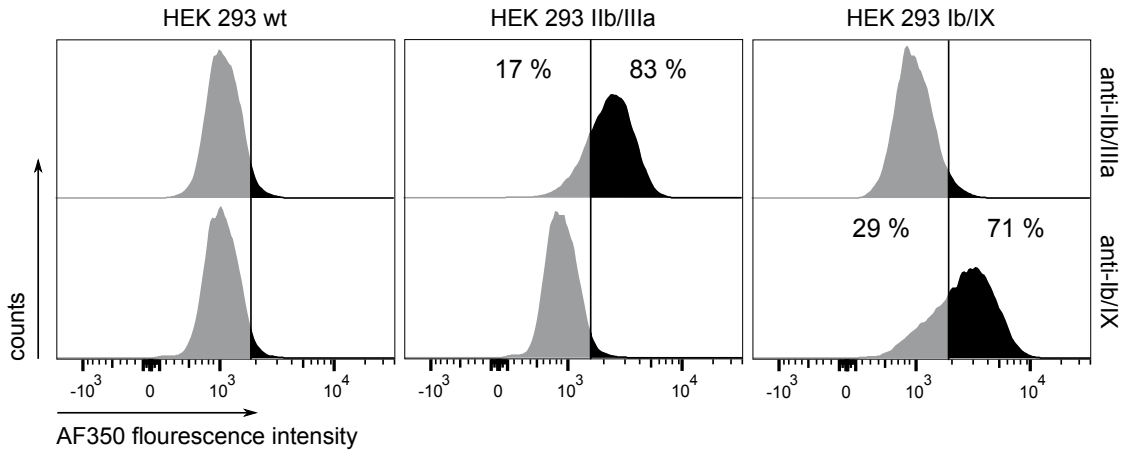

Figure 3.21: Presence of GPIIb/IIIa and GPIb/IX on the cell surface of HEK-293. Shown are histograms from flow cytometry experiments with stably transfected and sorted HEK-293 cells expressing either GPIIb/IIIa or GPIb/IX after staining with complex-specific antibodies (anti-GPIIb/IIIa or anti-GPIb/IX). Untransfected HEK-293 wt cells served as negative control. The chosen cut-off (vertical lines) for each HEK-293 cell line lead to an average of 95 % negative cells in all control experiments.

The FACS histograms showed a clear right shift of the AF350 fluorescence intensity peak in both HEK-293 IIb/IIIa and HEK-293 Ib/IX cells upon probing with the respective antibody, anti-IIb/IIIa and anti-Ib/IX, respectively (fig. 3.21). In contrast, untransfected HEK-293 wt cells as well as HEK-293 transfectants stained with control antibodies (antibodies against the not-expressed GP complex and the respective isotype controls) behaved similar to the unstained HEK-293 cells in the FACS experiment (fig. 3.21 and data not shown). An AF350 fluorescence intensity cut-off that lead to an average of 5 % positive cells in all control experiments resulted in 83 % and 71 % positive cells for HEK-293 IIb/IIIa and HEK-293 Ib/IX transfectants, respectively.

Since the applied antibodies bound only to intact receptors and not to their individual subunits or to misfolded proteins, the obtained FACS results showed that the GP complexes were actually present, assembled to complexes, and in a native-like conformation

on the surface of stably transfected HEK-293 cells.

3.2.3.3 Stability of gene expression over time

Fluorescence of eGFP and mCherry could be detected not only in whole cells, but also in lysates resulting from solubilization of HEK-293 cells in a detergent solution. This was also the first step for generation of nanodiscs, and should be executed with a mild detergent that does not denature the membrane proteins. As the fluorescence of both eGFP and mCherry depend on their 3D structure and thus on correct protein folding (Shaner et al., 2005), verification of fluorescence in the lysates (fig. 3.22) proved that at least the fluorescent proteins still possessed their native conformation.

Both cell lines showed fluorescence after excitation at 475 nm (for eGFP) and 570 nm (for mCherry). The HEK-293 Ib/IX cells showed more than twice as much green fluorescence as HEK-293 IIb/IIIa cells, whereas mCherry fluorescence was much more pronounced in HEK-293 IIb/IIIa. The most likely explanation of the unequal eGFP expression was that each GPIb/IX complex contained two copies of eGFP (bound to the GPIbβ subunits). As for the higher fluorescence of mCherry there was no hint in whole cells, neither with FACS nor with fluorescence microscopy, it could be due to unequal solubilization by the chosen detergent. This has to be kept in mind for further experiments.

The absolute fluorescence intensity was much higher for eGFP than for mCherry. Not only is the inherent brightness of eGFP more than twice as high as that of mCherry (Shaner et al., 2005), but also is the filter set used for detection of red fluorescence not ideal for mCherry. It would be better to excite at 587 nm instead of 570 nm, but then the excitation light would overlay the emission spectrum. For eGFP this problem was less pronounced.

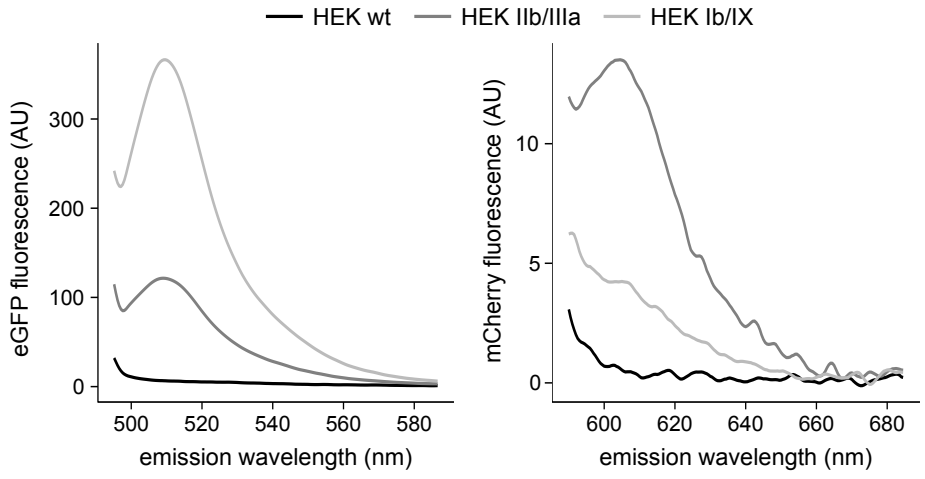

Figure 3.22: Representative fluorescence spectra of HEK-293 IIb/IIIa and HEK-293 Ib/IX lysates. Left: eGFP fluorescence, excitation wavelength 475 nm. Right: mCherry fluorescence, excitation wavelength 570 nm.

The quantification of eGFP fluorescence in cell lysates of HEK-293 transfectants via a standard curve generated from purified eGFP (fig. 3.23 A) allowed the determination

of the absolute number of GP complexes per cell (N_{GP}). The determined receptor copy numbers were very similar for both GPIIb/IIIa and GPIb/IX (fig. 3.23B).

In order to analyze the stability of the generated HEK-293 transfectants with respect to GP receptor expression, N_{GP} values were determined regularly over nine weeks (from passage P+1 to passage P+22), which corresponds to 70 cell divisions (at three passages per week, and one division every 24 hours). All in all, the copy number of both GP complexes fluctuated between 1.7 and 5.8 million copies per cell in this time, resulting for both HEK-293 transfectants in a medium copy number of 3.2 million GP complexes per cell. These numbers are in accordance with those published for other membrane proteins / receptors in the past (Andréll and Tate, 2013). They exceeded the reported copy numbers for GPIIb/IIIa and GPIb/IX receptors in platelets (100,000 and 50,000 receptors per cell, respectively (Saboor et al., 2013)) by more than 20-fold.

The expression rates of both HEK-293 cell lines did not decrease considerably over the course of 22 passages, which means that the cells could be cultured and used for at least this time period. Aging of the cells was of little importance, as the cells were only used as a raw material for protein production, and thus the only interesting parameter was the ongoing expression of the proteins of interest.

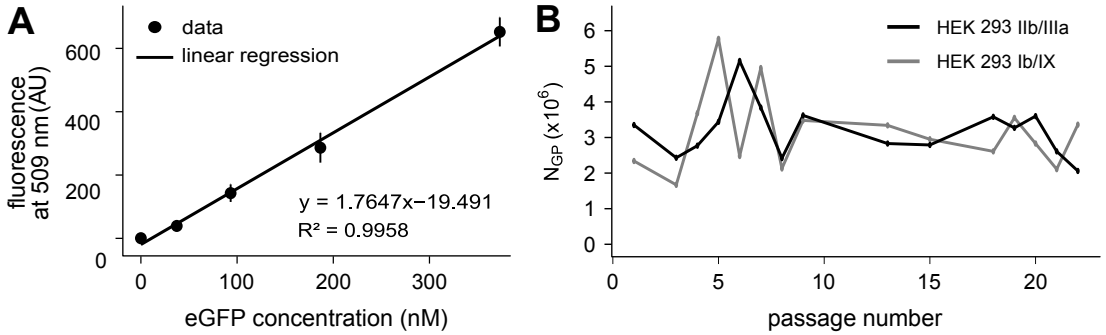

Figure 3.23: GP complex copy number per HEK-293 transfectant cell. (A) Standard curve, generated with purified eGFP dilutions, used for the determination of the concentration of eGFP in cell lysates. (B) GP complex copy numbers per cell (N_{GP}) were calculated for both HEK-293 Ib/IX and HEK-293 IIb/IIIa, between passages P+1 and P+22 according to equations 1 and 2. The curves cover data from two independent experiments.

3.2.3.4 Receptor functionality in HEK-293 cells

Functional glycoprotein receptors should be able to interact with their endogenous binding partners, fibrinogen for GPIIb/IIIa and von Willebrand factor for GPIb/IX (Kauskot and Hoylaerts, 2012). In order to test this hypothesis, glass slides were coated with the respective receptor ligand, and transfected HEK-293 cells were incubated for 1 hour at 37 °C on this surface. As negative controls, cells were exchanged for wild type HEK-293 or glass slides were coated with BSA.

Only for HEK-293 IIb/IIIa incubated on glass slides with fibrinogen, adhesion could be observed by transmission microscopy. The characteristic elongated shape of flattened cells indicated adherence of GPIIb/IIIa receptors to the fibrinogen surface. In contrast,

no adherence was observed for HEK-293 wt cells lacking GPIIb/IIIa, or if the glass slide had been coated with BSA instead of fibrinogen.

For HEK-293 Ib/IX cells however, no attachment could be observed beyond unspecific binding of round cells at all conditions, samples and negative controls alike. This result could be most probably explained by the binding characteristics of GPIb/IX. Naturally occurring GPIb/IX on thrombocytes is co-located with GPV, which links two copies of GPIb/IX complex. GPV is not necessary for vWF binding, but it stabilizes the connection (Canobbio et al., 2004). As this subunit is lacking in HEK-293 Ib/IX cells, the bond between the GP receptor and vWF could be too weak for cell adherence, or cells could be detached during washing steps.

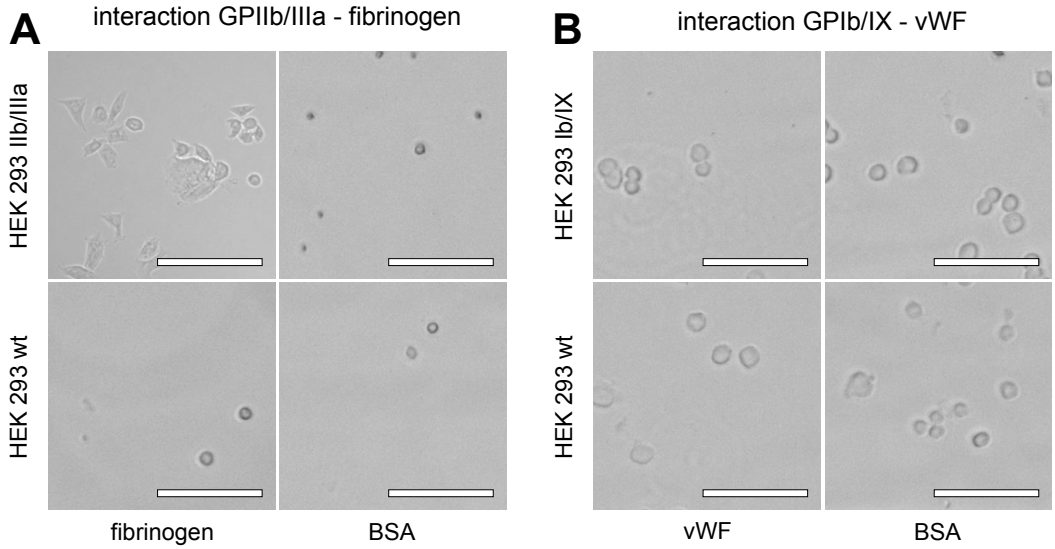

Figure 3.24: Adhesion assay for receptor functionality. Transmission microscopy images of HEK-293 IIb/IIIa, HEK-293 Ib/IX and HEK-293 wt cells incubated on glass slides coated with (A) fibrinogen or (B) vWF. Glass slides coated with BSA are shown as control. Images were taken in the transmission channel with a 10x objective. The scale bar equals 100 µm.

As the most crucial factor for the aim of this thesis, binding of patient autoantibodies to nanodiscs generated from transfected cells, was not directly dependent on functionality of receptors in whole cells, this experiment was suspended for later confirmation of receptor functionality in nanodiscs. Nevertheless, all other results so far hint to a native-like structure of the GP receptors, which is the necessary prerequisite for further experiments. The high and stable expression levels of the GP complexes in HEK-293 transfectants demonstrated the major advantage of this recombinant GP complex source over the endogenous platelet source, and enabled the generation of improved nanodiscs.

3.3 Nanodiscs with recombinant GPIIb/IIIa and GPIb/IX

After recombinant HEK-293 cell lines had been established as raw material for the production of GPIIb/IIIa and GPIb/IX complexes, the next step was the transfer of those proteins into lipid bilayer nanodiscs. The general protocol remained the same as for platelet nanodiscs, only the details had to be optimized for the new cell type. The focus was here less on nanodisc shape and size, but more on optimal performance in ELISA assays, as this was the necessary prerequisite for further experiments.

3.3.1 Adaption of nanodisc protocol for HEK-293 lysates

While the generation of nanodiscs always follows a common principle, the details of the protocol have to be adjusted for each combination of cell type and membrane protein. As the membrane proteins of interest were the same as in section 3.1 of this thesis, most parameters were kept the same for a first proof of concept experiment. Examples are the choice of detergent, the incubation conditions and the purification methods. Other details, such as the exact ratio of nanodiscs components, depend more on the type of cell lysate than on the membrane protein of interest. Those parameters were adjusted, based on experiences from previously published (Mak et al., 2017; Sun et al., 2019) and unpublished studies.

In a first experiment for the generation of nanodiscs from HEK-293 cells, the ratio of MSP, PEG-PE and lysate was varied in order to find the perfect mixture. Here, the amount of MSP was kept constant for all different nanodisc batches, while the amounts of lysate and PEG-PE were adjusted. After separation by SEC, a single nanodisc peak was the aim, with no aggregates or left-over MSP. By doing so, it was ensured that all available material from the HEK-293 cells was in fact incorporated into nanodiscs.

For nanodiscs from platelet material, the main elution peak could be found between about 9 ml and 12 ml elution volume. As the size of nanodiscs depends only on the length of the used MSP, it should be comparable for nanodiscs from HEK-293 cells. In figure 3.25 this peak is highlighted in grey.

Adjustment of the number of PEG-PE molecules is shown from left to right in figure 3.25. PEG-PE seemed to facilitate generation of nanodiscs in general. This was not surprising, as PEG-PE contains a lipid part, which can substitute a lack in membrane phospholipids. If neither enough endogenous phospholipids nor additional PEG-PE was available for the generation of nanodiscs, there was no characteristic peak observable between 9 and 12 ml.

With low amounts of PEG-PE, increase of the lysate amount mainly led to a rise of the aggregation peak. Even if the absorbance was higher than baseline between 9 ml and 12 ml with higher amounts of lysate, no clear separation of the nanodisc fraction was possible. However, additional PEG-PE seemed to allow incorporation of the excess membrane material into nanodiscs, and thus lowered the aggregation peak. At the same time, the peak consisting of leftover MSP1E3D1 disappeared. The optimal nanodisc protocol found here used 125 µg of HEK-293 cell lysate and 200 µg of PEG-PE for each 250 µg of MSP. This protocol resulted in the nanodisc curve highlighted in blue in figure 3.25 and was

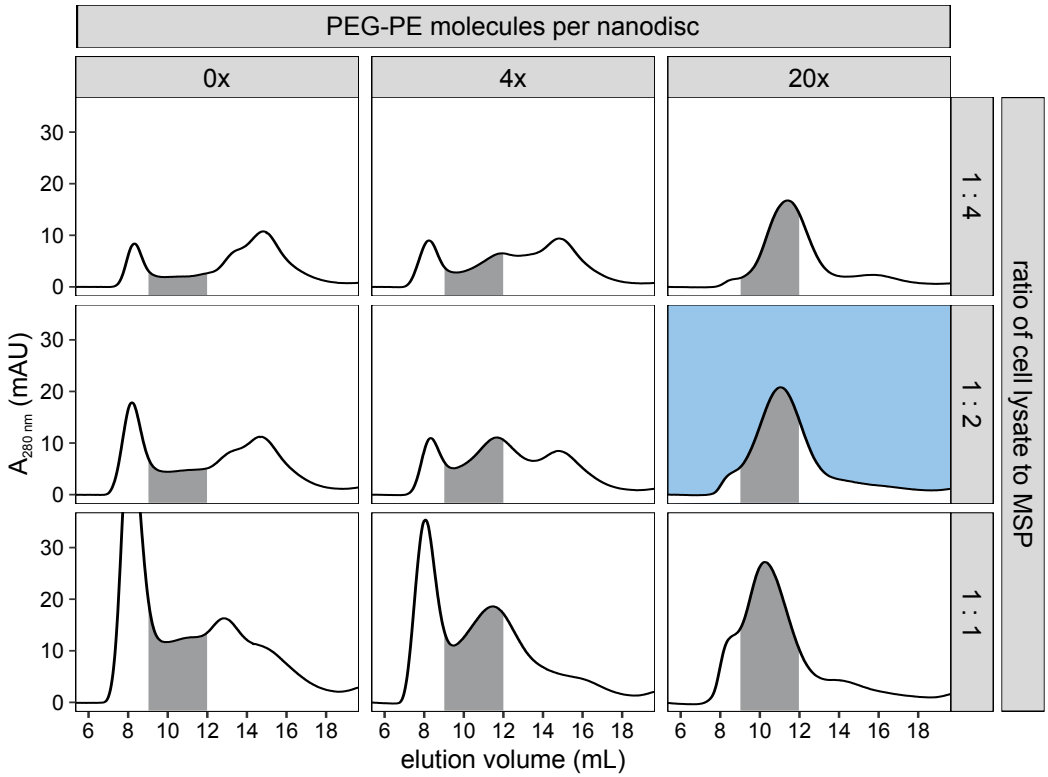

Figure 3.25: Variation of nanodisc generation protocol for HEK-293 lysates. Amounts of cells lysate and PEG-PE were varied, while the amount of MSP was kept constant. The best result is highlighted in blue.

used for all further experiments.

In conclusion, PEG-PE enabled incorporation of HEK-293 material into nanodiscs, which was important because of the contained GP receptors. A perfect peak of nanodiscs containing only PEG-PE and phospholipids would not be sufficient for further experiments.

3.3.2 ELISA with recombinant GP receptors in nanodiscs

After the raw material for the generation of nanodiscs had been changed successfully from platelets to HEK-293 cells, the experiments of section 3.1.4 could be repeated with the improved nanodiscs. ELISA was chosen as an assay format instead of SPR because of the better sensitivity and possible high-throughput, which would eventually facilitate the measurement of patient samples.

3.3.2.1 Proof of concept

For detection of the all GP subunits in a nanodisc-ELISA, the set-up was designed as follows (see fig. 3.26 A): A 96-well plate was coated with GFP- or RFP-nanobodies, which consist of only one single monomeric variable antibody domain. Those nanobodies were more stable than conventional antibodies, and showed excellent binding characteristics towards eGFP or mCherry, respectively. Additionally, as they have been derived from alpaca

antibodies, there was no danger of cross-reaction with potential detection or secondary antibodies (Vincke and Muyldermans, 2012).

In order to prevent unspecific binding of nanodiscs or antibodies to free spaces on the plastic plate, the surface was blocked with skim milk powder solution after the capture step. Different kinds of nanodiscs could now be added, with or without GP receptors incorporated. The eGFP and/or mCherry tags of the GP receptors bound to the nanobodies, and all nanodiscs not containing the recombinant GPs were washed away. Thus, GP-containing nanodiscs were specifically enriched on the surface.

Added anti-GP detection antibodies could now bind to the "extracellular" side of the nanodiscs. The GP complexes were perfectly orientated because of their directed immobilization. As their "intracellular" sides always pointed to the plastic surface of the plate, there was no steric inhibition for binding antibodies. A corresponding secondary antibody covalently bound to horseradish peroxidase (HRP) was then added, which in turn changed the color of the chromogenic ELISA substrate TMB (3,3',5,5'-Tetramethylbenzidine) from colorless to blue. The color changed to yellow (A_{max} at 450 nm) upon addition of a sulfuric acid stop solution.

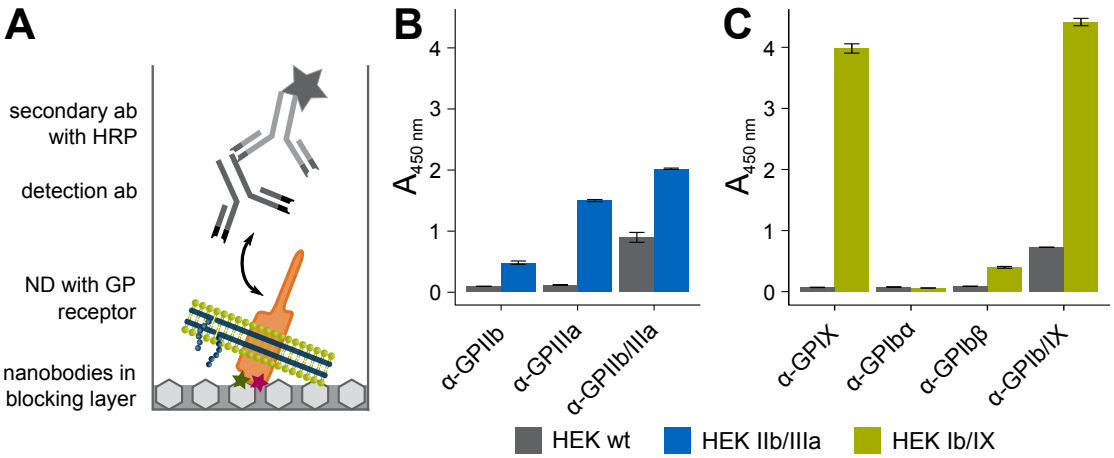

Figure 3.26: ELISA with nanodiscs generated from different HEK-293 cell types. (A) Schematic illustration of ELISA set-up. (B) Detection antibodies against GPIIb/IIIa complex and (C) detection antibodies against GPIb/IX complex bound only to the respective transfected cell lines, not to HEK-293 wt cells.

A first proof-of-concept experiment showed positive results. Nanodiscs from HEK-293 IIb/IIIa cells (fig. 3.26 B) and HEK-293 Ib/IX cells (fig. 3.26 C) were immobilized via RFP- and GFP-nanobodies respectively, and probed with different monoclonal detection antibodies against parts of the complexes as well as the complete complexes. As negative controls, nanodiscs from HEK-293 wt cells were used. Most antibodies resulted in a clear and specific signal for the GP nanodiscs, except anti-GPIbα. However, this was likely due to the antibody and not to the GPIb/IX complexes, as the other three antibodies did show a specific signal difference between GP and wt nanodiscs.

The complex-specific antibodies used here were the same as in the FACS experiments with whole HEK-293 cells (see section 3.2.3.2). They bound only to the complete GP complexes, not to the single subunits. This means that the GP complexes could in fact

be incorporated into nanodiscs in a folded and correctly assembled form.

3.3.2.2 Optimization of ELISA protocol

After the general feasibility of the ELISA with nanodiscs from HEK-293 cells had been proven, the assay was optimized with the aim of maximal signal difference between samples and negative controls as well as ease of handling and minimal use of material in order to reduce the costs.

The first simplification of the ELISA protocol concerned the raw material for generation of nanodiscs. In prior projects with nanodiscs from HEK-293 cells (Sun et al., 2019), the cells were used directly after harvesting, in order to prevent protein denaturation and degradation caused by freezing and thawing. The disadvantage of this approach is the dependence on a strict schedule dictated by the HEK-293 cells. However, the proteins of interest in this thesis are less complex, and could probably resist freezing upon addition of 10 % glycerol. In order to test this hypothesis, nanodiscs were generated from both fresh and frozen cells, and subjected to the same ELISA as described above.

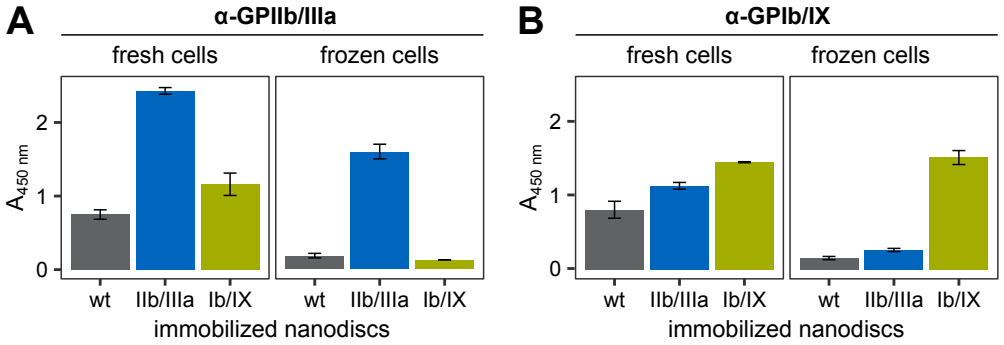

Figure 3.27: ELISA with nanodiscs from fresh or frozen HEK-293 cells. ELISA set-up as above with (A) anti-GPIIb/IIIa or (B) anti-GPIb/IX as detection antibody.

In this case, only the complex-specific antibodies were used for detection, as they are more sensitive towards protein unfolding and denaturation. Unexpectedly, freezing of cells even improved the signal-to-noise ratio of the ELISA assay. While specific signal decreased slightly for anti-GPIIb/IIIa and stayed the same for anti-GPIb/IX, the unspecific signals for all nanodiscs without the respective GP receptor decreased considerably after freezing of the raw material. Thus, the ELISA assay could generally be executed without the need for cell harvest on the same day.

The next step involved reduction of the ELISA components nanobodies, nanodiscs and detection antibodies. A titration of nanobodies resulted in unchanged ELISA signals between 10 and 0.1 µg per well (data not shown). For economical reasons, the lowest amount in this range was used for all further experiments.

Reduction of the detection antibody resulted in mixed results. While the anti-GPIIb/IIIa antibody could be diluted 1:5000 in PBS without decrease in signal, the anti-GPIb/IX antibody showed best results at a 1:1000 dilution. However, as those antibodies were bought at different concentrations, 1 mg/ml for anti-GPIIb/IIIa and 0.2 mg/ml for anti-GPIb/IX,

those dilutions actually resulted in the same final concentration.

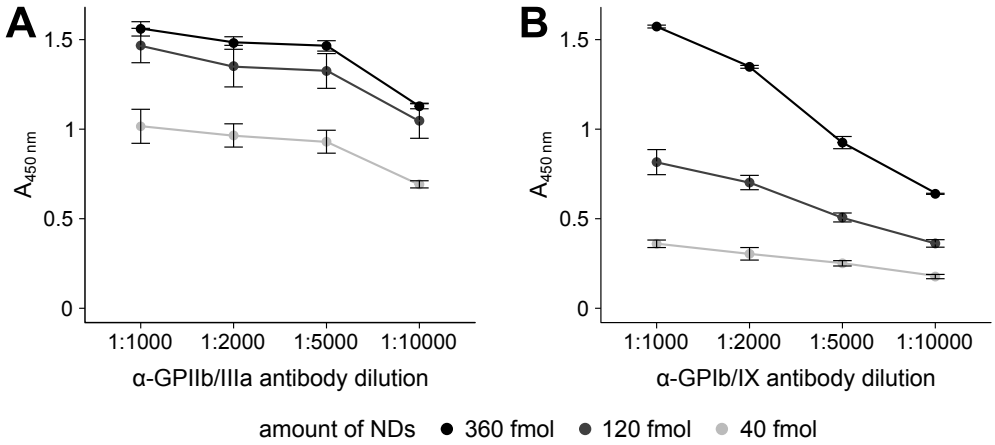

Figure 3.28: Titration of nanodisc amount (from 40 fmol to 360 fmol per well) and detection antibody dilution (from 1:1000 to 1:10000) for (A) nanodiscs with GPIIb/IIIa with anti-GPIIb/IIIa complex-specific antibody and (B) nanodiscs with GPIb/IX with anti-GPIb/IX complex-specific antibody.

Increase of the nanodisc concentration had the biggest effect on the specific ELISA signal. This effect was more pronounced for GPIb/IX than for GPIIb/IIIa, but for both conditions 120 fmol as the highest practicable nanodisc concentration was used for all further experiments. Nanodiscs generated from 250 µg of MSP with the corresponding amount of cell lysate and PEG-PE were thus sufficient for 10 ELISA wells.

3.3.2.3 Examination of nanodisc fractions

SEC diagrams of assembled nanodiscs showed again the characteristic peak between 9 ml and 13 ml (see fig. 3.29 A + B). Additionally, low amounts of cellular aggregates and free MSP1E3D1 could be observed as small peaks at 8 and 15 ml elution volume, respectively. The slightly asymmetrical nanodisc peak shape, with a shoulder at lower elution volumes, suggested the presence of a variety of generated nanodiscs.

The molecular weight of an empty nanodisc can be calculated from the weights of MSP1E3D1 (2 × 32 kDa), membrane phospholipids (120 × 0.77 kDa) and PEG-PE (20 × 2.8 kDa). This results in about 200 kDa in total, corresponding to the right end of the peak. In contrast, the peak maximum at 11.0 to 11.5 ml contained nanodiscs with an apparent molecular weight of 400 kDa to 450 kDa. Subtracting the weight of an empty nanodisc, 200 kDa to 250 kDa could be attributed to membrane proteins incorporated into those nanodiscs. This corresponds well to the molecular weight of a complete GPIb/IX (215 kDa) or GPIIb/IIIa (256 kDa) complex, including the fluorescent protein tags. Nanodiscs with a higher apparent molecular weight would then contain either multiple GP complexes, bigger membrane proteins or a mixture of several membrane proteins.

In order to verify this theory, SEC fractions were subjected to ELISA experiments with the set-ups described above (see fig. 3.26 C). Captured nanodisc fractions containing either GPIIb/IIIa or GPIb/IX were detected by the corresponding complex-specific antibody. As expected, the resulting ELISA signal intensity depended strongly on the applied

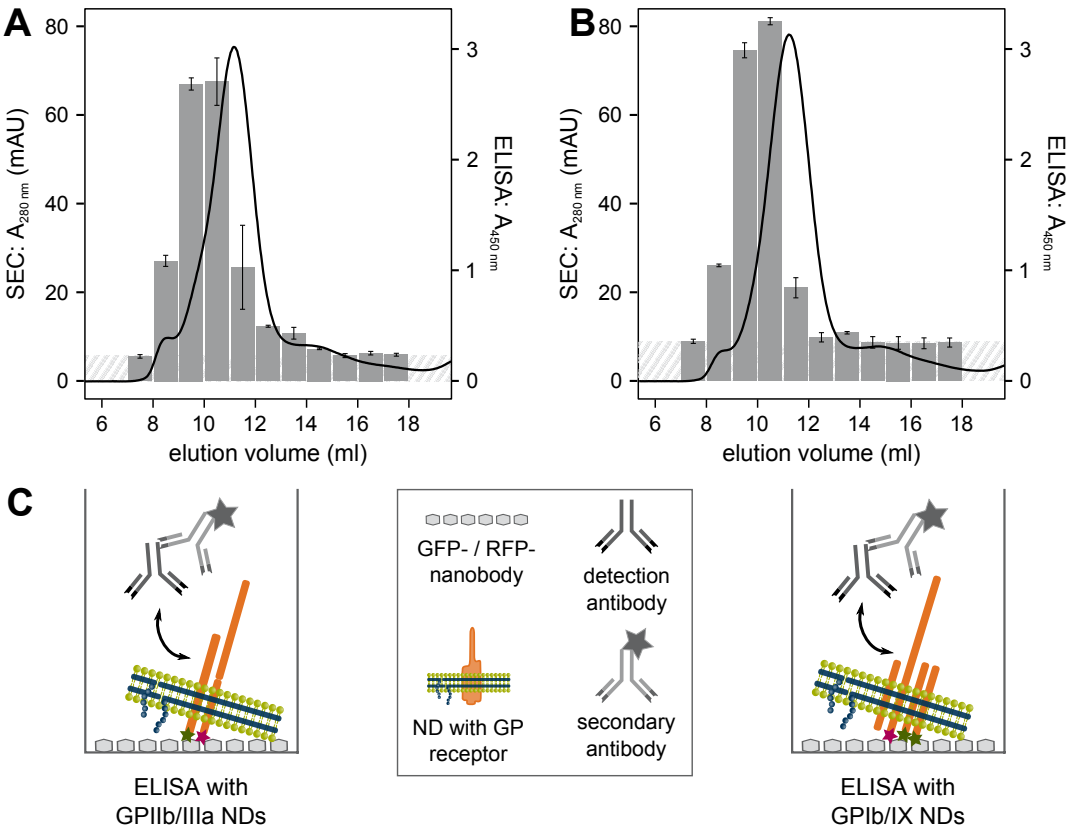

Figure 3.29: Verification of nanodisc assembly and integration of GPs. Nanodiscs from either (A) HEK-293 IIb/IIIa cells or (B) HEK-293 Ib/IX cells were separated by SEC (black lines) and 1 ml fractions were collected. The collected fractions were examined by ELISA (grey bars) with GP complex-specific antibodies. The ELISA set-up is shown in (C). Samples were measured in duplicates, error bars indicate the standard deviation and shaded background the level of unspecific signal.

fraction. The highest ELISA signals could be observed in fractions containing nanodiscs with an apparent molecular weight of 450 kDa to 1300 kDa, whereas only background signal intensities off less than 0.3 AU were seen for nanodiscs being smaller than 400 kDa (elution volume $>$ 11.3 ml). Those could impossibly have integrated the complete GP complex, which is necessary for binding of the complex-specific antibodies.

The obtained experimental results demonstrated that the nanodisc assembly protocol applied here allowed the extraction of intact recombinant GP complexes from HEK-293 cells, most probably still in connection with the surrounding membrane lipids, and their integration into nanodiscs. Hereby, the native-like structure of the complexes was preserved as verified by ELISA with complex-specific monoclonal antibodies.

3.3.2.4 Limit of detection of complex-specific antibodies

For the final ELISA set-up with optimized conditions, the limit of detection for the complex-specific antibodies was determined. Detection antibody in decreasing concentrations was added to nanodiscs with and without the respective GP receptor. Even at the lowest concentration, 3.1 ng/ml antibody, a marginal difference was still observed (see

fig. 3.30).

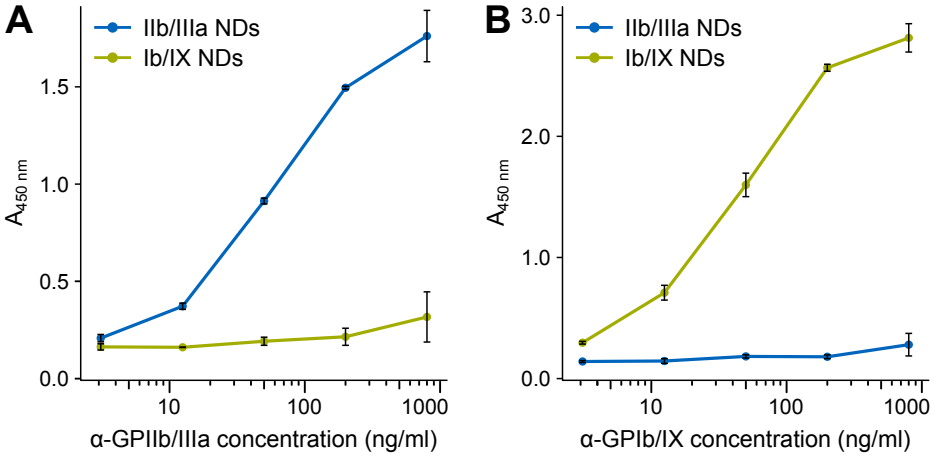

Figure 3.30: Limit of detection for ELISA with optimized set-up and complex-specific antibodies. Titration of detection antibody concentration (from 3.1 to 800 ng/ml) for (A) anti-GPIIb/IIIa complex-specific antibody and (B) anti-GPIb/IX complex-specific antibody.

Normal ranges for IgG in a healthy adult are about 4 to 22 mg/ml on average (Gonzalez-Quintela et al., 2008). In contrast, the concentration of specific antibody in polyclonal sera is typically between 50 and 200 µg/ml after successful immunization with the aim of antibody production (Lipman et al., 2005). This corresponds to about 1/100 of all antibodies.

For the determined limit of detection of less than 5 ng/ml, at the very least one in one million IgG molecules of the AITP patients should be directed against the GP complexes, if similar binding characteristics are assumed. This is much lower than the fraction of one in one hundred antibodies estimated above. Even if the antigenicity of autoantigens were much lower than that of optimized vaccines combined with adjuvants, there should be enough specific IgG molecules in the serum to allow detection with the presented assay set-up.

There are other possible complications that have to be taken into account as well, such as lower affinities of autoantibodies, or the necessary use of a different secondary antibody with human samples. In the ELISA experiments with monoclonal complex-specific antibodies, an anti-mouse antibody was used, whereas for patient samples an anti-human antibody would be necessary, which could potentially show worse binding characteristics. Additionally, the unspecific signal in serum samples would probably be higher than in buffer solutions. However, even if the properties of the tested monoclonal antibody assay set-up could not be replicated exactly for the measurement of patient autoantibodies, there is a wide margin of safety here.

3.3.3 Functionality of GP receptors in nanodiscs

The correct assembly and folding of GP receptors are necessary, but in some cases not sufficient prerequisites for their functionality (Braakman and Bulleid, 2011). In order to test the proper and specific functionality of GPIIb/IIIa and GPIb/IX complexes in

nanodiscs, the binding to their natural ligands, fibrinogen and vWF, respectively, was tested via SPR. These SPR experiments allowed a label-free real-time monitoring of the binding of nanodisc embedded GP receptors to their ligands (Cooper, 2002).

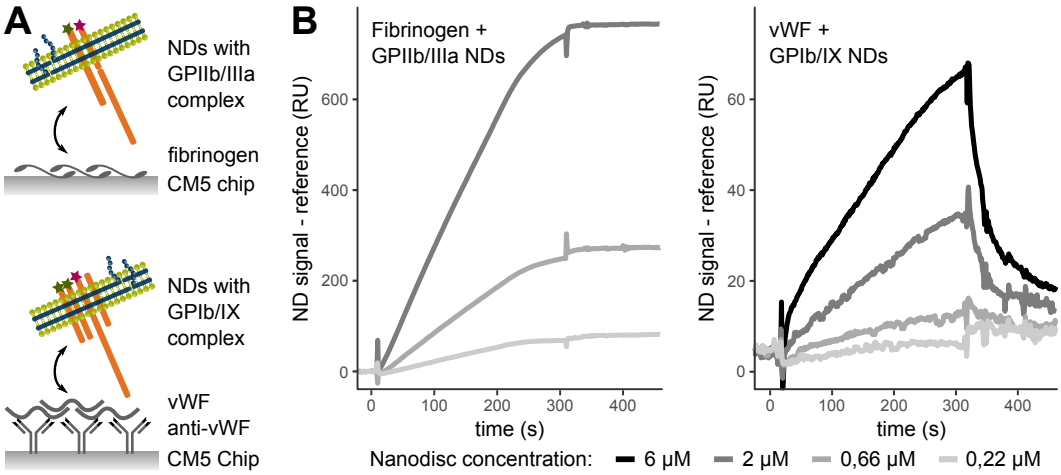

Figure 3.31: GP receptor functionality examined by SPR. (A) SPR set-ups for the analysis of interactions of GPIIb/IIIa nanodiscs with fibrinogen and of GPIb/IX NDs with vWF. (B) Corrected SPR results of different concentrations of NDs containing GPIIb/IIIa or GPIb/IX with their ligand.

The ligands were immobilized covalently on a CM5 chip via amine coupling. Fibrinogen was immobilized covalently to this surface in a direct manner, whereas vWF was affinity captured via a covalently attached anti-vWF antibody (fig. 3.31 A). Nanodiscs containing GPIIb/IIIa or GPIb/IX complexes were then injected onto the sample flow cell in different concentrations.

SPR reacts in general very sensitively to changes in the buffer composition during sample injection (Cooper, 2002). This leads to an immediate change of the signal, called bulk shift, at the beginning and the end of the sample injection phase (fig. 3.32). Besides, unspecific binding of nanodiscs to the SPR chip surface can also occur. In order to correct for both of these effects, SPR measurements were additionally carried out with control nanodiscs generated from wild type HEK-293 cells lacking the recombinant GP receptors. SPR sensorgrams of those reference runs were subtracted from the sensorgrams with GP nanodiscs, resulting in binding curves without any bulk shift or unspecific signal (fig. 3.31 B).

The corrected SPR signals for GP containing nanodiscs injected over the ligand flow cells increased with their concentration (see fig. 3.31 B). In contrast, injection of nanodiscs onto the reference flow cell, which was coated with a control protein, caused no signal increase (data not shown). This demonstrated that the recombinant GP receptors, integrated into the nanodiscs, specifically bound to their ligands, which is an indicator for their functionality.

However, significant differences between the SPR curves of the two kinds of GP receptor nanodiscs were visible in the association as well as in the dissociation phase. While GPIIb/IIIa nanodiscs bound very strongly to their ligand and exhibited minimal disso-

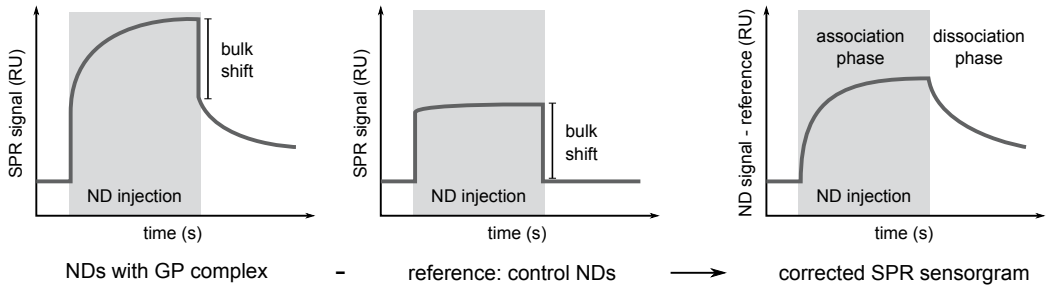

Figure 3.32: Schematic correction procedure for removal of bulk shift and unspecific binding from SPR curves.

ciation, GPIb/IX nanodiscs bound only weakly to the vWF, resulting in a much lower total signal (approximately 10 % of that of the GPIIb/IIIa system at the same nanodisc concentration), and dissociated rapidly. This is in accordance with earlier publications, reporting that the GPIb/IX receptor binds only weakly to vWF in the absence of GPV in the complex (Canobbio et al., 2004). This also explains the seemingly lacking GPIb/IX functionality in whole cells, the adhesion assay employed there was not suitable for detection of low-affinity binding.

This result shows that both GP receptors could be incorporated into nanodiscs in a functional and thus likely folded state. This was a necessary prerequisite for the following experiments with patient samples, as autoantibodies are reported to bind mostly to conformation-dependent epitopes (Kosugi et al., 1996).

3.4 Patient studies

After functionality and thus correct conformation of GP receptors incorporated into nanodiscs had been shown, as well as the general feasibility of the ELISA assay with monoclonal antibodies, the next step was verification of the results with patient samples. However, only samples from patients with autoantibodies against the GPIIb/IIIa complex were available, not against the GPIb/IX complex. For that reason, all of the following experiments were conducted only with nanodiscs containing this receptor.

3.4.1 Proof of concept ELISA with confirmed patient samples

For verification and optimization of the ELISA assay, a small number of patient samples were chosen (see table 3.1). Those samples had shown a clearly positive result in earlier studies and were well characterized. Additionally, different samples from persons without AITP were used as negative controls, and one sample from a patient with allo-ITP as positive control. The samples containing anti-GPIIb/IIIa antibodies as well as controls AB6 to AB8 were provided by Prof. Bakchoul from the Zentrum für Klinische Transfusionsmedizin in Tübingen, whereas the other negative controls were from voluntary donors in Munich. Those negative controls were added to test the quality of provided samples from Tübingen, as both their samples and controls were stored under the same conditions, whereas the samples from Munich were freshly drawn from voluntary donors and frozen as small aliquots. They were always thawed directly prior to the experiments.

Table 3.1: Description of samples from selected ITP patients and controls used for optimization of the ELISA assay.

Sample	age	sex	diagnosis	comment
ITP1	66	male	AITP	GPIIb/IIIa MAIPA dir. + indir. pos
ITP2	26	female	AITP	GPIIb/IIIa MAIPA dir. + indir. pos
ITP3	81	female	AITP	GPIIb/IIIa MAIPA dir. + indir. pos
HPA1	?	?	allo-ITP	no MAIPA results available
AB6	?	?	healthy control	from Tübingen
AB7	?	?	healthy control	from Tübingen
AB8	?	?	healthy control	from Tübingen
SM	27	female	healthy control	from Munich
AB	35	male	healthy control	from Munich
MS	30	male	healthy control	from Munich
RS	29	female	healthy control	from Munich

First, an initial ELISA set-up was developed based on results from experiments with monoclonal antibodies. After coating the 96-well plates with anti-RFP nanobodies, free binding sites were blocked with a solution of 5 % skim milk powder in PBS in order to reduce unspecific binding. 120 fmol nanodiscs generated from HEK-293 IIb/IIIa cells per well were incubated over night at 4 °C. After removal of unbound nanodiscs, patient

serum diluted 1:250 in PBS was added, and bound IgG was detected with a HRP-labeled secondary anti-human antibody. In between incubation steps, the ELISA plate was washed 3 times with 300 µl PBS per well.

This experimental set-up already allowed differentiation between positive and negative samples (fig. 3.33). Whereas all negative samples with the exception of AB8 were very similar, signal levels for the positive samples varied more.

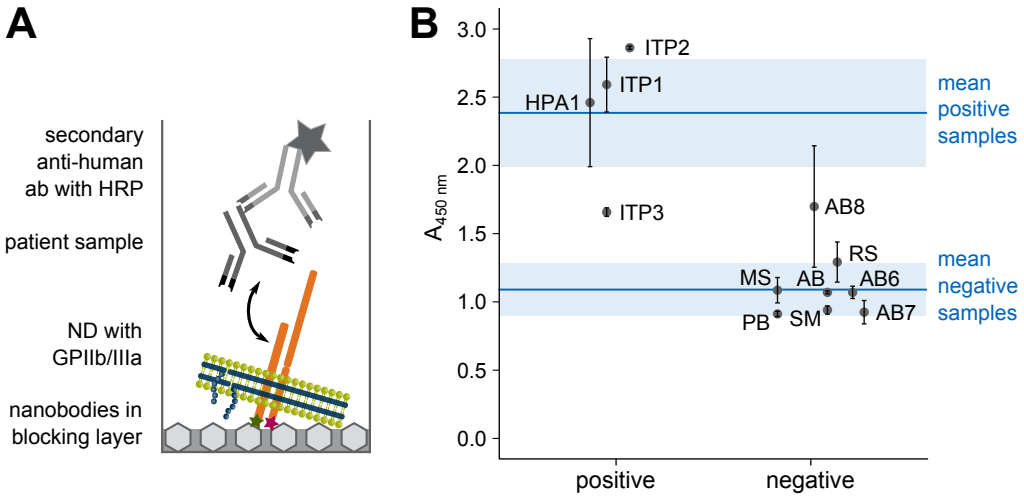

Figure 3.33: Measurement of patient samples by ELISA with nanodiscs generated from HEK-293 IIb/IIIa. (A) Schematic illustration of ELISA set-up. (B) ELISA results for positive and negative samples and controls. Each grey point represents the mean of duplicate measurements of one sample, with standard deviation, while blue lines depict mean values for all positive and negative samples, respectively, with light blue shadows for standard deviations.

However, signal differences between the samples were not clear enough, and there was partial overlap between low positive samples and high negative ones. For this reason, the ELISA set-up was improved with the following aims:

- positive samples should result in signals > 2.5
- negative samples should result in signals < 0.5
- without any serum sample, the unspecific signal of secondary antibody on the coating layer with nanodiscs should be < 0.2.

3.4.2 Optimization of ELISA for patient samples

3.4.2.1 Blocking of free binding sites

Blocking conditions were optimized for a serum pool of all negative controls in equal amounts. Different common blocking solutions (Studentsov et al., 2002) for ELISA were tested, alone or in combination, in order to obtain values < 0.5 as specified above (see fig. 3.34). All reagents were solubilized in PBS.

First of all, all blocking conditions tested were a huge improvement in contrast to no blocking at all, which resulted in an A_{450nm} of 4.3 (data not shown). This is not surprising, as all serum samples contain large amounts of IgG that bind to free, unblocked sites on the plastic surface and can be detected by the anti-human secondary antibody.

However, there were considerable differences between the blocking solutions. Skim milk powder, which had been used up to this point, was actually one of the worst choices tested here. It showed similar blocking capacities as the different PEG variants, with ELISA signals in the range of 0.8 to 1.1. Additionally, skim milk seemed to react strongly with specific samples (data not shown). A little better was a solution of 1 % BSA in PBS, but still above the desired limit of 0.5 for negative samples. Only two blocking solutions met this requirement, 0.05 % Tween 20 with and without BSA, resulting in an absorbance of about 0.4.

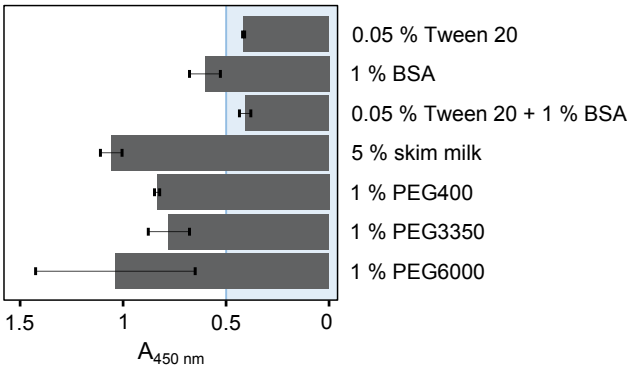

Figure 3.34: Optimization of blocking conditions for ELISA with serum samples. All blocking reagents were dissolved in PBS. Grey bars depict the mean of duplicate measurements with standard deviation. Blue background represents desired maximum value for negative samples.

So in theory, blocking with Tween 20 should be enough to keep unspecific binding low. However, this detergent is easily soluble in aqueous solutions, and can be washed away in subsequent incubation and washing steps. For this reason, stabilizing BSA was added for the blocking step, and PBS-T was used for washing of the ELISA plates. Here it was important that the plates were not be washed prior to incubation with RFP nanobodies, as this inhibited immobilization.

3.4.2.2 Amount of nanodiscs

As the amount of nanodisc per well had been show to have a considerable impact in ELISA with monoclonal antibodies, it was tested here as well. All positive samples as well as four different negative samples were applied to ELISA plates coated with either 60 fmol, 120 fmol or 240 fmol of nanodiscs generated from HEK-293 IIb/IIIa cells (see fig. 3.35).

The impact of the nanodisc amount was not as big as with monoclonal antibodies, but a general trend of more signal with more nanodiscs could be observed nonetheless, and was more pronounced in the positive samples. This was an indication that the concentration of anti-GPIIb/IIIa antibodies in the samples was quite low, so that the number of available binding sites was not the limiting factor. As a compromise between signal strength and waste of material, the nanodisc amount was set as 120 fmol per well for all further experiments.

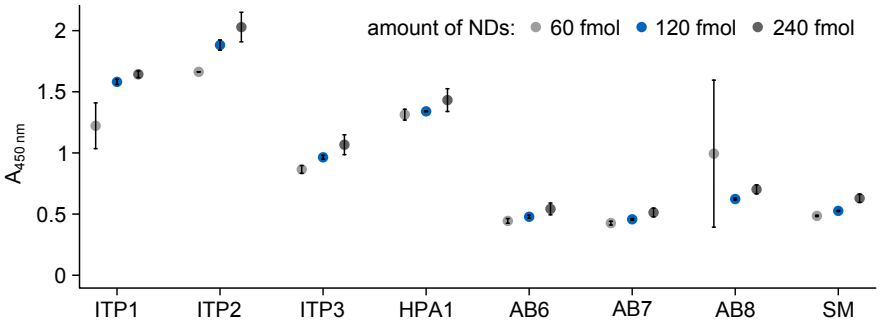

Figure 3.35: Optimization of nanodisc amount for ELISA with serum samples. Points depict the mean of duplicate measurements with standard deviation. The optimal result for further experiments is highlighted in blue. The light blue shaded area indicates the desired level of 0.5 for negative controls.

3.4.2.3 Sample dilution

The signal for negative samples was about 0.5 in the last experiment, as desired. The only exception was AB8, which always resulted in slightly higher signals. The positive samples resulted in signals that ranged from 1.0 to 1.9. Even if those samples could be differentiated without problems, the case might be not so clear for more ambiguous samples. For this reason, the signal difference between positive and negative samples should be increased. One possible factor to optimize was the sample incubation. Due to constraints in the amount of available serum, only two samples were tested here, ITP1 and SM.

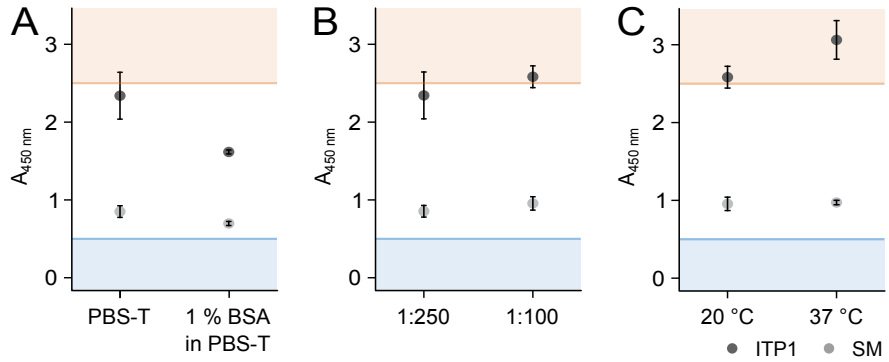

Figure 3.36: Optimization of sample incubation conditions for ELISA with patient samples. Variation of (A) dilution buffer, (B) dilution factor and (C) incubation temperature. The positive sample ITP1 (dark grey) and the negative control SM (light grey) were measured in duplicates at all conditions. The desired limits for negative samples and positive samples are depicted in blue and orange, respectively.

One after the other, sample dilution, dilution buffer and incubation temperature were optimized (see fig. 3.36). PBS-T (PBS with 0.05 % Tween 20, as determined above as washing buffer) was tested as sample dilution buffer with and without addition of 1 % BSA. Addition of BSA led to a signal reduction for the ITP sample from 2.3 to 1.6, whereas the negative control was barely influenced (see fig. 3.36A). A dilution of 1:100 resulted in higher ELISA signals above the desired limit of 2.5 for ITP1, whereas results for the negative sample SM were similar for both dilutions (see fig. 3.36B). Finally, increase of the incubation temperature from 20 °C to 37 °C resulted in the highest signal so far (see fig.

3.36C). Additionally, as antibodies in the body are exposed to an ambient temperature of 37 °C as well, those conditions mimic the naturally occurring antigen-antibody interaction even more better.

Those steps led to an increase in the ratio of SM to ITP1 from 1:2 to 1:3. However, the negative controls were higher than desired, at around 1. The absolute values were always dependent on the incubation time of TMB before stopping with sulfuric acid. For that reason it was important to test competing conditions on the same ELISA plate, and to observe both positive and negative signals, or the ratio of both respectively.

3.4.2.4 Secondary antibody

Most autoantibodies found in chronic ITP patients are of the IgG class, but IgM and sporadically IgA antibodies are also detected (Kiefel et al., 1996). However, IgG autoantibodies seem to be the main mediator of antibody-driven autoimmunity. Most prevalent are IgGs of the IgG1 subclass, and while IgG2, IgG3, and IgG4 subclass autoantibodies can be also found in patients, they are often accompanied by IgG1 antibodies (Hymes et al., 1980).

There were two different polyclonal anti-human IgG antibodies in stock that could be used as HRP-coupled secondary antibody, Dako P0214 and Acris R1333HRP. Those antibodies required very different working concentrations, otherwise results with both antibodies were very similar (data not shown). The Acris antibody required only about 1/7th of the concentration of the Dako antibody in order to result in the same ELISA signal (0.2 ng/µl and 1.3 ng/µl, respectively). A possible explanation was the storage of the Acris antibody as aliquots at -20 °C, whereas the Dako antibody had been kept at 4 °C for several years. This could compromise the binding characteristics and lead to degradation of the antibody. Thus, the Acris antibody was chosen for further experiments.

3.4.2.5 Conclusion

After optimization of the ELISA assay, differentiation between positive and negative samples was easier than before. Although the desired limits of > 2.5 for positive samples and < 0.5 for negative samples were not entirely reached, a clear separation of the samples was possible. As the absolute final signal intensities depend strongly on the incubation time of TMB, the ratio of positive and negative samples was much more important than the absolute values.

In order to test the final assay set-up and to verify its reproducibility, the same patient and control samples were measured twice with the original and the improved assay, on two different days (see fig. 3.37). For this purpose, all values were normalized on the signal intensity of ITP1, which was set as 100 %.

The important point was that the improved assay did in fact allow better separation of positive and negative samples. Whereas the original assay resulted in nearly the same signal for ITP3 and AB8, the improved assay could clearly differentiate between those ambiguous samples. Generally, the signals for positive samples increased, whereas the

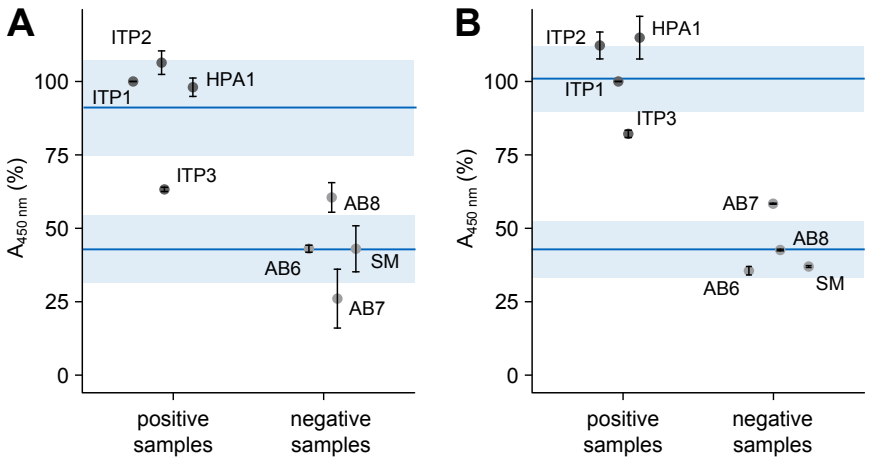

Figure 3.37: Comparison of ELISA (A) before and (B) after optimization. All samples were measured in quadruplicates on two different days with a completely new ELISA plate and nanodiscs on each day. A_{450nm} values were normalized on the value for ITP1. Blue lines indicate the mean value of all positive and negative samples, respectively, with standard deviations in light blue.

unspecific signals decreased.

Assay reproducibility was acceptable with both set-ups. While the values were slightly different between experiments, the differentiation between positive and negative samples was repeatedly possible.

3.4.3 ELISA with serum and isolated IgG fraction

In order to make sure that the ELISA actually detected binding of IgG in the serum samples, and not only unspecific binding of other serum components associated with IgG, the IgG fraction of different serum samples was isolated (see fig. 3.38A). This was achieved by protein-A/G affinity columns, which bind specifically to all human IgG subclasses. The flow-through then contained all other serum components and no IgG, as verified by SDS PAGE (data not shown).

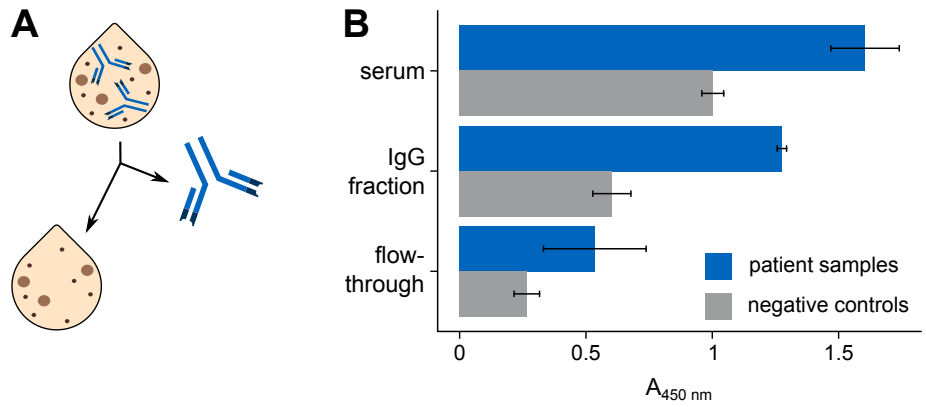

Figure 3.38: ELISA with isolated IgG fraction. (A) Schematic illustration of separation of serum in IgG fraction an flow-through. (B) Results of ELISA with whole serum, isolated IgG fraction and flow-through of two patient samples (blue) and four controls (grey).

For this experiment, samples from two patients (ITP1 and ITP2) and four negative

controls (from a different cohort than above due to limited sample amounts) were used. All three types of sample material, the serum used as starting material as well as the isolated IgG fraction and the flow-through, were subjected to the same ELISA set-up according to the optimized conditions specified above (see fig. 3.38B).

For the serum samples, the result was as expected, with the patient samples resulting in higher ELISA signals than the controls. The use of isolated IgG instead of serum decreased all signals. However, the negative samples decreased more than the patient samples, which means that the signal difference could be increased by use of isolated IgG. In contrast, the flow-through resulted in very low signals, with no significant difference between positive and negative samples.

Thus, the binding part of patient samples seemed to be in fact the IgG fraction, even if other serum components led to a not inconsiderable amount of unspecific signal.

3.4.4 Patient study

Prior ELISA experiments with monoclonal antibodies against the GPIIb/IIIa complex or with a few selected patient samples allowed a clear separation of samples with and without antibodies. In order to verify these results, a study with a bigger number of serum samples was conducted.

3.4.4.1 Study population

This study comprised 150 subjects all together, of which 69 were from AITP-positive subjects from the Zentrum für Klinische Transfusionsmedizin in Tübingen (see fig. 3.39). The patients were diagnosed by process of exclusion, and clinical data such as platelet count, age and sex were available for most of those samples. Additionally, 61 of the samples were tested by indirect MAIPA assay, which detects free serum IgG autoantibodies, and 38 by direct MAIPA measuring platelet-associated IgG.

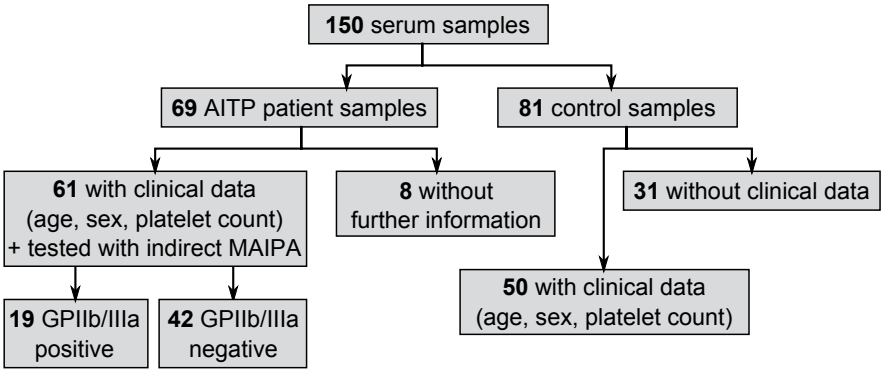

Figure 3.39: Overview of study population.

As negative controls, there were 81 healthy controls from two different populations. 50 control samples were from the Klinikum rechts der Isar in Munich, consisting of left-over material from the orthopedic unit, with platelet counts above 100,000 per µl. For those subjects, platelet count, age and sex were known. In contrast, for 31 negative controls

from Tübingen no information was available except that they were not diagnosed with AITP.

Distribution of age and sex showed some difference between patient samples and negative controls. Whereas 64 % of patients were female, only 48 % of controls were so. The mean age of patients was 52 ± 23 years, and that of negative controls was 62 ± 20 years. The platelets counts were of course quite different (see fig. 3.40), as the primary symptom of patients was their low platelet number. Surprisingly, although AITP is officially diagnosed only for platelet counts lower than 100,000 per microliter, 6 patients were above that range. This could possibly mean that patients had been treated against AITP successfully, this has to be kept in mind for further discussion of the results.

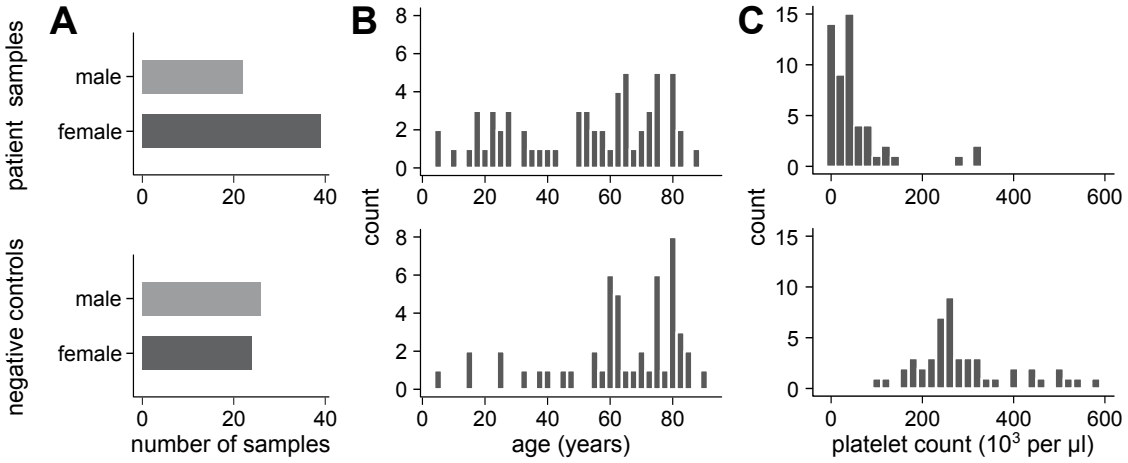

Figure 3.40: Comparison of age, sex and platelet count of study population. Statistics of (A) sex, (B) age and (C) platelet count of ITP patients (upper panels) and negative controls (lower panels). Patients with missing data were omitted.

The AITP patients could be further divided by their prior characterization. Most of the patient samples were tested for anti-GPIIb/IIIa antibodies either by indirect MAIPA measuring free serum antibodies (61 samples) or direct MAIPA measuring platelet-associated antibodies (38 samples). 54 patients had data for platelet counts, and 61 for age and sex (see fig. 3.39). However, no data concerning the severity of symptoms, prior treatment or other clinical information was available.

3.4.4.2 Manufacturing of ELISA plates

As a maximum of 22 samples could be measured on one ELISA plate, samples were run on a total of 12 assay plates. The study comprised serum samples from Munich as well as from Tübingen, which were all measured with the same batch of ELISA plates. For this purpose, enough ELISA plates for all samples were prepared in advance up to the nanodisc immobilization step. Then they were transported to Tübingen where the measurements took place.

The necessary prerequisite for this was that the ELISA plates could be stored for several days with immobilized nanodiscs. There are different storage possibilities, the plates can be stored dry or with different storage buffers, frozen or cooled at 4 °C.

The best compromise between assay functionality and ease of handling provided cool storage of the dried plates at 4 °C. The advantage of dried plates is that the plates are less sensitive to a change in the surrounding temperature, and that they need not be stored upright. In order to test this storage condition, a dummy plate was prepared in the same way as the planned assay plates, and tested for antibody binding after up to ten days. As control for unspecific binding of the antibody, not only GPIIb/IIIa nanodiscs were immobilized, but GPIb/IX nanodiscs without the GPIIb/IIIa receptor as well. Wild type nanodiscs were not suited for this purpose, as they did not bind to the ELISA plate at all.

The ELISA protocol was followed as usual, but after nanodisc incubation at 4 °C over night, only one set of wells was finished immediately (day 1). The other wells were washed, tapped dry on a paper towel, and left open to dry for two hours. Then the plate was closed with an adhesive film and stored at 4 °C. At different time points in the next ten days, some wells were uncovered, washed again with PBS-T and the rest of the ELISA protocol was executed. This means that the rest of the plate was subjected to a change in temperature from 4 °C to room temperature and back on each measurement day. This should sufficiently simulate any disturbances that could occur during transportation.

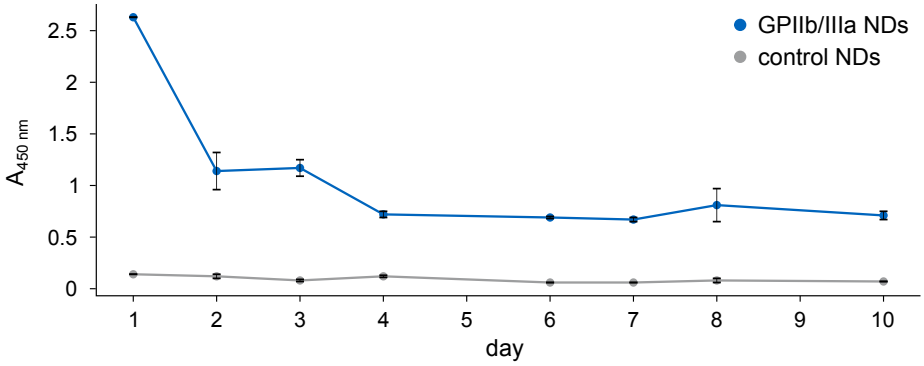

Figure 3.41: Measurement of GPIIb/IIIa ELISA plates after up to 10 days of dry storage. All samples were measured as duplicates and normalized to the signal of freshly and directly coated secondary antibody.

Although the ELISA signal decreased considerably from freshly prepared control nanodiscs on day 1 to the stored nanodiscs on day 2, from this point on the signal remained almost constant for at least 10 days (see fig. 3.41). The wells containing GPIIb/IIIa nanodiscs could always be distinguished from control nanodiscs, which ensured that the signal did not come from unspecific binding of antibody to degraded nanodiscs.

Although this storage method was not ideal compared to the fresh ELISA plate, it was considered good enough for the execution of the planned study. The tested time span of ten days allowed manufacturing of ELISA plates on Thursday/Friday, storage over the weekend, and measurement from Monday to Friday the next week. For future studies, the storage methods could be optimized, for example by storage under buffer or with different additives. As an alternative, the plates could be prepared freshly on each measurement day. However, this approach could potentially introduce higher variations between plates, due to inconsistencies in the raw material (passage number of HEK-293 cells, exact amount

of raw material) or the nanodisc generation process. Additionally, if all plates are prepared at the same time with the same batch of reagents, small deviations of reagent dilution and incubation times can be avoided.

3.4.4.3 Correction between ELISA plates

Even with the most reproducible manufacturing of ELISA plates, the absolute A_{450nm} values of each plate varied considerably. They depended strongly on the incubation time of TMB, so it was difficult to achieve exactly reproducible absolute values from one plate to the other. Thus, there had to be found a way to normalize the results between the plates. Usually, each plate would have been run with its own calibrator, a dilution series of known concentrations of a standard substance, and control samples with known concentrations of the analyte. However, for this assay this would have required a human or humanized antibody binding to the GPIIb/IIIa complex, as the present anti-GPIIb/IIIa antibodies were either from rabbit (anti-GPIIb and anti-GPIIIa) or from mouse (anti-GPIIb/IIIa). Those antibodies were recognized by a different secondary antibody than the patient samples, which made them unsuitable for a calibration curve. For this reason, four well-characterized serum samples were measured repeatedly on each ELISA plate: ITP1 and ITP2 as positive samples, and AB6 and SM as negative controls.

All 150 serum samples were subjected to the newly developed ELISA with conditions as described above. The samples were measured in duplicates, and the results given as A_{450nm} values. In order to determine the repeatability of this assay, two measures of the coefficient of variability (CV) were used. The inter-assay CV describes the plate-to-plate consistency and is calculated from the mean values of all samples that were measured at least twice on different plates. In this case, it was determined as 6.8 %, which is far below the generally acceptable limit of 10 % (Schultheiss and Stanton, 2009). This confirmed that measurements between plates were in fact reproducible, that the plates worked repeatably on the different measurement days, and that the signals were not due to random effects.

The intra-assay CV, in contrast, describes the precision of measurements between duplicates, i.e. the same sample on the same ELISA plate, measured in two separate wells. It is calculated as mean of the individual CVs for all duplicates. All duplicates with a CV higher than 10 % were discarded and the measurement repeated. Additionally, half of all samples were repeated randomly. Subsequently, the total intra-assay CV was determined as 2.48 % in this study, which was much lower than the generally acceptable limit of 10 % (Schultheiss and Stanton, 2009). The most common cause of a high intra-assay CV are small pipetting errors and irreproducible working methods, which can thus be excluded.

In order to control for reproducibility of the four calibration samples across all 12 ELISA plates used for this study, first all results were normalized to that of ITP1 on the respective plate. This resulted in very reproducible results for the sample ITP2 at 98.2 ± 2.0 % of the ITP1 value over all plates, whereas the negative samples resulted in 39.9 ± 6.1 % for AB6 and 39.9 ± 8.7 % for SM. The controls were subjected to more random variations (see fig. 3.42), but could be clearly distinguished from the positive samples.

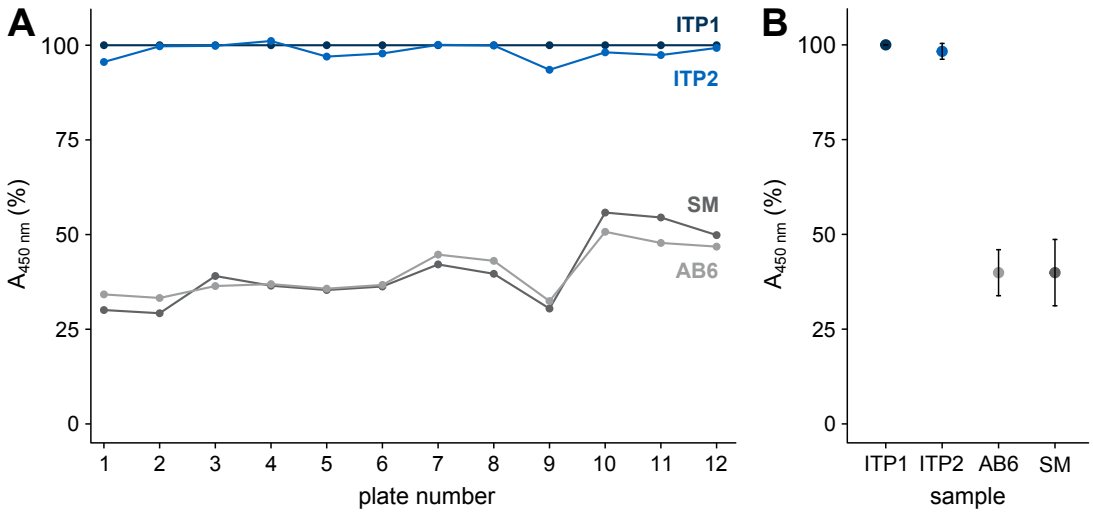

Figure 3.42: Reproducibility of ELISA plates in study. Four samples were included in every ELISA used in the study, the results were normalized to ITP1. (A) Results for each ELISA plate. (B) Mean values and standard deviation for each sample.

In order to obtain a correction factor for each ELISA plate for comparison with the first plate, all four samples were normalized relative to plate #1, and resulting percentages were averaged for each plate. This resulted in correction factors between 0.61 and 1.48, which were multiplied with all values from the respective plate.

3.4.4.4 Study results

The normalized results of all samples are shown in fig. 3.43. Mean ELISA results of all 150 samples are shown, divided into patient and control groups. Although the group "AITP patients" comprised samples with and without anti-GPIIb/IIIa antibodies (as detected by MAIPA), its mean value was significantly higher than that of negative controls (2.02 $\pm$ 0.74 and 1.54 $\pm$ 0.52, respectively, p = 0.00001037 calculated with t-test in R). This means that the assay was generally able to differentiate between serum samples from AITP patients and healthy controls in this study.

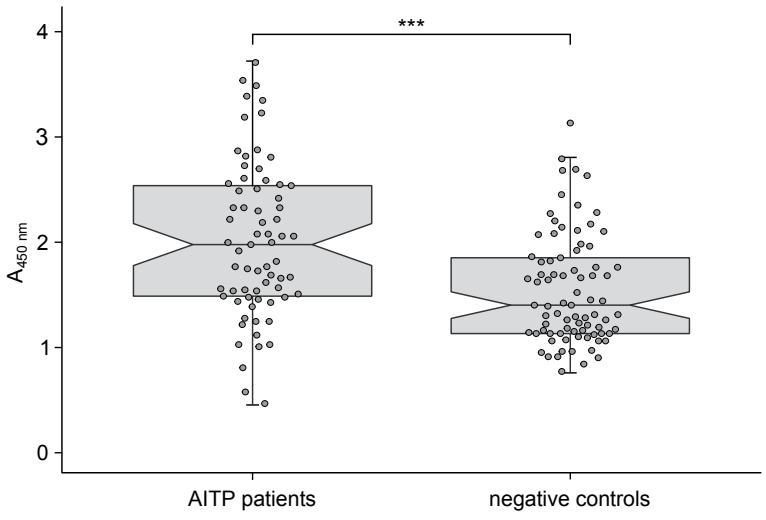

Figure 3.43: Result of patient study: Comparison of ELISA result of patient samples (n=69) and negative controls (n=81).

For a more detailed evaluation, the samples were divided into different subgroups. First of all, the two cohorts of negative samples were compared. The samples from Munich were freshly collected, frozen at -80 °C and thawed only once. In contrast, sample age or storage conditions were unknown for the samples from Tübingen, as well as other factors leading to a possible sample degradation. However, both control cohorts were nearly indistinguishable, resulting in the same mean ELISA result (1.55 ± 0.54 for samples from Munich, and 1.53 ± 0.50 for samples from Tübingen). Thus, it can be assumed that the high unspecific binding of the control samples was not due to sample degradation.

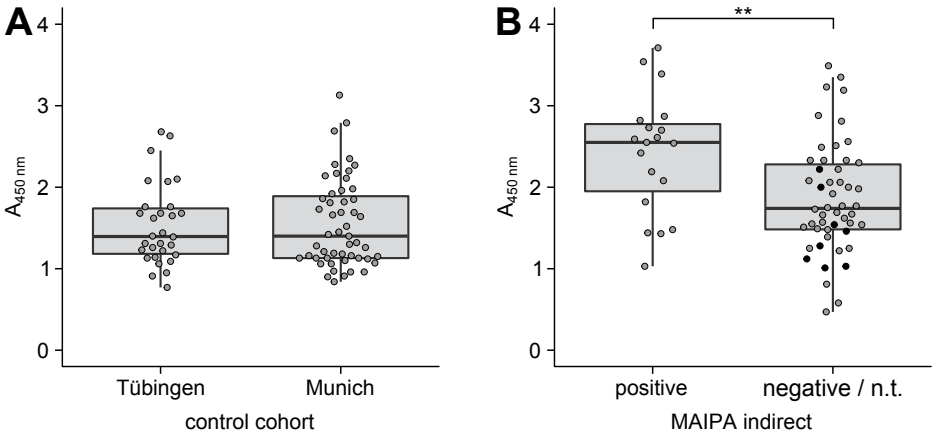

Figure 3.44: Comparison of patient and control subgroups. (A) Negative controls from Tübingen and Munich, respectively. (B) Comparison of serum samples from AITP subgroups divided by indirect MAIPA results. In the negative/n.t. group, negative samples are shown in grey, samples that had not been tested in black.

The patient samples can be divided by different criteria, but the most reasonable is by indirect MAIPA result. This assay tests for autoantibodies in the patient serum, just like the here developed nanodisc ELISA. The results for sera from the 19 AITP patients with a positive indirect MAIPA were significantly higher than for those with a negative indirect MAIPA, or those that had not been tested (2.41 ± 0.74 and 1.86 ± 0.68, respectively, $p = 0.004212$). Thus, the samples with a positive indirect MAIPA resulted in a higher mean than that of all AITP patients. However, there were still many negative samples with a high ELISA result, the mean here was higher than that of the healthy controls.

In conclusion, the results from this patient study are a promising start. Patient samples could generally be differentiated from healthy controls, but the separation is not unambiguous. However, patients were diagnosed by process of exclusion, which consists of a clinical presentation in combination with the exclusion of other causes for the low platelet count. This means that it is not known which samples do in fact contain autoantibodies.

It would be better to have a patient collective chosen according to MAIPA results, or even better multiple tests. A different possibility would be examination of patients before and after treatment. If a high autoantibody titer is correlated with severity of symptoms, then patients with less symptoms (for example after treatment) should show less autoantibodies. Finally, a higher total number of samples would be helpful for a more meaningful statistical analysis.

4 Conclusion and outlook

4.1 Conclusion

Aim of this thesis was the development of a new assay format for the detection of autoantibodies in AITP based on the platelet glycoprotein receptors GPIIb/IIIa and GPIb/IX incorporated into nanodiscs. So far, most assays had been based on human platelets as a source for the native-like antigen needed for antibody binding. By recombinant expression of both antigens in a stable HEK-293 cell culture, different drawbacks of this approach could be circumvented. The GP receptors could be reliably produced in virtually unlimited amounts, and the added intracellular fluorescent tags were useful for both culturing of cells and assay development. Confirmation of correct protein assembly and structure by experiments with complex-specific antibodies was supplemented by at least partial verification of receptor functionality in intact HEK-293 cells for GPIIb/IIIa.

Although the functionality could not be shown for both receptors in whole cells, they were both able to bind to their natural ligand upon incorporation into nanodiscs. For the nanodisc generation, a fast and easy protocol was first established with human platelets as raw material, and then later optimized for proteins expressed in HEK-293 cells. Correct assembly of nanodiscs as well as incorporation of the proteins of interest was shown by SEC and WB. Whereas the fraction of nanodiscs containing the desired proteins was very low with human platelets as starting material, it could be increased considerably by use of recombinant receptors. This allowed detection of incorporated proteins with less sensitive methods, which was the crucial point for development of the intended assay. Detection of monoclonal antibody binding was now easily possible by ELISA, with very low limits of detection.

The ELISA set-up was then optimized for detection of anti-GPIIb/IIIa autoantibodies in serum samples. Although the desired difference between well characterized samples with and without antibodies could not be completely achieved, differentiation between both was reliably possible. The assay with GPIIb/IIIa nanodiscs was finally validated with a bigger number of patient samples, whereas for GPIb/IX no samples were available. 150 serum samples were measured in total, of which 69 were from AITP patients and 81 from healthy controls. Inter-assay and intra-assay CV were well below generally acceptable limits. This was possible because of large-scale manufacturing of all ELISA plates prior to the study, and subsequent storage until use.

Results of the patient study were promising. The mean ELISA results were significantly higher for patients diagnosed with AITP than for healthy controls, although the patient group contained samples with and without autoantibodies against GPIIb/IIIa. In addition, samples from AITP patients were divided into positive and negative subgroups according to their prior testing for free anti-GPIIb/IIIa serum autoantibodies by indirect MAIPA assay. Here, the positive group showed again significantly higher mean signals than the negative group. The results of this preliminary study demonstrated the basic

suitability and the high potential of the newly developed assay for the diagnosis of AITP.

4.2 Outlook

Although the assay still had some drawbacks like the high unspecific binding of serum and thus the not entirely satisfactory separation of positive and negative samples, those first results were very promising and could be used as a starting point for future bigger studies. Final validation of the proposed assay is only possible by measurement of a large enough number of patient samples and controls, ideally with both the GPIIb/IIIa and GPIb/IX nanodisc ELISA.

For this purpose, the assay itself should be further optimized, mainly concerning the reduction of unspecific binding of antibodies to the nanodisc surface. While serum samples always tend to show a higher background signal than buffer solutions, it would be interesting to determine the exact source of the unspecific signal. Antibodies binding unspecifically to free surface areas or the blocking agent itself could be inhibited by further optimization of blocking, for example with casein or commercial mixtures.

However, another possibility are antibodies against different surface components of HEK-293 cells. Those were likely included into the nanodiscs next to the GP receptors of interest. If the incorporation of interfering proteins could be reduced, perhaps the unspecific signal of negative samples would be lower. A promising approach would be the reduction of the nanodisc size in order to reduce available membrane space. As the nanodisc diameter depends mostly on the length of the scaffold protein, different variants should be tested and compared.

Additionally, a useful approach would be repetition of the patient study with nanodiscs from wild type HEK-293 cells as control. Thus, the signal could be subtracted from that with GP receptor nanodiscs, which would hopefully lead to a better separation of samples. Alternatively, both approaches could be combined: Reduction of unspecific signal, and correction with control nanodiscs.

It would also be important to characterize the samples more extensively. Not only determination of MAIPA results for all patient samples as well as negative controls, but also severity and duration of symptoms, progression of platelet counts, applied treatment and the patient's response to it would be useful as context for the ELISA results. Ideally, multiple samples from the same patients before and after treatment could be compared, perhaps with a differentiation between cases with complete recovery and relapse. Those samples could be examined in respect to different glycoprotein receptors, not only those handled in this thesis. GPV and GPIb/IIa are promising candidates here.

Correlation with multiple tests, not only with MAIPA would be useful. A new assay can by definition never be better than the gold standard. If the new assay shows a result that is different from the gold standard, it is automatically considered wrong. But if the gold standard has a lower sensitivity than the new assay, the abnormal finding could in fact be correct. For this reason, correlation of three or four different assay principles would be interesting, with computational analysis of the results, and again correlation with disease

severity, platelet counts or response to treatment. For this, a cooperation with multiple laboratories would be necessary, that receive the same anonymized samples and negative controls for testing.

If the new assay format proves to be better than the now used assays for detection of AITP, a more reliable diagnosis would improve the living quality of patients, reduce uncertainty and enable more personalized therapy. A dependable prediction of which treatment options will work in which patient would reduce unnecessary side effects, which are quite severe in for example splenectomy or immune suppression. Additionally, costs caused by unnecessary treatment and hospital stays could potentially be reduced.

Finally, the diagnostic assay format presented here is not only limited to the application in AITP, other autoantibody targets could be incorporated into nanodiscs as well. Thus, the work presented in this thesis could be used as a starting point for a variety of other assays.

A Bibliography

D. G. Abraham, E. M. Nutt, R. A. Bednar, B. Bednar, R. J. Gould, and L. T. Duong. Arginine-glycine-aspartic acid mimics can identify a transitional activation state of recombinant αIIbβ3 in human embryonic kidney 293 cells. *Molecular Pharmacology*, 52 (2):227–236, 1997.

P. E. Abrahamson, S. A. Hall, M. Feudjo-Tepie, F. S. Mitrani-Gold, and J. Logie. The incidence of idiopathic thrombocytopenic purpura among adults: A population-based study and literature review. *European Journal of Haematology*, 83(2):83–89, 2009.

N. Akkaladevi, L. Hinton-Chollet, H. Katayama, J. Mitchell, L. Szerszen, S. Mukherjee, E. P. Gogol, B. L. Pentelute, R. J. Collier, and M. T. Fisher. Assembly of anthrax toxin pore: Lethal-factor complexes into lipid nanodiscs. *Protein Science: A Publication of the Protein Society*, 22(4):492–501, 2013.

G. Anderluh, M. Besenicar, A. Kladnik, J. H. Lakey, and P. Macek. Properties of nonfused liposomes immobilized on an L1 Biacore chip and their permeabilization by a eukaryotic pore-forming toxin. *Analytical Biochemistry*, 344(1):43–52, 2005.

J. Andréll and C. G. Tate. Overexpression of membrane proteins in mammalian cells for structural studies. *Molecular Membrane Biology*, 30(1-2):52–63, 2013.

D. M. Arnold, I. Nazy, R. Clare, A. M. Jaffer, B. Aubie, N. Li, and J. G. Kelton. Misdiagnosis of primary immune thrombocytopenia and frequency of bleeding: Lessons from the McMaster ITP Registry. *Blood Advances*, 1(25):2414–2420, 2017.

R. H. Aster and D. W. Bougie. Drug-induced immune thrombocytopenia. *New England Journal of Medicine*, 357(6):580–587, 2007.

D. Atkinson and D. M. Small. Recombinant lipoproteins: Implications for structure and assembly of native lipoproteins. *Annual Review of Biophysics and Biophysical Chemistry*, 15:403–456, 1986.

T. Bakchoul, O. Meyer, A. Agaylan, S. Bombard, G. Bein, U. J. H. Sachs, A. Salama, and S. Santoso. Rapid detection of HPA-1 alloantibodies by platelet antigens immobilized onto microbeads. *Transfusion*, 47(8):1363–1368, 2007.

T. H. Bayburt and S. G. Sligar. Single-molecule height measurements on microsomal cytochrome P450 in nanometer-scale phospholipid bilayer disks. *Proceedings of the National Academy of Sciences of the United States of America*, 99(10):6725–6730, 2002.

T. H. Bayburt and S. G. Sligar. Membrane protein assembly into Nanodiscs. *FEBS letters*, 584(9):1721–1727, 2010.

T. H. Bayburt, J. W. Carlson, and S. G. Sligar. Reconstitution and imaging of a membrane protein in a nanometer-size phospholipid bilayer. *Journal of Structural Biology*, 123(1): 37–44, 1998.

T. H. Bayburt, Y. V. Grinkova, and S. G. Sligar. Self-assembly of discoidal phospholipid bilayer nanoparticles with membrane scaffold proteins. *Nano Letters*, 2(8):853–856, 2002.

T. H. Bayburt, Y. V. Grinkova, and S. G. Sligar. Assembly of single bacteriorhodopsin trimers in bilayer nanodiscs. *Archives of Biochemistry and Biophysics*, 450(2):215–222, 2006.

P. Berchtold, D. Müller, D. Beardsley, K. Fujisawa, C. Kaplan, R. Kekomäki, E. Lipp, M. C. Morell-Kopp, V. Kiefel, R. McMillan, A. E. G. K. von dem Borne, and P. Imbach. International study to compare antigen-specific methods used for the measurement of antiplatelet autoantibodies. *British Journal of Haematology*, 96(3):477–483, 1997.

J. Borch, P. Roepstorff, and J. Møller-Jensen. Nanodisc-based co-immunoprecipitation for mass spectrometric identification of membrane-interacting proteins. *Molecular & Cellular Proteomics : MCP*, 10(7), 2011.

R. D. Bowditch, P. Tani, K. C. Fong, and R. McMillan. Characterization of autoantigenic epitopes on platelet glycoprotein IIb/IIIa using random peptide libraries. *Blood*, 88(12): 4579–4584, 1996.

I. Braakman and N. J. Bulleid. Protein folding and modification in the mammalian endoplasmic reticulum. *Annual Review of Biochemistry*, 80(1):71–99, 2011.

F. Brohm. *Über Purpura*. PhD thesis, Heidelberg, 1883.

K. A. Butash, P. Natarajan, A. Young, and D. K. Fox. Reexamination of the effect of endotoxin on cell proliferation and transfection efficiency. *BioTechniques*, 29(3):610–614, 616, 618–619, 2000.

Y. Cai, Y. Liu, K. J. Culhane, B. T. DeVree, Y. Yang, R. K. Sunahara, and E. C. Y. Yan. Purification of family B G protein-coupled receptors using nanodiscs: Application to human glucagon-like peptide-1 receptor. *PLOS ONE*, 12(6):e0179568, 2017.

I. Canobbio, C. Balduini, and M. Torti. Signalling through the platelet glycoprotein Ib-V–IX complex. *Cellular Signalling*, 16(12):1329–1344, 2004.

E. T. Castellana and P. S. Cremer. Solid supported lipid bilayers: From biophysical studies to sensor design. *Surface Science Reports*, 61(10):429–444, 2006.

L. Catani, M. E. Fagioli, P. L. Tazzari, F. Ricci, A. Curti, M. Rovito, P. Preda, G. Chirumbolo, M. Amabile, R. M. Lemoli, S. Tura, R. Conte, M. Baccarani, and N. Vianelli. Dendritic cells of immune thrombocytopenic purpura (ITP) show increased capacity to

present apoptotic platelets to T lymphocytes. *Experimental Hematology*, 34(7):879–887, 2006.

H. Cherif, A. Greinacher, and N. Lubenow. Patient was wrongly diagnosed and repeatedly treated for immune thrombocytopenia for 50 years. *Lakartidningen*, 115, 2018.

D. B. Cines and V. S. Blanchette. Immune thrombocytopenic purpura. *New England Journal of Medicine*, 346(13):995–1008, 2002.

D. B. Cines, A. Cuker, and J. W. Semple. Pathogenesis of immune thrombocytopenia. *La Presse Médicale*, 43(4, Part 2):e49–e59, 2014.

Y. C. Cohen, B. Djulbegovic, O. Shamai-Lubovitz, and B. Mozes. The bleeding risk and natural history of idiopathic thrombocytopenic purpura in patients with persistent low platelet counts. *Archives of Internal Medicine*, 160(11):1630–1638, 2000.

B. S. Coller. αIIbβ3: Structure and function. *Journal of Thrombosis and Haemostasis*, 13:S17–S25, 2015.

M. A. Cooper. Optical biosensors in drug discovery. *Nature Reviews Drug Discovery*, 1 (7):515–528, 2002.

N. Crawford, K. S. Authi, and N. Hack. Isolation and characterization of platelet membranes prepared by free flow electrophoresis. *Methods in Enzymology*, 215:5–20, 1992.

B. R. Curtis and J. G. McFarland. Detection and identification of platelet antibodies and antigens in the clinical laboratory. *Immunohematology*, 25(3):125–135, 2009.

L. de la Rivière. On pestilential feavers. In *The Practice of Physick*. Streator, London, 1658.

F. J. de Sauvage, K. Carver-Moore, S. M. Luoh, A. Ryan, M. Dowd, D. L. Eaton, and M. W. Moore. Physiological regulation of early and late stages of megakaryocytopoiesis by thrombopoietin. *The Journal of Experimental Medicine*, 183(2):651–656, 1996.

I. G. Denisov, Y. V. Grinkova, A. A. Lazarides, and S. G. Sligar. Directed self-assembly of monodisperse phospholipid bilayer Nanodiscs with controlled size. *Journal of the American Chemical Society*, 126(11):3477–3487, 2004.

H. Denys. Études sur la coagulation du sang dans un cas de purpura avec diminution considerable des plaquettes. In *La Cellule*, pages 445–562. 1887.

H. Duan, N. R. Civjan, S. G. Sligar, and M. A. Schuler. Co-incorporation of heterologously expressed Arabidopsis cytochrome P450 and P450 reductase into soluble nanoscale lipid bilayers. *Archives of Biochemistry and Biophysics*, 424(2):141–153, 2004.

U. H. N. Dürr, M. Gildenberg, and A. Ramamoorthy. The magic of bicelles lights up membrane protein structure. *Chemical Reviews*, 112(11):6054–6074, 2012.

R. Escher, D. Müller, M. Vogel, S. Miescher, B. M. Stadler, and P. Berchtold. Recombinant human natural autoantibodies against GPIIb/IIIa inhibit binding of autoantibodies from patients with AITP. *British Journal of Haematology*, 102(3):820–828, 1998.

M. Filizola, S. A. Hassan, A. Artoni, B. S. Coller, and H. Weinstein. Mechanistic insights from a refined three-dimensional model of integrin αIIbβ3. *Journal of Biological Chemistry*, 279(23):24624–24630, 2004.

M. Freigassner, H. Pichler, and A. Glieder. Tuning microbial hosts for membrane protein production. *Microbial Cell Factories*, 8:69, 2009.

A. L. Frelinger, R. F. Grace, A. J. Gerrits, M. A. Berny-Lang, T. Brown, S. L. Carmichael, E. J. Neufeld, and A. D. Michelson. Platelet function tests, independent of platelet count, are associated with bleeding severity in ITP. *Blood*, 126(7):873–879, 2015.

K. Fujisawa, P. Tani, and R. McMillan. Platelet-associated antibody to glycoprotein IIb/IIIa from chronic immune thrombocytopenic purpura patients often binds to divalent cation-dependent antigens. *Blood*, 81(5):1284–1289, 1993.

T. Gao, J. Petrlova, W. He, T. Huser, W. Kudlick, J. Voss, and M. A. Coleman. Characterization of de novo synthesized GPCRs supported in nanolipoprotein discs. *PloS One*, 7(9):e44911, 2012.

R. M. Garavito and S. Ferguson-Miller. Detergents as tools in membrane biochemistry. *The Journal of Biological Chemistry*, 276(35):32403–32406, 2001.

J. N. George. Platelet immunoglobulin G: Its significance for the evaluation of thrombocytopenia and for understanding the origin of alpha-granule proteins. *Blood*, 76(5): 859–870, 1990.

N. P. Goette, A. C. Glembotsky, P. R. Lev, M. Grodzielski, G. Contrufo, M. S. Pierdominici, Y. R. Espasandin, D. Riveros, A. J. García, F. C. Molinas, P. G. Heller, and R. F. Marta. Platelet apoptosis in adult immune thrombocytopenia: Insights into the mechanism of damage triggered by auto-antibodies. *PloS One*, 11(8):e0160563, 2016.

A. Gonzalez-Quintela, R. Alende, F. Gude, J. Campos, J. Rey, L. M. Meijide, C. Fernandez-Merino, and C. Vidal. Serum levels of immunoglobulins (IgG, IgA, IgM) in a general adult population and their relationship with alcohol consumption, smoking and common metabolic abnormalities. *Clinical and Experimental Immunology*, 151(1): 42–50, 2008.

R. Grisshammer. Understanding recombinant expression of membrane proteins. *Current Opinion in Biotechnology*, 17(4):337–340, 2006.

R. Grozovsky, S. Giannini, H. Falet, and K. M. Hoffmeister. Regulating billions of blood platelets: Glycans and beyond. *Blood*, 126(16):1877–1884, 2015.

K. Grushin, M. A. White, and S. Stoilova-McPhie. Reversible stacking of lipid nanodiscs for structural studies of clotting factors. *Nanotechnology Reviews*, 6(1):139–148, 2017.

C. E. Hagemeyer and K. Peter. Targeting the platelet integrin GPIIb/IIIa. *Current Pharmaceutical Design*, 16(37):4119–4133, 2010.

F. Hagn, M. Etzkorn, T. Raschle, and G. Wagner. Optimized phospholipid bilayer nanodiscs facilitate high-resolution structure determination of membrane proteins. *Journal of the American Chemical Society*, 135(5):1919–1925, 2013.

F. Hagn, M. L. Nasr, and G. Wagner. Assembly of phospholipid nanodiscs of controlled size for structural studies of membrane proteins by NMR. *Nature Protocols*, 13(1):79–98, 2018.

M. Hamidpour, M. Behrendt, B. Griffiths, L. Partridge, and N. Lindsey. The isolation and characterisation of antiplatelet antibodies. *European Journal of Haematology*, 76 (4):331–338, 2006.

R. J. Hansen and J. P. Balthasar. IVIG effects on autoantibody elimination. *Allergy*, 59 (10):1124; author reply 1124, 2004.

W. J. Harrington, V. Minnich, J. W. Hollingsworth, and C. V. Moore. Demonstration of a thrombocytopenic factor in the blood of patients with thrombocytopenic purpura. *The Journal of Laboratory and Clinical Medicine*, 38(1):1–10, 1951.

G. Hayem. *Du Sang et de Ses Alterations Anatomiques*. G. Masson, Paris, 1889.

R. He, D. M. Reid, C. E. Jones, and N. R. Shulman. Extracellular epitopes of platelet glycoprotein Ib alpha reactive with serum antibodies from patients with chronic idiopathic thrombocytopenic purpura. *Blood*, 86(10):3789–3796, 1995.

Y. He, Y.-x. Zhao, M.-q. Zhu, Q. Wu, and C.-g. Ruan. Detection of autoantibodies against platelet glycoproteins in patients with immune thrombocytopenic purpura by flow cytometric immunobead array. *Clinica Chimica Acta; International Journal of Clinical Chemistry*, 415:176–180, 2013.

Y. He, K. Wang, and N. Yan. The recombinant expression systems for structure determination of eukaryotic membrane proteins. *Protein & Cell*, 5(9):658–672, 2014.

H. E. Heemstra, R. L. de Vrueh, S. van Weely, H. A. Büller, and H. G. M. Leufkens. Predictors of orphan drug approval in the European Union. *European Journal of Clinical Pharmacology*, 64(5):545–552, 2008.

U. M. Hegde. Platelet antibodies in immune thrombocytopenia. *Blood Reviews*, 6(1): 34–42, 1992.

N. M. Heikal and K. J. Smock. Laboratory testing for platelet antibodies. *American Journal of Hematology*, 88(9):818–821, 2013.

H. Heimpel. Immunthrombozytopenie – eine therapeutische Herausforderung. *Oncology Research and Treatment*, 33(Suppl. 3):1–1, 2010.

E. Hiller. Basic principles of hemostasis. In R. Munker, E. Hiller, J. G. MD, and R. Paquette, editors, *Modern Hematology*, pages 327–345. Humana Press, 2007. ISBN 978-1-58829-557-6 978-1-59745-149-9.

R. Hoffman, E. J. B. Jr, L. E. Silberstein, H. Heslop, J. Weitz, and J. Anastasi. *Hematology: Basic Principles and Practice*. Elsevier Health Sciences, 2012. ISBN 1-4557-4041-1.

B. D. Hornstein, D. Roman, L. M. Arévalo-Soliz, M. A. Engevik, and L. Zechiedrich. Effects of circular dna length on transfection efficiency by electroporation into hela cells. *PLoS ONE*, 11(12), 2016.

M. Hou, D. Stockelberg, J. Kutti, and H. Wadenvik. Glycoprotein IIb/IIIa autoantigenic repertoire in chronic idiopathic thrombocytopenic purpura. *British Journal of Haematology*, 91(4):971–975, 1995.

E. J. Houwerzijl, N. R. Blom, J. J. L. van der Want, M. T. Esselink, J. J. Koornstra, J. W. Smit, H. Louwes, E. Vellenga, and J. T. M. de Wolf. Ultrastructural study shows morphologic features of apoptosis and para-apoptosis in megakaryocytes from patients with idiopathic thrombocytopenic purpura. *Blood*, 103(2):500–506, 2004.

K. Hymes, P. H. Schur, and S. Karpatkin. Heavy-chain subclass of round antiplatelet IgG in autoimmune thrombocytopenic purpura. *Blood*, 56(1):84–87, 1980.

S. Inagaki, R. Ghirlando, J. F. White, J. Gvozdenovic-Jeremic, J. K. Northup, and R. Grisshammer. Modulation of the interaction between neurotensin receptor NTS1 and Gq protein by lipid. *Journal of Molecular Biology*, 417(1-2):95–111, 2012.

A. Ishchenko, E. E. Abola, and V. Cherezov. Crystallization of membrane proteins: An overview. *Methods in Molecular Biology (Clifton, N.J.)*, 1607:117–141, 2017.

P. J. M. Johnson, A. Halpin, T. Morizumi, L. S. Brown, V. I. Prokhorenko, O. P. Ernst, and R. J. Dwayne Miller. The photocycle and ultrafast vibrational dynamics of bacteriorhodopsin in lipid nanodiscs. *Physical chemistry chemical physics: PCCP*, 16(39): 21310–21320, 2014.

H. Kashiwagi and Y. Tomiyama. Pathophysiology and management of primary immune thrombocytopenia. *International Journal of Hematology*, 98(1):24–33, 2013.

H. Katayama, J. Wang, F. Tama, L. Chollet, E. P. Gogol, R. J. Collier, and M. T. Fisher. Three-dimensional structure of the anthrax toxin pore inserted into lipid nanodiscs and lipid vesicles. *Proceedings of the National Academy of Sciences of the United States of America*, 107(8):3453–3457, 2010.

A. Kauskot and M. F. Hoylaerts. Platelet receptors. *Handbook of Experimental Pharmacology*, (210):23–57, 2012.

T. Kawai, J. M. M. Caaveiro, R. Abe, T. Katagiri, and K. Tsumoto. Catalytic activity of MsbA reconstituted in nanodisc particles is modulated by remote interactions with the bilayer. *FEBS Letters*, 585(22):3533–3537, 2011.

P. Kaznelson. Verschwinden der hämorrhagischen Diathese bei einem Falle von essentieller Thrombopenie nach Milzexstirpation. *Wien Klin Wochenschr*, 29:1451–1454, 1916.

V. Kiefel and C. Müller-Eckhardt. *Transfusionsmedizin und Immunhämatologie: Grundlagen - Therapie - Methodik*. Springer, Berlin, 2010. ISBN 978-3-642-12764-9.

V. Kiefel, S. Santoso, M. Weisheit, and C. Mueller-Eckhardt. Monoclonal antibody–specific immobilization of platelet antigens (MAIPA): A new tool for the identification of platelet-reactive antibodies. *Blood*, 70(6):1722–1726, 1987.

V. Kiefel, E. Freitag, H. Kroll, S. Santoso, and C. Mueller-Eckhardt. Platelet autoantibodies (IgG, IgM, IgA) against glycoproteins IIb/IIIa and Ib/IX in patients with thrombocytopenia. *Annals of Hematology*, 72(4):280–285, 1996.

J. H. Kim, S.-R. Lee, L.-H. Li, H.-J. Park, J.-H. Park, K. Y. Lee, M.-K. Kim, B. A. Shin, and S.-Y. Choi. High cleavage efficiency of a 2a peptide derived from porcine teschovirus-1 in human cell lines, zebrafish and mice. *PLOS ONE*, 6(4):e18556, 2011.

S. Kosugi, Y. Tomiyama, M. Shiraga, H. Kashiwagi, H. Mizutani, Y. Kanakura, Y. Kurata, and Y. Matsuzawa. Platelet-associated anti-glycoprotein (GP) IIb-IIIa autoantibodies in chronic immune thrombocytopenic purpura mainly recognize cation-dependent conformations: Comparison with the epitopes of serum autoantibodies. *Thrombosis and Haemostasis*, 75(2):339–345, 1996.

R. Kuai, L. J. Ochyl, K. S. Bahjat, A. Schwendeman, and J. J. Moon. Designer vaccine nanodiscs for personalized cancer immunotherapy. *Nature materials*, 16(4):489–496, 2017.

M. Kuwana, Y. Okazaki, J. Kaburaki, Y. Kawakami, and Y. Ikeda. Spleen is a primary site for activation of platelet-reactive T and B cells in patients with immune thrombocytopenic purpura. *Journal of Immunology*, 168(7):3675–3682, 2002.

M. Kuwana, Y. Kurata, K. Fujimura, K. Fujisawa, H. Wada, T. Nagasawa, S. Nomura, T. Kojima, H. Yagi, and Y. Ikeda. Preliminary laboratory based diagnostic criteria for immune thrombocytopenic purpura: Evaluation by multi-center prospective study. *Journal of Thrombosis and Haemostasis*, 4(9):1936–1943, 2006.

M. P. Lambert and T. B. Gernsheimer. Clinical updates in adult immune thrombocytopenia. *Blood*, 129(21):2829–2835, 2017.

C. Lavenu-Bombled, C. Guitton, A. Dupuis, M.-J. Baas, C. Desconclois, M. Dreyfus, R. Li, C. Caron, C. Gachet, E. Fressinaud, and F. Lanza. A novel platelet-type von Willebrand disease mutation (GP1BA p.Met255Ile) associated with type 2B "Malmö/New York" von Willebrand disease. *Thrombosis and Haemostasis*, 116(6):1070–1078, 2016.

J. C. G. Ledingham. The experimental production of purpura in animals by the introduction of anti-blood-plate sera: A preliminary communication. *The Lancet*, 183(4737): 1673–1676, 1914.

A. J. Leitz, T. H. Bayburt, A. N. Barnakov, B. A. Springer, and S. G. Sligar. Functional reconstitution of Beta2-adrenergic receptors utilizing self-assembling Nanodisc technology. *BioTechniques*, 40(5):601–602, 604, 606, passim, 2006.

A. Lepage, M. Leboeuf, J. P. Cazenave, C. de la Salle, F. Lanza, and G. Uzan. The alpha(IIb)beta(3) integrin and GPIb-V-IX complex identify distinct stages in the maturation of CD34(+) cord blood cells to megakaryocytes. *Blood*, 96(13):4169–4177, 2000.

R. Li and J. Emsley. The organizing principle of the platelet glycoprotein Ib–IX–V complex. *Journal of Thrombosis and Haemostasis*, 11(4):605–614, 2013.

R. Li, K. M. Hoffmeister, and H. Falet. Glycans and the platelet life cycle. *Platelets*, 27 (6):505–511, 2016.

S. Li, L. Wang, C. Zhao, L. Li, J. Peng, and M. Hou. CD8+ T cells suppress autologous megakaryocyte apoptosis in idiopathic thrombocytopenic purpura. *British Journal of Haematology*, 139(4):605–611, 2007.

H. A. Liebman. Immune thrombocytopenia (ITP): An historical perspective. *ASH Education Program Book*, 2008(1):205–205, 2008.

N. S. Lipman, L. R. Jackson, L. J. Trudel, and F. Weis-Garcia. Monoclonal versus polyclonal antibodies: Distinguishing characteristics, applications, and information resources. *ILAR journal*, 46(3):258–268, 2005.

A. J. Lochowicz and B. R. Curtis. Clinical applications of platelet antibody and antigen testing. *Laboratory Medicine*, 42(11):687–692, 2011.

J. A. López, B. Leung, C. C. Reynolds, C. Q. Li, and J. E. Fox. Efficient plasma membrane expression of a functional platelet glycoprotein Ib-IX complex requires the presence of its three subunits. *Journal of Biological Chemistry*, 267(18):12851–12859, 1992.

S.-Z. Luo, X. Mo, V. Afshar-Kharghan, S. Srinivasan, J. A. López, and R. Li. Glycoprotein Ibα forms disulfide bonds with 2 glycoprotein Ibβ subunits in the resting platelet. *Blood*, 109(2):603–609, 2007.

A. Lusitano. *Curationum Medicinalum Centuriae Quatuor*. Froben, Basileae, 1556.

S. Ly, F. Bourguet, N. O. Fischer, E. Y. Lau, M. A. Coleman, and T. A. Laurence. Quantifying interactions of a membrane protein embedded in a lipid nanodisc using fluorescence correlation spectroscopy. *Biophysical Journal*, 106(2):L05–L08, 2014.

S. Mak, R. Sun, M. Schmalenberg, C. Peters, and P. B. Luppa. Express incorporation of membrane proteins from various human cell types into phospholipid bilayer nanodiscs. *Biochemical Journal*, 474(8):1361–1371, 2017.

F. Marino. Recherches sur les plaquettes du sang. *Comptes Rendus des Seances de la Societe de Biologie et de Ses Filiales*, 58:194–196, 1905.

M. T. Marty, K. C. Wilcox, W. L. Klein, and S. G. Sligar. Nanodisc-solubilized membrane protein library reflects the membrane proteome. *Analytical and bioanalytical chemistry*, 405(12):4009–4016, 2013.

A. Matzdorff, O. Meyer, H. Ostermann, V. Kiefel, W. Eberl, T. Kühne, I. Pabinger, and M. Rummel. Immunthrombozytopenie - aktuelle Diagnostik und Therapie: Empfehlungen einer gemeinsamen Arbeitsgruppe der DGHO, ÖGHO, SGH, GPOH und DGTI. *Oncology Research and Treatment*, 41(Suppl. 2):5–36, 2018.

R. McMillan. Antiplatelet antibodies in chronic adult immune thrombocytopenic purpura: Assays and epitopes. *Journal of Pediatric Hematology/Oncology*, 25 Suppl 1:S57–61, 2003.

R. McMillan. The pathogenesis of chronic immune thrombocytopenic purpura. *Seminars in Hematology*, 44(4 Suppl 5):S3–S11, 2007.

R. McMillan, J. Lopez-Dee, and R. Bowditch. Clonal restriction of platelet-associated anti-GPIIb/IIIa autoantibodies in patients with chronic ITP. *Thrombosis and Haemostasis*, 85(5):821–823, 2001.

O. Meyer, A. Agaylan, H.-H. Borchert, T. Aslan, S. Bombard, H. Kiesewetter, and A. Salama. A simple and practical assay for the antigen-specific detection of platelet antibodies. *Transfusion*, 46(7):1226–1231, 2006.

J. H. Morrissey, V. Pureza, R. L. Davis-Harrison, S. G. Sligar, Y. Z. Ohkubo, and E. Tajkhorshid. Blood clotting reactions on nanoscale phospholipid bilayers. *Thrombosis research*, 122(Suppl 1):S23–S26, 2008.

K. Mörs, C. Roos, F. Scholz, J. Wachtveitl, V. Dötsch, F. Bernhard, and C. Glaubitz. Modified lipid and protein dynamics in nanodiscs. *Biochimica Et Biophysica Acta*, 1828 (4):1222–1229, 2013.

A. Najaoui, T. Bakchoul, J. Stoy, G. Bein, M. J. Rummel, S. Santoso, and U. J. Sachs. Autoantibody-mediated complement activation on platelets is a common finding in patients with immune thrombocytopenic purpura (ITP). *European Journal of Haematology*, 88(2):167–174, 2012.

A. Nath, W. M. Atkins, and S. G. Sligar. Applications of phospholipid bilayer nanodiscs in the study of membranes and membrane proteins. *Biochemistry*, 46(8):2059–2069, 2007.

T. Nebe. Hämatologische Labordiagnostik bei Thrombozyten. *LaboratoriumsMedizin*, 38 (5), 2014.

C. Neunert, W. Lim, M. Crowther, A. Cohen, L. Solberg, and M. A. Crowther. The American Society of Hematology 2011 evidence-based practice guideline for immune thrombocytopenia. *Blood*, 117(16):4190–4207, 2011.

C. Neunert, N. Noroozi, G. Norman, G. R. Buchanan, J. Goy, I. Nazi, J. G. Kelton, and D. M. Arnold. Severe bleeding events in adults and children with primary immune thrombocytopenia: A systematic review. *Journal of thrombosis and haemostasis: JTH*, 13(3):457–464, 2015.

S. Nomura. Advances in diagnosis and treatments for immune thrombocytopenia. *Clinical Medicine Insights: Blood Disorders*, 9:15–22, 2016.

B. Olsson, P.-O. Andersson, M. Jernås, S. Jacobsson, B. Carlsson, L. M. S. Carlsson, and H. Wadenvik. T-cell-mediated cytotoxicity toward platelets in chronic idiopathic thrombocytopenic purpura. *Nature Medicine*, 9(9):1123–1124, 2003.

J. Perdomo, F. Yan, and B. H. Chong. A megakaryocyte with no platelets: Anti-platelet antibodies, apoptosis, and platelet production. *Platelets*, 24(2):98–106, 2013.

E. J. Petersen, E. Posthumus, and J. J. Sixma. Functional expression of single chain glycoprotein Ib alpha on the surface of COS cells and BHK cells. *Thrombosis and Haemostasis*, 76(5):768–773, 1996.

L. Porcelijn, E. Huiskes, M. Schipperus, B. van der Holt, M. de Haas, J. J. Zwaginga, and Dutch HOVON 64 Study Group. Lack of detectable platelet autoantibodies is correlated with nonresponsiveness to rituximab treatment in ITP patients. *Blood*, 129 (25):3389–3391, 2017.

D. Proverbio, C. Roos, M. Beyermann, E. Orbán, V. Dötsch, and F. Bernhard. Functional properties of cell-free expressed human endothelin A and endothelin B receptors in artificial membrane environments. *Biochimica Et Biophysica Acta*, 1828(9):2182–2192, 2013.

T. Raschle, S. Hiller, T.-Y. Yu, A. J. Rice, T. Walz, and G. Wagner. Structural and functional characterization of the integral membrane protein VDAC-1 in lipid bilayer nanodiscs. *Journal of the American Chemical Society*, 131(49):17777–17779, 2009.

T. Raschle, C. Lin, R. Jungmann, W. M. Shih, and G. Wagner. Controlled co-reconstitution of multiple membrane proteins in lipid bilayer nanodiscs using dna as a scaffold. *ACS chemical biology*, 10(11):2448–2454, 2015.

R. P. Richter, R. Bérat, and A. R. Brisson. Formation of solid-supported lipid bilayers: an integrated view. *Langmuir*, 22(8):3497–3505, 2006.

M. Rijkers, B. L. van den Eshof, P. F. van der Meer, F. P. J. van Alphen, D. de Korte, F. W. G. Leebeek, A. B. Meijer, J. Voorberg, and A. J. G. Jansen. Monitoring storage induced changes in the platelet proteome employing label free quantitative mass spectrometry. *Scientific Reports*, 7(1):11045, 2017.

T. K. Ritchie, Y. V. Grinkova, T. H. Bayburt, I. G. Denisov, J. K. Zolnerciks, W. M. Atkins, and S. G. Sligar. Reconstitution of membrane proteins in phospholipid bilayer nanodiscs. *Methods in enzymology*, 464:211–231, 2009.

T. K. Ritchie, H. Kwon, and W. M. Atkins. Conformational analysis of human ATP-binding cassette transporter (ABCB1) in lipid nanodiscs and inhibition by the antibodies MRK16 and UIC2. *Journal of Biological Chemistry*, page jbc.M111.284554, 2011.

F. Rodeghiero and M. Ruggeri. ITP and international guidelines: What do we know, what do we need? *La Presse Médicale*, 43(4, Part 2):e61–e67, 2014.

S. Rodriguez Bueno. *Atlas of Haemostasis, Volume III.* GRU, 2011. ISBN 978-84-615-0364-3.

C. Roos, M. Zocher, D. Müller, D. Münch, T. Schneider, H.-G. Sahl, F. Scholz, J. Wachtveitl, Y. Ma, D. Proverbio, E. Henrich, V. Dötsch, and F. Bernhard. Characterization of co-translationally formed nanodisc complexes with small multidrug transporters, proteorhodopsin and with the E. coli MraY translocase. *Biochimica et Biophysica Acta (BBA) - Biomembranes*, 1818(12):3098–3106, 2012.

J. E. Rouck, J. E. Krapf, J. Roy, H. C. Huff, and A. Das. Recent advances in nanodisc technology for membrane protein studies (2012–2017). *FEBS Letters*, 591(14):2057–2088, 2017.

J. Roy, H. Pondenis, T. M. Fan, and A. Das. Direct capture of functional proteins from mammalian plasma membranes into nanodiscs. *Biochemistry*, 54(41):6299–6302, 2015.

M. Saboor, Q. Ayub, S. Ilyas, and Moinuddin. Platelet receptors: An instrumental of platelet physiology. *Pakistan Journal of Medical Sciences*, 29(3):891–896, 2013.

U. J. H. Sachs. Diagnostik der Autoimmunthrombozytopenie. *Hämostaseologie*, 28(1): 72–76, 2008.

T. Sailer, K. Lechner, S. Panzer, P. A. Kyrle, and I. Pabinger. The course of severe autoimmune thrombocytopenia in patients not undergoing splenectomy. *Haematologica*, 91(8):1041–1045, 2006.

S. Sakaguchi. Naturally arising Foxp3-expressing CD25+CD4+ regulatory T cells in immunological tolerance to self and non-self. *Nature Immunology*, 6(4):345–352, 2005.

M. Sakakura, H. Wada, I. Tawara, T. Nobori, T. Sugiyama, N. Sagawa, and H. Shiku. Reduced CD4+CD25+ T cells in patients with idiopathic thrombocytopenic purpura. *Thrombosis Research*, 120(2):187–193, 2007.

S. Schlegel, M. Klepsch, D. Gialama, D. Wickström, D. J. Slotboom, and J.-W. de Gier. Revolutionizing membrane protein overexpression in bacteria. *Microbial Biotechnology*, 3(4):403–411, 2010.

M. A. Schuler, I. G. Denisov, and S. G. Sligar. Nanodiscs as a new tool to examine lipid-protein interactions. *Methods in Molecular Biology*, 974:415–433, 2013.

O. C. Schultheiss and S. J. Stanton. Assessment of salivary hormones. In *Methods in Social Neuroscience*, pages 17–44. Guilford Press, New York, NY, US, 2009. ISBN 978-1-60623-040-4.

A. M. Seddon, P. Curnow, and P. J. Booth. Membrane proteins, lipids and detergents: Not just a soap opera. *Biochimica et Biophysica Acta (BBA) - Biomembranes*, 1666 (1–2):105–117, 2004.

J. B. Segal and N. R. Powe. Prevalence of immune thrombocytopenia: Analyses of administrative data. *Journal of Thrombosis and Haemostasis*, 4(11):2377–2383, 2006.

J. W. Semple. Immune pathophysiology of autoimmune thrombocytopenic purpura. *Blood Reviews*, 16(1):9–12, 2002.

N. C. Shaner, P. A. Steinbach, and R. Y. Tsien. A guide to choosing fluorescent proteins. *Nature Methods*, 2(12):905–909, 2005.

S. Sharma and S. Wilkens. Biolayer interferometry of lipid nanodisc-reconstituted yeast vacuolar H+-ATPase. *Protein Science : A Publication of the Protein Society*, 26(5): 1070–1079, 2017.

A. W. Shaw, M. A. McLean, and S. G. Sligar. Phospholipid phase transitions in homogeneous nanometer scale bilayer discs. *FEBS letters*, 556(1-3):260–264, 2004.

J. R. Sheng, S. Grimme, P. Bhattacharya, M. H. B. Stowell, M. Artinger, B. S. Prabahakar, and M. N. Meriggioli. In vivo adsorption of autoantibodies in myasthenia gravis using Nanodisc-incorporated acetylcholine receptor. *Experimental Neurology*, 225(2):320–327, 2010.

A. Shih, I. Nazi, J. G. Kelton, and D. M. Arnold. Novel treatments for immune thrombocytopenia. *La Presse Médicale*, 43(4, Part 2):e87–e95, 2014.

N. Shirzad-Wasei, O. J. van, P. H. Bovee-Geurts, L. J. Kusters, G. J. Bosman, and W. J. DeGrip. Rapid transfer of overexpressed integral membrane protein from the host membrane into soluble lipid nanodiscs without previous purification. *Biological Chemistry*, 396(8):903–915, 2015.

N. R. Shulman, V. J. Marder, and R. S. Weinrach. Similarities between known antiplatelet antibodies and the factor responsible for thrombocytopenia in idiopathic purpura. Physiologic, serologic and isotopic studies. *Annals of the New York Academy of Sciences*, 124(2):499–542, 1965.

Y. Skaik, A. Battermann, O. Hiller, O. Meyer, C. Figueiredo, A. Salama, and R. Blasczyk. Development of a single-antigen magnetic bead assay (SAMBA) for the sensitive detection of HPA-1a alloantibodies using tag-engineered recombinant soluble $B3$ integrin. *Journal of Immunological Methods*, 391(1-2):72–80, 2013.

D. Stegner, J. M. M. vanEeuwijk, O. Angay, M. G. Gorelashvili, D. Semeniak, J. Pinnecker, P. Schmithausen, I. Meyer, M. Friedrich, S. Dütting, C. Brede, A. Beilhack, H. Schulze, B. Nieswandt, and K. G. Heinze. Thrombopoiesis is spatially regulated by the bone marrow vasculature. *Nature Communications*, 8(1):127, 2017.

Y. Y. Studentsov, M. Schiffman, H. D. Strickler, G. Y. F. Ho, Y.-Y. S. Pang, J. Schiller, R. Herrero, and R. D. Burk. Enhanced enzyme-linked immunosorbent assay for detection of antibodies to virus-like particles of human papillomavirus. *Journal of Clinical Microbiology*, 40(5):1755–1760, 2002.

R. Sun, S. Mak, J. Haschemi, P. Horn, F. Boege, and P. B. Luppa. Nanodiscs incorporating native $B1$ adrenergic receptor as a novel approach for the detection of pathological autoantibodies in patients with dilated cardiomyopathy. *The Journal of Applied Laboratory Medicine*, 3(7), 2019.

A. L. Szymczak and D. A. A. Vignali. Development of 2A peptide-based strategies in the design of multicistronic vectors. *Expert Opinion on Biological Therapy*, 5(5):627–638, 2005.

A. M. Taylor, J. Storm, L. Soceneantu, K. J. Linton, M. Gabriel, C. Martin, J. Woodhouse, E. Blott, C. F. Higgins, and R. Callaghan. Detailed characterization of cysteine-less P-glycoprotein reveals subtle pharmacological differences in function from wild-type protein. *British Journal of Pharmacology*, 134(8):1609–1618, 2001.

D. Terrell, L. A. Beebe, J. George, B. R. Neas, S. K. Vesely, and J. Segal. The prevalence of immune thrombocytopenic purpura (ITP). *Blood*, 112(11):1277–1277, 2008.

J. A. Thomas and C. G. Tate. Quality control in eukaryotic membrane protein overproduction. *Journal of Molecular Biology*, 426(24):4139–4154, 2014.

P. Thomas and T. G. Smart. HEK293 cell line: A vehicle for the expression of recombinant proteins. *Journal of Pharmacological and Toxicological Methods*, 51(3):187–200, 2005.

M. Trahey, M. J. Li, H. Kwon, E. L. Woodahl, W. D. McClary, and W. M. Atkins. Applications of lipid nanodiscs for the study of membrane proteins by surface plasmon resonance. *Current protocols in protein science*, 81:29.13.1–29.13.16, 2015.

C. Tzitzilonis, C. Eichmann, I. Maslennikov, S. Choe, and R. Riek. Detergent/nanodisc screening for high-resolution nmr studies of an integral membrane protein containing a cytoplasmic domain. *PLOS ONE*, 8(1):e54378, 2013.

E. F. van Leeuwen, J. T. van der Ven, C. P. Engelfriet, and A. E. von dem Borne. Specificity of autoantibodies in autoimmune thrombocytopenia. *Blood*, 59(1):23–26, 1982.

L. N. Varghese, J.-P. Defour, C. Pecquet, and S. N. Constantinescu. The thrombopoietin receptor: Structural basis of traffic and activation by ligand, mutations, agonists, and mutated calreticulin. *Frontiers in Endocrinology*, 8:59, 2017.

D. Varon and S. Karpatkin. A monoclonal anti-platelet antibody with decreased reactivity for autoimmune thrombocytopenic platelets. *Proceedings of the National Academy of Sciences of the United States of America*, 80(22):6992–6995, 1983.

C. Vincke and S. Muyldermans. Introduction to heavy chain antibodies and derived Nanobodies. *Methods in Molecular Biology (Clifton, N.J.)*, 911:15–26, 2012.

J. R. Vrbensky, J. E. Moore, D. M. Arnold, J. W. Smith, J. G. Kelton, and I. Nazy. The sensitivity and specificity of platelet autoantibody testing in immune thrombocytopenia: A systematic review and meta-analysis of a diagnostic test. *Journal of Thrombosis and Haemostasis*, 17(5):787–794, 2019.

H. J. Weiss, M. H. Rosove, B. A. Lages, and K. L. Kaplan. Acquired storage pool deficiency with increased platelet-associated IgG. Report of five cases. *The American Journal of Medicine*, 69(5):711–717, 1980.

P. Werlhof. *Disquisitio Medica et Philolo- Gica de Variolis et Anthracibus, Signis Differentiis, Medelis Disserit Etc.* Nicolai Foersteri, 1735.

K. C. Wilcox, M. R. Marunde, A. Das, P. T. Velasco, B. D. Kuhns, M. T. Marty, H. Jiang, C.-H. Luan, S. G. Sligar, and W. L. Klein. Nanoscale synaptic membrane mimetic allows unbiased high throughput screen that targets binding sites for alzheimer's-associated aβ oligomers. *PLOS ONE*, 10(4):e0125263, 2015.

V. J. Woods, E. H. Oh, D. Mason, and R. McMillan. Autoantibodies against the platelet glycoprotein IIb/IIIa complex in patients with chronic ITP. *Blood*, 63(2):368–375, 1984.

F. M. Wurm. Production of recombinant protein therapeutics in cultivated mammalian cells. *Nature Biotechnology*, 22(11):1393–1398, 2004.

R. Yan, X. Mo, A. M. Paredes, K. Dai, F. Lanza, M. A. Cruz, and R. Li. Reconstitution of the platelet glycoprotein ib-ix complex in phospholipid bilayer nanodiscs. *Biochemistry*, 50(49):10598–10606, 2011.

F. Ye, G. Hu, D. Taylor, B. Ratnikov, A. A. Bobkov, M. A. McLean, S. G. Sligar, K. A. Taylor, and M. H. Ginsberg. Recreation of the terminal events in physiological integrin activation. *The Journal of Cell Biology*, 188(1):157–173, 2010.

J. Yu, S. Heck, V. Patel, J. Levan, Y. Yu, J. B. Bussel, and K. Yazdanbakhsh. Defective circulating CD25 regulatory T cells in patients with chronic immune thrombocytopenic purpura. *Blood*, 112(4):1325–1328, 2008.

J. Zhai, M. Ding, T. Yang, B. Zuo, Z. Weng, Y. Zhao, J. He, Q. Wu, C. Ruan, and Y. He. Flow cytometric immunobead assay for quantitative detection of platelet autoantibodies in immune thrombocytopenia patients. *Journal of Translational Medicine*, 15(1):214, 2017.

S. Zhang, A. Garcia-D'Angeli, J. P. Brennan, and Q. Huo. Predicting detection limits of enzyme-linked immunosorbent assay (ELISA) and bioanalytical techniques in general. *Analyst*, 139(2):439–445, 2013.

W. Zhang, W. Deng, L. Zhou, Y. Xu, W. Yang, X. Liang, Y. Wang, J. D. Kulman, X. F. Zhang, and R. Li. Identification of a juxtamembrane mechanosensitive domain in the platelet mechanosensor glycoprotein Ib-IX complex. *Blood*, 125(3):562–569, 2015.

A. Zufferey, R. Kapur, and J. W. Semple. Pathogenesis and therapeutic mechanisms in immune thrombocytopenia (ITP). *Journal of Clinical Medicine*, 6(2), 2017.

B Appendix

B.1 Abbreviations

A	ACE	antigen capture ELISA
	AITP	autoimmune thrombocytopenia
	ApoA-1	apolipoprotein A-1
	APS	ammonium persulfate
	AU	absorbance units
B	BGH	bovine growth hormone
	BSA	bovine serum albumin
C	CD	cluster of differentiation
	CHAPS	3-[(3-cholamidopropyl)dimethylammonio]-1-propanesulfonate
	CHO	Chinese hamster ovary
	CMC	critical micelle concentration
	CMV	human cytomegalovirus
	CV	coefficient of variability
D	Da	Dalton
	DDM	n-dodecyl-β-D-Maltoside
	DMEM	Dulbecco's modified Eagle medium
	DMSO	dimethyl sulfoxide
	DNA	deoxyribonucleic acid
	DPBS	Dulbecco's phosphate-buffered saline
E	EDC	1-ethyl-3-(3-dimethylaminopropyl)carbodiimide
	eGFP	enhanced green fluorescent protein
	ELISA	enzyme-linked immunosorbent assay
	ER	endoplasmatic reticulum
F	FACS	fluorescence-activated cell sorting
	FBS	fetal bovine serum
	Fc	flow cell
	FC-12	n-dodecyl-phosphocholine
G	GP	glycoprotein
H	HDL	high-density lipoprotein
	HEK	human embryonic kidney
	HEPES	4-2-hydroxyethylpiperazine-1-ethanesulfonic acid
	HRP	horseradish peroxidase
	HSA	human serum albumin
I	Ig	immunoglobulin
	IMAC	immobilized metal ion affinity chromatography
	ITP	immune thrombocytopenia

	IVIg	intravenous Ig
M	MACE	modified antigen capture ELISA
	MAIPA	monoclonal antibody immobilization of platelet antigens
	MCS	multiple cloning site
	MSP	membrane scaffold protein
	MW	molecular weight
	MWCO	molecular weight cut-off
N	ND	nanodisc
	NHS	N-hydroxysuccinimide
	NMR	nuclear magnetic resonance
O	OG	octyl-β-D-glucopyranoside
P	PaIgG	platelet-associated IgG
	PAGE	polyacrylamide gel electrophoresis
	PBS	phosphate-buffered saline
	PC	L-α-phosphatidyl-choline
	PCR	polymerase chain reaction
	PEG-PE	1,2-dioleoyl-sn-glycero-3-phosphoethanol-amine-N-[methoxy(polyethylene glycol)-2000]
	PLT	platelet
	PRP	platelet-rich plasma
	PVDF	polyvinylidene difluoride
R	RFP	red fluorescent protein
	RT	room temperature
S	SD	standard deviation
	SDS	sodium dodecyl sulfate
	SEC	size exclusion chromatography
	SPR	surface plasmon resonance
T	TBS	tris-buffered saline
	Tc cell	cytotoxic T cell
	TEMED	tetramethylethylenediamine
	TEV	Tobacco Etch Virus
	Th cell	T helper cell
	TMB	3,3',5,5'-tetramethylbenzidine
	TPO	thrombopoietin
	TPO-RA	thrombopoietin receptor agonist
	Treg	regulatory T cell
V	vWF	von Willebrand factor
W	WB	Western Blot
	wt	wild type

B.2 List of Figures

B.3 List of Tables

B.4 Eidesstattliche Erklärung

Ich erkläre an Eides statt, dass ich die bei der Fakultät für Chemie der TU München zur Promotionsprüfung vorgelegte Arbeit mit dem Titel:

Einbau von Thrombozyten-Rezeptoren in Nanodiscs für den Nachweis von Autoantikörpern in Autoimmun-Thrombozytopenie

am Institut für Klinische Chemie und Pathobiochemie am Klinikum rechts der Isar unter der Anleitung und Betreuung durch Prof. Dr. Peter B. Luppa ohne sonstige Hilfe erstellt und bei der Abfassung nur die gemäß § 6 Abs. 6 und 7 Satz 2 angegebenen Hilfsmittel benutzt habe.

⊗ Ich habe keine Organisation eingeschaltet, die gegen Entgelt Betreuerinnen und Betreuer für die Anfertigung von Dissertationen sucht, oder die mir obliegenden Pflichten hinsichtlich der Prüfungsleistungen für mich ganz oder teilweise erledigt.

⊗ Ich habe die Dissertation in dieser oder ähnlicher Form in keinem anderen Prüfungsverfahren als Prüfungsleistung vorgelegt.

○ Die vollständige Dissertation wurde in _____ veröffentlicht. Die promotionsführende Einrichtung hat der Vorveröffentlichung zugestimmt.

⊗ Ich habe den angestrebten Doktorgrad noch nicht erworben und bin nicht in einem früheren Promotionsverfahren für den angestrebten Doktorgrad endgültig gescheitert.

○ Ich habe bereits am _____ bei der Fakultät für _____ der Hochschule _____ unter Vorlage einer Dissertation mit dem Thema _____ die Zulassung zur Promotion beantragt mit dem Ergebnis: _____

Die öffentlich zugängliche Promotionsordnung der TUM ist mir bekannt, insbesondere habe ich die Bedeutung von § 28 (Nichtigkeit der Promotion) und § 29 (Entzug des Doktorgrades) zur Kenntnis genommen. Ich bin mir der Konsequenzen einer falschen Eidesstattlichen Erklärung bewusst.
Mit der Aufnahme meiner personenbezogenen Daten in die Alumni-Datei bei der TUM bin ich

⊗ einverstanden
○ nicht einverstanden

München, den _____

Stefanie Mak